

1. LEG 185 SUMMARY: INPUTS TO THE IZU-MARIANA SUBDUCTION SYSTEM¹

Shipboard Scientific Party²

ABSTRACT

Subduction zones are the primary regions on Earth today where crust recycling takes place, and through geologic time they have been sites of continent formation. Many key chemical elements important for understanding crustal growth are subducted in the sedimentary column (e.g., Th, rare earth elements, Ba, and Be) and in the uppermost oxidized portions of the volcanic section of oceanic basement (e.g., K, B, U, CO₂, and H₂O). The principal objective of Leg 185 was to core two sites in Mesozoic crust in the west Pacific, which is being subducted into the Mariana and Izu-Bonin subduction systems, in order to determine the inputs into the “west Pacific subduction factory.” Hole 801C was first drilled in the oldest (~170 Ma) crust in the Pacific Ocean during Ocean Drilling Program (ODP) Leg 129. During Leg 185 the hole was deepened to 936 meters below seafloor (mbsf), and at Site 1149, located on magnetic Anomaly M11 (~132 Ma) 100 km east of the Izu-Bonin Trench, the complete sedimentary sequence (410 m) and an additional 133 m of highly altered volcanic basement were drilled.

Using the recovered core and the logging results, it is possible to reconstruct the volcanic section for Hole 801C. Eight volcanic sequences have been defined by the combined efforts of Legs 129 and 185, some with massive lava flows up to 20 m thick and others with thin pillows and sheet flows of <1 m. The uppermost unit is a ~60-m sequence of alkali basalts drilled during Leg 129 and radiometrically dated at ~157 Ma. This unit is separated from the underlying tholeiites of normal oceanic crust by an ~20-m-thick ochreous Si-Fe-rich hydrothermal deposit. A similar deposit is present 100 m lower in the hole. These hydrothermal deposits and numerous interpillow sediments observed in the upper volcanic sequences define the alteration character of the basement,

¹Examples of how to reference the whole or part of this volume.

²Shipboard Scientific Party addresses.

which is confined to three zones downcore and appears to be controlled by local permeability structures. The pattern of alteration for basement at Site 801 contrasts with that from other deeply drilled sections in oceanic crust where oxidative alteration decreases continuously with depth. The estimated seafloor spreading rate for Site 801 is 160 km/m.y. Both the alteration and lava sequences may be typical of fast-spreading environments, such as the present-day East Pacific Rise.

Preliminary estimates of the geochemical budget for K were made for volcanic sections of ocean basement at Site 801 using gamma-ray intensities from downhole logs and multisensor track measurements, in addition to chemical analyses of core samples and estimates of the volume percentages of veins and alteration types. The K content of the entire core indicates a three- to four-fold enrichment as a result of low-temperature alteration. Similar estimations will be possible for other key elements following shore-based analyses of a unique suite of 120 community samples taken shipboard.

The deep basement penetration in Hole 801C provided ideal samples for probing the causes of the Jurassic Quiet Zone (JQZ). From paleomagnetic measurements on cores and geophysical logs we discovered as many as six reversals downhole. Given the spreading rates estimated for the region, the reversals must relate to rapid fluctuations in field polarity. Therefore, at Site 801 the JQZ may result from a canceling out of normal and reversed polarities associated with an unstable and relatively weak magnetic field.

Site 1149 basement is dramatically different in character from Site 801. It is pervasively altered at low temperatures to red dusky brown and preserves multicolored halos around veins and fractures. Dominated by thin flows, hyaloclastite, and flow breccia, the volcanic facies are normal-mid-ocean-ridge basalt in the upper section and enriched mid-ocean-ridge basalt at the base of Hole 1149B.

The sediments being subducted into trenches must, in part, control geochemical differences in the composition of arc magmas. Both the Mariana and Izu-Bonin margins are characterized by complete subduction of the sedimentary section on the downgoing plate, thus simplifying the dynamics of the subduction problem. Although the subducting sediments have been reasonably well sampled in the Pigafetta and East Mariana Basins (Mariana region), earlier drilling attempts to recover the sedimentary section in the Nadezhda Basin, seaward of the Izu-Bonin Trench, had largely been thwarted by difficult drilling conditions. Thus, an important objective of Leg 185 was met by continuously coring and logging the ~400 m sedimentary section at Site 1149. The uppermost sediments consist of pelagic clays with admixtures of volcanic ash and biosiliceous material for which paleomagnetic data define an excellent record of 6 m.y. of sedimentation in the west Pacific. These are underlain by barren diagenetically altered pelagic clays (characterized by low sedimentation rates), which overlie radiolarian cherts and clays and a lower unit of chert intercalated with marl and chalk above basement. The basal sediments have been dated from nannofossil assemblages (*Tubodiscus verena* and *Rucinolithus wisei*) as lowermost Hauterivian to uppermost Valanginian, in accord with the assigned M-11 magnetic lineation. The lower sedimentary units preserve a record of high rates of biogenic sedimentation (~18 m/m.y.) as the site passed beneath the equatorial zone of high biological productivity. Shipboard sediment chemistry also documents a well-preserved record of hydrothermal input into the basal sediments.

The sedimentary sequence at Site 1149 is substantially different from that being subducted at the Mariana Trench, the latter being characterized by an extensive mid-Cretaceous volcanoclastic sequence derived from the local seamounts and having a lower carbonate content, which may explain some of the geochemical differences between the two arc systems.

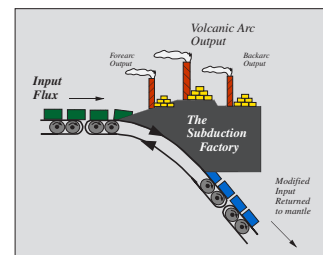
In an attempt to establish the *JOIDES Resolution* as a platform for microbiological studies, Leg 185 was the first ODP leg to conduct a series of on-site contamination tests while undertaking a systematic study of the deep biosphere in oceanic sediments and basement. These contamination tests involved adding highly sensitive tracers (i.e., perfluorocarbons and fluorescent microspheres) to the drilling fluids and the core barrel to evaluate the potential extent of contamination of the cores by the drilling process. The particulate tracer was not found in the samples used for microbiological experiments, suggesting these samples were uncontaminated. Some thin sections contained the particulate tracer, probably introduced during preparation of thin sections. The results of the chemical tracer experiments indicate that, on average, $\sim 0.3 \mu\text{L}$ of drilling fluid/gram cored material was present. In addition, samples of sediments and basalts were placed in cultures aboard ship for further shore-based study. Possible microbial tracks observed in the 170-Ma volcanic glass are intriguing evidence for a deep biosphere active at the extreme depths (>930 mbsf) sampled during Leg 185.

INTRODUCTION

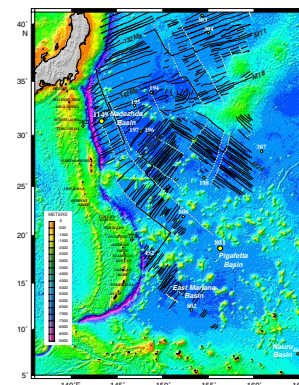
The primary objective of Leg 185 was to determine the geochemical composition of the sediments and upper volcanic section of oceanic crust being subducted into the western Pacific arc system. These data are required as part of the subduction equation, which involves quantifying the inputs and outputs, both into the arc and back into the mantle, of the subduction factory (Fig. F1). These processes are important, as the majority of chemical recycling on Earth is currently taking place in the subduction factory. These “factories” were probably the main sites of crustal production through geologic time (Armstrong, 1968; Karig and Kay, 1981; Reymer and Schubert, 1984; McLennan, 1988). Despite the fact that there is good evidence for transport of fluid and sedimentary components from the subducted plate to the arc system (Morris et al., 1990; Hawkesworth et al., 1997; Elliott et al., 1997), there are few quantitative constraints on the recycling equation and its effect on the dynamics of crust formation and destruction. The Ocean Drilling Program (ODP) since the late 1980s has, as a part of several drilling legs, tackled this problem (see “[Historical Perspectives](#),” p. 6), but Leg 185 was the first ODP leg for which the objectives were specifically applied to coring oceanic crust and sedimentary sections representative of the different inputs into the subduction factory; in this case the Mariana and Izu-Bonin arcs of the west Pacific Ocean (Fig. F2).

Many of the key elements for understanding crustal growth are sequestered in the sedimentary column (e.g. Th, rare earth elements [REEs], Ba, and Be) and in the uppermost oxidized portions of the volcanic section of oceanic basement (e.g., K, B, U, CO_2 , and H_2O). The input of these and other elements may vary as a function of sediment composition (Plank and Langmuir, 1998) or the nature of the volcanic basement (Staudigel et al., 1995; Alt and Teagle, 1999). For example, the absence of significant carbonate in the sediments may influence the

F1. Input to and output from “The Subduction Factory,” p. 35.



F2. Topography of study area showing magnetic lineations, p. 36.



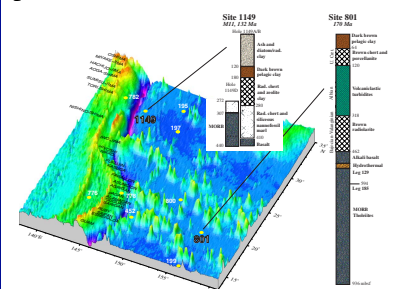
CO₂ emitted at an arc volcano. The presence of organic-rich sediments or hydrothermal sediment may influence the input of metals in different arcs. Alkaline off-axis volcanics and associated volcanoclastic sediments, when subducted, may significantly add to the alkali inventory of the subduction factory.

The igneous section of oceanic crust inherits many of its physical and geochemical characteristics from the spreading ridge. Significant differences in eruption style, ridge morphology, and structure occur depending on the rate of spreading (see review in Perfit and Chadwick, 1998). Similarly, the hydrothermal systems vary as a function of the longevity and depth of the magma chamber (e.g., Gillis, 1995; Haymon et al., 1991) and, on average, the alteration characteristics; therefore, the geochemical inventory of crust must vary as a function of spreading rate. As crust ages and moves away from the spreading axis, it is cooled initially by hydrothermal activity and later warms again as it equilibrates with the geothermal gradient. The chemical changes occurring during this transition are important, not only in controlling the compositions of the oceans and the retroactions with continental erosion (Staudigel et al., 1995; Alt and Teagle, 1999), but also in fixing key elements that will later be fed into the subduction factory. Some of these elements will migrate into the arc crust, whereas others will be recycled into the mantle, possibly to return to the oceanic crust as hot-spot magma. Although the chemical maturation of crust must continue for several tens of millions of years after its formation (Stein and Stein, 1994) and probably throughout its history, the most significant alteration is at the ridge axis and for ~10–30 m.y. following crustal accretion (Staudigel et al., 1986; Alt and Teagle, 1999).

In an analogous fashion, the history of sedimentation on the oceanic crust as it transits different oceanic regimes will influence the composition of the input into the subduction factory (Plank and Langmuir, 1993). Nearby intraplate volcanoes may add a significant flux of volcanoclastic material to the sedimentary sequence. This may have very different characteristics in key isotope ratios, especially Pb, that the arc may inherit or that may be recycled back into the mantle. When proximal to active margins, the upper sediments may contain significant quantities of terrigenous turbidites. As the oceanic plate approaches the trench, the final contribution to the sedimentary pile will include ash from the volcanic arc. For margins that are not undergoing frontal accretion of sediments, this component will be recycled into the mantle or underplated beneath the forearc.

The oldest oceanic crust on Earth is subducting into the Izu-Mariana arc system. In addition to providing geochemical data to input into the subduction equation, the two sites studied provide important geochemical constraints on the nature and history of Mesozoic oceanic crust. Site 801, in the Pigafetta Basin (Fig. F3), is within the Jurassic Quiet Zone (JQZ). It is the oldest crust drilled by ODP or the Deep Sea Drilling Project (DSDP), radiometrically dated at ~170 Ma (Pringle, 1992). The second site, Site 1149 in the Nadezhda Basin (Fig. F3), is on the same flow line as Site 801 but is on magnetic Anomaly M11 and, as such, has an estimated age of ~132 Ma. Both sites originated at fast-spreading mid-ocean ridges in the Southern Hemisphere and then migrated northward, but at different times and rates. Thus, in addition to the “subduction factory experiment,” Leg 185 scientists had an unparalleled opportunity to (1) assess the paleoequatorial sedimentation history of the Pacific Ocean since Mesozoic time, (2) place limits on the

F3. Perspective map of Izu and Mariana arcs and Leg 185 sites, p. 37.



ages of the oldest magnetic anomalies in the ocean basins, and (3) study the nature of the JQZ.

With the exception of relatively soft sediments, drilling rarely recovers entire sedimentary and igneous sections; thus, calculating the geochemical inventory is problematic. The gaps in the data have to be filled in by combining detailed core description and logging the drill hole for both physical parameters (e.g., resistivity, porosity, velocity), and geochemical composition. In addition to the regular inventory of ODP logs, the geochemical logging tool was used during Leg 185.

The ultimate long-term goal of studies of the subduction factory is to create a complete geochemical mass balance of the inputs, outputs, and residues lost from the system. Geochemists and geophysicists argue strongly for the recycling of oceanic crust and sediments to the mantle (Hofmann, 1997; Van der Hilst et al., 1997). Given adequate control on the subduction equation, it may ultimately be possible to identify the recycled products of the factory, not only in the arc volcanoes, but as they reappear as mantle plumes on the Earth's surface after being recycled into the mantle. The Izu-Mariana system was chosen as the first of these studies because it is relatively simple:

1. It is characterized only by limited, if any, sediment accretion in the forearc.
2. It has a well-defined subduction geometry with a relatively steeply dipping slab defined beneath the Mariana arc that penetrates the 670-km discontinuity contrasted with a more shallowly dipping slab beneath the Izu-Bonin arc (Van der Hilst et al., 1997).
3. It has a wide aperture of outputs from forearc across the arc to the backarc.
4. The arc and forearc regions have already been the subject of ODP drilling during Legs 125 and 126, which penetrated serpentinite mounds associated with forearc dewatering (Fryer, 1992), as well as excellent sections of deep-sea ash that record >15 m.y. of arc volcanic activity (Arculus et al., 1995).

Too often postcruise research on ODP samples produces a data set dispersed among many individual investigators. During Leg 185 the investigators developed a novel approach and chose to work on a common set of samples. The geochemical database thus developed for Leg 185 will be a unique contribution to the Geochemical Earth Reference Model (GERM) (Staudigel et al., 1998) and to the NSF MARGINS Program (Plank et al., 1998), and the communal samples will be a legacy of the leg. Additionally, Hole 801C, now at a depth of 936 mbsf, remains as an ODP legacy hole in the oldest oceanic crust on Earth.

An important objective of Leg 185 involved the study of the deep biosphere at both sites. Bacteria have been located in near-ridge axis hydrothermal systems and within the sediment column as deep as 800 m (Parkes et al., 1994). In addition, textural evidence suggests that bacteria living off nutrients associated with basaltic glass alteration, may thrive in the basaltic crust (Thorseth et al., 1995; Fisk et al., 1998; Furnes and Staudigel, 1999). The fascinating possibility that bacterial activity may exist in oceanic crust as old and as deep as that at Sites 801 and 1149 provided the motivation for sampling the basement and sediment for bacteria culturing and DNA extraction in the search for extremophile life. To control the extent of contamination from surface waters, drilling mud, and drilling tools, a series of tests for contami-

nants were undertaken as part of the operations at Sites 801 and 1149 (see “[Methods for Quantifying Potential Microbial Contamination during Deep Ocean Coring](#)” [Smith et al., 2000]).

HISTORICAL PERSPECTIVES

The two sites drilled during this leg are in Mesozoic crust, in the oldest part of the Pacific Ocean Basin, and in extreme water depths, which provided a challenge to drilling technology. These sites are the most recent part of an unfolding drama of drilling by DSDP and ODP in the west Pacific abyssal plains over the past three decades.

It was apparent in 1968 after DSDP Leg 3 that the deep ocean basins were formed by seafloor spreading and, so, were very young relative to the age of the Earth. The same evidence from rifted continental margins that led Wegener and DuToit to propose continental drift then could be used to infer that the Atlantic and Indian Ocean Basins were no older than ~200 m.y. and probably somewhat younger. However, no such clues applied to the Pacific Basin because it is geologically isolated from the surrounding continents by subduction zones. Thus, in the late 1960s it seemed possible that the world’s oldest deep ocean rocks lay somewhere in the western Pacific, more than 10,000 km away from the nearest spreading ridge.

DSDP Legs 6 and 7 in 1969 were the first to search the western Pacific for the Earth’s oldest oceanic crust and sediments. The search ultimately took 20 yr and 10 legs of DSDP/ODP (Legs 6, 7, 17, 20, 32, 33, 60, 61, 89, and 129) to achieve the final goal. Many people were involved; the most persistent members of the “Old Pacific Club” included B.C. Heezen, E.L. Winterer, S.O. Schlanger, R. Moberly, I. Premoli Silva, R. Larson, Y. Lancelot, W. Sliter, D. Bukry, R.G. Douglas, and H.P. Foreman. During the early legs, drilling sites were targeted with single-channel seismic records characterized by acoustically opaque chert layers that obscured the underlying volcanic basement. Often the coring was frustrated by these impenetrable cherts, as well as by volcanoclastic sediments and basalts of Cretaceous age. To those who shipped out repeatedly and returned home with more questions than answers, what had started as an oceanographic exercise turned into an ongoing quest for the “old Pacific.”

Leg 129 brought the *Resolution*, with improved drilling capabilities, where the *Glomar Challenger* failed. Also, preparations for Leg 129 led by Yves Lancelot and Roger Larson included four multichannel seismic expeditions to the area searching for seismic “windows” through the Cretaceous volcanoclastic sediments and solid basalts. This combination of improved science and technology was finally successful 10 yr ago, in 1989, at Site 801 in the Pigafetta Basin where Jurassic sediments of Bajocian–Bathonian age were discovered overlying ~170-Ma oceanic crust (Lancelot, Larson, et al., 1990). If older material exists in the area, tectonic reconstructions suggest it would not exceed that at Site 801 by more than 10 m.y. By comparison, the next oldest deep-ocean sites are ~5–15 m.y. younger: Site 534 near the continental margin of North Carolina in the North Atlantic and Site 765 in the Argo Abyssal Plain in the Indian Ocean (Table T1). Thus, the original suggestion that the Earth’s oldest deep-ocean crust lies in the western Pacific is correct but, coincidentally, not by much.

Just before Leg 129 in the Pacific Ocean, Plank and Ludden (1992) completed the first attempt at quantifying the sedimentary geochemi-

T1. The oldest crust drilled by ODP, p. 60.

cal budget in an ODP drill core. Drilling at Site 765 penetrated ~1000 m of sediment, derived from the northwestern Australian margin, and ~250 m into the basement. The main objective was to characterize the crust subducting beneath the Sunda Arc of Indonesia. The idea of characterizing the inputs to subduction zones arose from a proposition by J. Natland and C. Langmuir in 1987–1988. The idea was extensively debated in the ODP Planning Committee and the Indian Ocean and West Pacific Ocean Regional Panels. Despite the fact that Leg 123 had been successful, the idea took several years to root itself firmly within the panel structure as a viable scientific approach. One remark was particularly pointed: “How can you learn something about milk by studying grass when you don't know anything about cows?”

The “cow model” is in fact an excellent way to convey the competing models for subduction recycling studies. In the context of subduction recycling studies, the cow is the subduction factory, the grass is the oceanic crust and sediment being subducted, and the milk is the volcanic output at the arc. The grass control model is that the same breed of cow eating different flavors of grass will produce different flavors of milk (Fig. F4A). The cow control model emphasizes the cow over the grass—different breeds will produce different flavors of milk, even if they eat the same kind of grass (Fig. F4B). The grass control model predicts that the “flavor” of the subducted input (carbonate-rich pelagic or volcanoclastic sediments) has a strong effect on the flavor of the volcanic output despite slight differences in subduction style from one margin to the next. The cow control model would predict that given similar subducted input, the different characteristics of the subduction zone (dip of the subducted plate, thermal structure, convergence rate) will lead to differences in the volcanic output. Thus, the central question is for the real Earth system, where both the grass and cow vary, whether the grass or the cow is the dominant control on the flavor of the milk—whether the subducted sediments or the physics of the subduction zone are the dominant control on the volume and composition of the volcanic output. Work thus far indicates grass (sediment input) control (Plank and Langmuir, 1993). Nonetheless, the cow (subduction zone) must play a role, and subduction factory studies need excellent control on the composition of the subducted input before we resolve its effect.

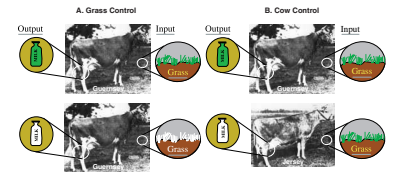
Drilling into the serpentinite mounds and the ash layers in the Izu-Bonin forearc (Leg 126; Leg 125; Fryer, 1992) recorded the magmatic output of the arc and the early dewatering of the subducting plate in the Izu-Bonin arc. Leg 170 in the Costa Rica accretionary prism (Kimura, Silver, et al., 1997) focused on problems of sediment accretion and fluid evolution in an accretionary prism and has been the latest in a series of initiatives over the past 10 yr by ODP to explore active margin accretionary assemblages (e.g., Barbados, Nankai, and Cascadia).

Consequently, ODP has come to embrace the idea of using drilling to understand geochemical mass balance. Hopefully, Leg 185 will be the first of several legs dedicated to this problem in arc systems with different tectonic regimes and sedimentary input. The U.S. MARGINS Program and the international GERM have adopted this approach as an essential part of their strategy.

IZU-MARIANA ARC

The Izu-Mariana arc system involves subduction of the ancient Pacific plate beneath the relatively young Philippine Sea plate with the re-

F4. Competing models for input-output studies, p. 38.



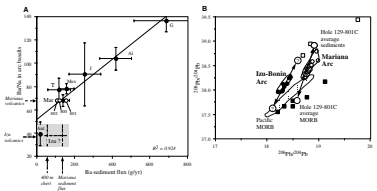
sulting production of an island arc chain of volcanoes and marginal backarc basins (Fig. F3).

There are several reasons why the Izu-Mariana margin is favorable for studying material recycling in subduction zones. The first is that significant progress has already been made on many parts of the flux equation. Serpentine seamounts, which represent forearc sites of fluid outflow, have already been drilled (Leg 125; Fryer, 1992), as have most of the sedimentary components being subducted at the Mariana Trench (Leg 129; Lancelot, Larson, et al. 1990) (see “[Western Pacific Stratigraphy](#),” p. 9). The Izu and Mariana volcanic arcs and the Mariana Trough and Sumisu Rift backarcs are among the best characterized intraoceanic convergent margins, both in space and time (Legs 125 and 126; Gill et al., 1994; Arculus et al., 1995; Elliott, et al., 1997; Ikeda and Yuasa, 1989; Stern et al., 1990; Tatsumi et al., 1992; Woodhead and Fraser, 1985; Taylor and Nesbitt, 1998). Thus, major parts of the forearc, arc, and backarc output, as well as the sedimentary input, have already been characterized. The other advantage to the Izu-Mariana system is that the problem is simplified here because (1) the upper plate is oceanic and, therefore, upper crustal contamination is minimized; and (2) sediment accretion in the forearc is nonexistent (Taylor, 1992) and, therefore, sediment subduction is complete.

Despite the simple oceanic setting and the shared plate margin, there are clear geochemical differences between the Izu and Mariana arcs. The Mariana arc erupts basalts in which both subducted sedimentary and altered oceanic crustal components can be identified (e.g., Elliott et al., 1997), and the arc conforms well to the global trend in Ba sediment input vs. Ba arc output (Fig. F5A). On the other hand, the Izu arc erupts basalts that are among the most depleted of any arc on Earth in trace element concentrations (e.g., REEs, Ba, and Sr). In addition to the contrast in elemental concentrations, there are also clear differences in the isotopic composition of Mariana and Izu basalts, such as $^{207}\text{Pb}/^{204}\text{Pb}$ and $^{206}\text{Pb}/^{204}\text{Pb}$, which may derive from isotopic differences in the input to the two trenches (Fig. F5B).

The divergence of compositions between the volcanics of these two oceanic arcs provides the simplest test for how the composition of the subducting crust affects them. The key missing information is the composition of the incoming crustal sections, specifically the basaltic basement subducting at the Mariana Trench and the sediment and basement sections subducting at the Izu Trench. The low trace element concentrations of Izu volcanics may derive from a lower flux of these elements at the trench, and their distinctive isotopic composition may be inherited from the composition of the sediments subducting there. These hypotheses can be tested by drilling the subducting sediment and basement sections feeding the two arc systems. Alternatively, differences in the fluxes cycled to the arcs may derive from different operations of the subduction factory in the two areas. For example, along-strike changes (e.g., dip, age, and depth) in the subducting slab could affect where material exits the slab and enters the arc melting regime. The changes in the geometry of the slab and its relationship to the volcanic arc may signal a change in where the volcanoes are sampling the slab material. Distinguishing between these two models—the input model vs. the slab model—requires good control on the subducted inputs, which was a primary objective of Leg 185.

F5. Correlation between Ba flux and Ba enrichment, p. 39.



WESTERN PACIFIC STRATIGRAPHY

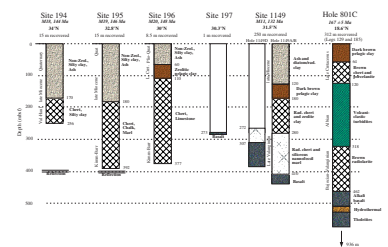
The ancient crust of the western Pacific plate is the primary input to the >2000-km-long Izu-Mariana subducting margin. Ideally, this input would be constrained by drilling several holes through the sedimentary section and deeply into oceanic crust along the length of the trench. Because of the great expense and time it takes to drill in ~6000-m water depth, we are limited in practice to a few drill holes and extending this information regionally using sedimentation and plate-motion models, along with seismic stratigraphy. Understanding the context of sedimentation and plate history in the western Pacific is thus important in order to maximize the information gained from a small number of reference sites, such as Leg 185 Sites 801 and 1149.

The crust subducting into the Mariana Trench is characterized by sea-floor divided into the Jurassic East Mariana and Pigafetta Basins (Fig. F2). Based on magnetic anomaly lineations, this region was thought to contain the Earth's oldest in situ oceanic crust formed at fast-spreading rates (160 km/m.y. at Site 801). The basic goal of Leg 129 was to sample Jurassic oceanic crust. Earlier attempts to recover Jurassic sediments and basement in the western Pacific had been thwarted by extensive mid-Cretaceous volcanics and sills and by problems with the drill string sticking in chert horizons. While drilling two holes (ODP Sites 800 and 802) that encountered Cretaceous basalt, Leg 129 was the first to succeed in recovering Jurassic oceanic basement in the Pacific Ocean, and Hole 801C rocks are still the oldest sampled in the ocean basins, at 167 ± 5 Ma (Pringle, 1992).

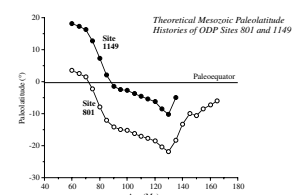
Complete sedimentary sections were sampled during Leg 129 at three sites in the East Mariana and Pigafetta Basins (ODP Sites 800–802) (Fig. F2). Before this leg, the recovery from nine DSDP and ODP sites averaged <50 m each (Fig. F2). Taking Hole 801C as typical of the region, the sedimentary stratigraphy consists of Cenozoic brown pelagic clay overlying Coniacian to Campanian cherts and porcelanite, Albian seamount volcanoclastics, and Bajocian to Valanginian radiolarites (Fig. F6) (Lancelot, Larson, et al., 1990). This sedimentary history reflects the plate history, which begins in the Southern Hemisphere in a zone of high biological productivity, as recorded by the Jurassic radiolarites (Fig. F7) (Lancelot, Larson, et al., 1990). The plate then moved southward until the Early Cretaceous when it began to move northward again, collecting volcanoclastics from the nearby Cretaceous Magellan Seamounts and then more siliceous sediments as it again entered the high-productivity zone 5° – 10° south of the paleoequator. The Cenozoic was characterized by very slow accumulation of deep brown pelagic clays, with minimal biogenic input, as is expected for the open-ocean environment. This history is typical for the western margin of the East Mariana Basin and the Pigafetta Basin. This stratigraphy, particularly the clay/chert and volcanoclastic intervals, can be traced regionally from seismic records (Abrams, et al., 1992). Although recovery was generally low (<30%), Leg 129 provided adequate sampling of the different sedimentary components to characterize the sedimentary geochemical flux into the Mariana Trench (Plank and Langmuir, 1998). This contrasts with the lack of a single, continuously drilled sedimentary section along the entire 1000 km of the Izu-Bonin margin to the north.

Previous drilling in the Nadezhda Basin, seaward of the Izu-Bonin Trench, was about as successful as drilling to the south prior to Leg 129. The chert horizons plagued drilling during Leg 20, which placed five

F6. Lithologic columns for Leg 20 sites, Hole 801C, and Site 1149, p. 40.



F7. Theoretical Mesozoic paleolatitude histories of Leg 185 sites, p. 41.



holes in the region, none of which was to hit basement except DSDP Hole 197, where only 1 m of undatable tholeiite was recovered (Fig. F6). Thus, the age of the M-series magnetic anomaly had never been tested in this region. Along the Izu-Bonin Trench, magnetic anomalies predict that the oceanic crust decreases in age from Jurassic (>M18) in the south to Early Cretaceous (M11) at Site 1149 (Fig. F2). It was unknown if the extensive mid-Cretaceous volcanism that took place in the south extended north into the Nadezhda Basin.

Average recovery of sediments in the Nadezhda Basin was extremely low (<15 m) for previous DSDP sites, again because of sticking problems and spot coring. Leg 20 cores indicate an upper ash- and diatom-rich clay unit overlying a brown pelagic clay and Cretaceous chert and chalk (Fig. F6). The paleolatitude history for Site 1149 predicts a longer duration beneath equatorial zones of high biological productivity, and, therefore, extensive chert and chalk sequences (Fig. F7). Water-gun seismic profiles collected during a presite seismic survey show a prominent reflection at ~0.2 s two-way traveltime (TWT) that corresponds to the chert horizon and another prominent reflection at 0.42 s TWT (Fig. F8) that corresponds with probable basement. Postcruise investigations will determine if these distinctive reflections can be identified throughout the Nadezhda Basin.

Site 1149 lies within the same spreading compartment as Site 801, along a flow line in crust ~35 m.y. younger (Fig. F2), formed at a slower spreading rate than Site 801 (100 mm/yr full rate). Roughly 100 km from the trench, Site 1149 lies seaward of the main faulting of the plate as it bends into the subduction zone (Fig. F2). The main objective at Site 1149 was to drill through the inferred 400-m-thick sedimentary sequence and into basement subducting along the Izu-Bonin margin, which would enable a comparison with the fluxes to the south into the Mariana Trench.

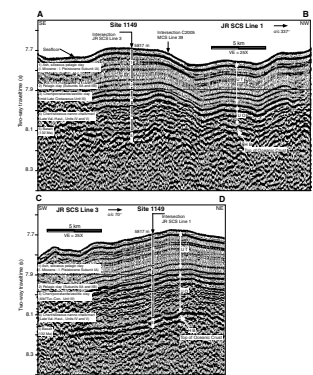
SCIENTIFIC OBJECTIVES

As discussed above, previous drilling has already laid the foundation to much of the crustal flux equation at the Izu and Mariana subduction systems and provided a strong rationale for continuing the effort to determine the mass balance fluxes across the subduction zones. The missing part of the flux equation is largely the input: (1) the altered oceanic crust seaward of the Mariana Trench—Site 801—and (2) both the incoming sediment and basaltic sections approaching the Izu-Bonin Trench—Site 1149. In addition, both sites are located along the same flow line in Mesozoic Pacific oceanic crust (from ~170 to 130 Ma) and provide an unparalleled opportunity to study the geochemical and physical nature of old Pacific crust and its tectonic, sedimentation, and magnetic histories.

Site 801

The primary motivation for returning to Hole 801C, seaward of the Mariana Trench (Fig. F2), was to sample the upper oxidative zone of alteration of this oldest in situ oceanic crust. Previous drilling during Leg 129 only penetrated 63 m into “normal” Jurassic basement. Based on basement rocks from Hole 504B and other basement sites with sufficient penetration, the upper oxidative zone of alteration, which contains the lion’s share of some element budgets (e.g., K, B, etc.), lies in

F8. Seismic stratigraphy at Site 1149, p. 42.



the upper 200–300 m of the basaltic crust (e.g., Alt et al., 1986; Gillis et al., 1992). The objectives of coring and logging at this site were to

1. Calculate the geochemical fluxes attending the upper oxidative alteration of the oceanic crust in Hole 801C;
2. Compare igneous compositions, structure, and alteration with other drilled sections of in situ oceanic crust (in particular Hole 504B, contrasting a young site in Pacific crust with the oldest site in Pacific crust);
3. Help to constrain general models for seafloor alteration that depend on spreading rate and age (Hole 801C is in the world's oldest oceanic crust that was formed at a fast-spreading ridge, so it embodies several end-member characteristics); and
4. Test models for the origin of the magnetic Jurassic Quiet Zone. Site 801 is located in an area of very low amplitude uncorrelated magnetic anomalies, the JQZ. This quiet zone has been suggested to result from (1) oceanic crust of a single polarity with only small anomalies from field intensity fluctuations, (2) oceanic crust with magnetic reversals so numerous as to "cancel each other out" when measured at the sea surface, or (3) oceanic crust with a more normal frequency of magnetic reversals acquired when the dipole field intensity was anomalously low. Deepening Hole 801C permitted testing of the above hypotheses, and in particular, the third hypothesis of magnetic reversals during a period of anomalously low field intensity as fresh, unaltered volcanic glass was obtained. Such material can yield reliable paleointensity information (Pick and Tauxe, 1993) on the very fine, single-domain grains of titanium-free magnetite within the volcanic glass.

Site 1149

The primary motivation for drilling at Site 1149, a site ~100 km seaward of the Izu-Bonin Trench, was to provide the first complete section of sediment and altered oceanic crust entering this subduction zone. Previous drilling in the Nadezhda Basin failed to penetrate resistant cherts, so most of the sediment column was unsampled. Only 1 m of basalt had been previously recovered from basement in this vast area. The objectives of coring and logging at this site were to

1. Provide estimates of the sediment and altered basalt inputs (geochemical fluxes) into the Izu-Bonin subduction zone;
2. Contrast crustal inputs to the Izu-Bonin Trench with those for the Mariana Trench, to test whether along-strike differences in the volcanics can be explained by along-strike variations in the crustal inputs;
3. Compare basement alteration characteristics to those at Hole 801C (on 170-Ma crust along the same flow line);
4. Provide constraints on the Early Cretaceous paleomagnetic time scale; and
5. Provide constraints on mid-Cretaceous carbonate compensation depth (CCD) and equatorial circulation fluctuations.

In addition to serving as an important reference site for crustal inputs to the Izu-Bonin Trench, Site 1149 can also address additional paleomagnetic and paleoceanographic problems (objectives 4 and 5 above).

According to Nakanishi et al. (1992), Site 1149 is approximately on magnetic Anomaly M12. Its basement age should be ~133 Ma and correspond to the Valanginian Stage of the Early Cretaceous, according to recent time-scale calibrations (Harland et al., 1990; Gradstein et al., 1994; Channell et al., 1995). However, those age estimates are poorly constrained but may be tested by drilling. Specifically, a reasonably precise date on the magnetic Anomaly M12 at Site 1149 could test the proposed new time scale of Channell et al. (1995) and our proposed magnetic anomaly interpretation (see *“Geophysics,”* p. 21).

Based on its theoretical Cretaceous paleolatitude history, Site 1149 may have formed at ~5°S, migrated south to 10°S in its early history, and then gradually moved north, crossing the paleoequator as the Pacific plate accelerated its northward motion ~85–90 Ma (Fig. F7). A site such as Site 1149 with an Early Cretaceous basement age (~135 Ma), an equatorial paleolatitude history during the mid-Cretaceous, and a predictable subsidence history for the Cretaceous is ideal for testing proposed CCD variations (Thierstein, 1979; Arthur et al., 1985). In addition, Erba (1992), following Roth (1981), has shown that certain species of nannofossils can be characterized as “high fertility indices” and used as approximate indicators of the paleoequatorial upwelling zone. Using these high fertility indices, potential fluctuations in the equatorial circulation system could be studied at Site 1149 for the mid-Cretaceous, when it was located near the paleoequator (especially from 115 to 95 Ma).

Microbiological Objectives

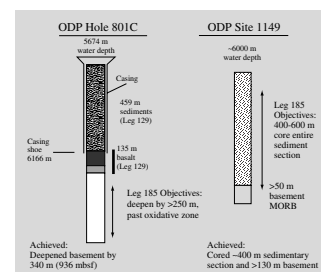
The deep water (~6000 m) and proposed penetration into old oceanic basement provided an intriguing target in the search for hidden bacterial life forms. Leg 185 was the first ODP leg to incorporate microbiology as a major new initiative. The microbiology objectives for Leg 185 were to

1. Determine the amount of potential biological contamination created by the APC, extended core barrel (XCB), and rotary core barrel (RCB) coring;
2. Develop a sample-handling strategy for routine microbiological sampling; and
3. Conduct culturing experiments with several media at both atmospheric and in situ pressures.

DRILLING STRATEGY

The drilling strategy for Hole 801C, an ODP legacy hole drilled during Leg 129 (Lancelot, Larson, et al., 1990), was to reenter and deepen the hole by an additional 250 m (to a maximum of 400 m total basement depth) past the upper oxidative alteration zone of the basaltic crust (Fig. F9; Table T2). During Leg 129 only 63 m of the normal tholeiites was cored. Based on data from Hole 504B and other basement sites with sufficient penetration, the upper oxidative zone of alteration, which contains important element budgets (e.g., K, B), lies in the upper 200–300 m of the basaltic crust (Alt et al., 1986; Staudigel et al., 1995). The transition from volcanics to sheeted dikes may not lie much deeper: 500–600 m in Hole 504B (Detrick et al., 1994); 450 m to Layer 2B (Carbotte et al., 1997); and only a few hundred meters at Hess Deep

F9. Drilling objectives for Leg 185 sites, p. 43.



T2. Leg 185 operational summary, p. 61.

(Francheteau et al., 1992). By drilling >250 m, the expectation was that we would penetrate the oxidation zone, as well as a significant portion of Layer 2A, and possibly into the dikes.

The drilling strategy at Site 1149 was to core the entire sedimentary section, inferred to be 400–600 m thick, and as far into the upper oxidative alteration zone of the basaltic basement as possible, to a maximum of 430 m (Fig. F9; Table T2). Previous drilling hundreds of kilometers to the east had failed to penetrate successfully through resistant cherts, so most of the sediment column was still unsampled.

SAMPLING STRATEGY

Communal and Composite Basement Samples for Geochemical Studies

Too often ODP cores are sampled by individual investigators who perform a unique set of analyses. This process produces a dispersed data set, often making it difficult to relate the different studies. Our overall objective is to have the investigators work on a common set of samples. This is a novel approach and requires good organization, communication, and cooperation at all stages. The benefits, however, are substantial, and the geochemical database archived for Leg 185 will be a unique contribution to the GERM initiative.

In addition to personal samples taken for specific studies in the cores, such as vein-rock interaction, microbiology, in situ laser, and ion probe analyses, a representative suite of rocks was sampled for use by the scientific party for geochemical analysis. These samples were taken within each geochemical unit to represent the major lithologies in the cores: massive flows, pillowed or sheet flows, interflow material, breccia, and also the different alteration types: veins, halos, and pervasively altered basalt. A representative group of samples was taken for each of the different lithologic divisions. In all, the sample set comprises 118 samples.

Samples were described, crushed, and powdered following the procedures detailed in “[Preparation of Composites](#),” p. 25, in the “Explanatory Notes” chapter. Each sample was subdivided for a thin section, a slab for crushing and powdering, and an archive piece. For most samples an aliquot of clean chips was also archived. A summary description of each sample, the sampling interval, and the weight of powder and rock chips was recorded. Communal and composite sample tables summarizing these data are available (see the “[Supplementary Materials](#)” contents list). The communal samples will serve as the base sample set for all geochemical work. The geochemical results, in combination with the geophysical logs, core descriptions, and physical properties data, will be used to construct a numerical average for all elements for the composition of Hole 801C and Site 1149 basement. A subset of these samples will be utilized to build a physical mixture of different lithologies, a “composite” sample, which will be prepared following the procedures outlined in “[Preparation of Composites](#),” p. 25, in the “Explanatory Notes” chapter. The composite samples will also be analyzed by various geochemical procedures to determine the bulk geochemistry of Hole 801C and Site 1149 basalts. The composite samples must be large enough in volume to accommodate future analytical efforts and, therefore, represent the legacy of the site.

Initial shore-based analyses of the communal samples will focus on inductively coupled plasma-atomic emission spectrometry analysis for

major elements and selected trace elements (Sr, Ba, and some trace metals), and CO₂ and H₂O determinations. In addition, 20 samples will be taken for representative key lithologies and distributed for general analysis. Using the geochemical data, additional subsets will be selected for more detailed geochemical and isotopic analysis. Although subject to interpretation of the shore-based geochemical data and detailed analysis of logs, a composite sample will be prepared that is representative of each of the major sequences. The analyses proposed for the communal samples and the composites are given in Table T3. The data will be updated on a regular basis on the Leg 185 World Wide Web site; distribution and curation of the samples will be controlled by the Leg 185 co-chief scientists.

Glass Samples

Fresh glass is important for determining the chemical composition of magmas because it is unaffected by mineral accumulation and post-eruption alteration. Glass is also usually chemically homogeneous so that chemical analyses made with microbeam techniques are applicable to the bulk sample. Fresh glass from flow and pillow margins and from hyaloclastites was identified under the binocular microscope during the routine description of the cores. The locations of most of the pieces that contain glass are given in Table T4. A subset of ~50 glasses was sampled aboard ship for a coordinated effort to obtain a wide variety of analyses on the same samples (Table T4). Glass chips and thin sections will be analyzed first by electron microprobe for the major elements. This will determine how many different compositions are present in the cores. Based on the major element analyses, selected thin sections and chips will be distributed among the other investigators who wish to conduct laser and ion beam microanalyses and water measurements by Fourier transform infrared spectroscopy. Samples will also be distributed for mass spectroscopy for heavy isotopes, halogens, Li, and B. Some samples were dispensed on board the ship for magnetic intensity measurements, with additional samples to be available after thin-section billets are cut. Thin sections examined for evidence of microbial activity will also be measured for the extent of chemical and microbial alteration.

Communal Sediment Samples

A communal protocol was also developed for the sediments recovered at Site 1149. These samples were selected from either interstitial water squeeze cakes or specially selected discrete samples. The squeeze cakes, which result from the compression of a cleaned 10-cm-long whole round, are excellent materials because they are a collected average of hundreds of grains of sediment. Care was taken to exclude ash layers and other discrete layers. The squeeze cakes were also complemented by additional large samples (~50 cm³) taken on the sampling table. All lithologies were targeted to ensure good coverage of the complete sedimentary sequence. Shipboard and shore-based analyses of the interstitial waters and sedimentary material will include stable and radiogenic isotopes; elemental concentrations of major, trace, and rare earth elements, bulk mineralogy, clay mineralogy, and a host of other important parameters.

T3. Proposed analyses of the communal and composite samples, p. 62.

T4. Proposed analyses on communal glass samples, p. 63.

Analysis of Logs

An important aspect of the construction of a reference site involves integrating the geophysical and geochemical logs with the core information to create a complete crustal section. In the case of the basement logging at Site 801, of particular interest is determining the relative proportions of interflow material, thick flows, and thin sheet flows or pillows. The strategy involves an integration of the FMS logs, geochemical data, and core lithology data for the Hole 801C basement. The porosity-sensitive logs (resistivity, velocity, density, and neutron porosity) will be studied for Hole 801C to characterize old oceanic crust formed at a fast-spreading rate. In addition, a modeling study of the temperature log in Hole 801C will be undertaken to further constrain the porosity/permeability of basement.

Given the interest in the magnetic reversal history of Jurassic oceanic crust, the magnetic logs will be used to establish the magnetic polarity stratigraphy of Hole 801C basement from the log data and to construct a model of the surface magnetic field using the various polarity intervals as input. The combined geochemical and geophysical logs will be essential to reconstructing the sedimentary section at Site 1149, which had low recovery but high-quality logging data in the chert-bearing units.

Microbiology

The majority of the microbiology data will be generated in shore-based studies. The major efforts will be to determine community composition by DNA extraction, in situ hybridization, characterization of microbes isolated from enrichment cultures, and culturing of microbes from samples maintained at in situ pressure. Culturing at high pressure and at 1 atm will be done at different shore-based laboratories. These studies will be coordinated with additional study of igneous rocks, veins, and sediment from which biological samples were collected. Rock samples will be examined by scanning electron microscope for microbes and microbial alteration textures. The amount of microbial vs. chemical alteration will be measured in thin sections, and the types and compositions of secondary minerals will be ascertained by electron microprobe. The lithology of sediments used for cultures and ATP measurements will be determined from smear slides.

SITE 801 PRINCIPAL RESULTS

Site 801: A Jurassic Basement Reference Site

Leg 185, Hole 801C
Days on site: 28 April–19 May 1999
Latitude: 18°38.53798'N
Longitude: 156°21.58813'E
Water depth (m): 5673.60
Total cored section (m): 339.3
Interval drilled (mbsf): 594.3–935.7
Core recovery (%): 47

ODP Hole 801C was first drilled during Leg 129 in December 1989 as part of a series of drill sites aimed at recovering Jurassic sediment and oceanic crust in the Pacific Ocean (Lancelot, Larson, et al., 1990). Rocks

from Hole 801C are the oldest sampled in the ocean basins (at ~170 Ma) (Pringle, 1992). During Leg 144, the hole was reentered and logged, and a drill-string packer experiment was conducted (Haggerty, Silva, Rack, et al., 1995; Larson et al., 1993). Leg 185 succeeded in deepening Hole 801C by an additional 359 m, to a total depth in basement of 474 m (Table T2), placing this site as the DSDP and ODP drill hole with the sixth greatest penetration into normal oceanic crust. Recovery was good (47%), and a complete suite of ODP downhole logs was run to 850 mbsf. Although the reentry cone needs to be cleared of cuttings, which hampered logging by flowing back into the hole, it is in good condition and remains as ODP's legacy site in the Earth's oldest oceanic crust.

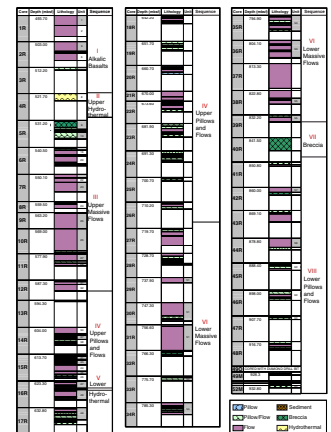
Basement Stratigraphy and Geochemistry

The basaltic section at Site 801 is overlain by a sedimentary section characterized by an upper (56 m) pelagic clay unit, which overlies a 63-m-thick chert-porcelanite unit. These sedimentary units are underlain by thick (192 m) volcanoclastic turbidites of probable Albian age, which represent redeposited material from the Magellan Seamounts. A second chert-radiolarite unit (125 m) underlies the volcanoclastics and gives way to 20 m of Callovian red radiolarites and claystones. These overlie basement at 461.6 mbsf at Site 801.

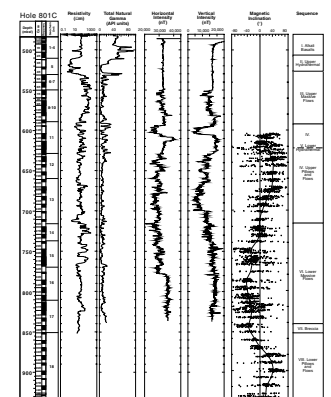
A stratigraphic column of the entire basement section is given in Figure F10. This section includes a composite of the rocks drilled on both Leg 129 and Leg 185 in Hole 801C. On the basis of flow morphology, geochemistry, and mineralogy, the basement section has been divided into eight major sequences (I–VIII). These sequences have been subdivided into 18 geochemical units, 60 lithologic units, and ~250 individual cooling units. The cooling units (pillows, flows, breccia, etc.) are organized into eruptive packages of similar textures and mineralogy; these are the lithologic units. The geochemical units require distinct batches of magma from the magma chamber or melting regime. We discuss here the features of the main sequences only.

The uppermost basement (Sequence I) is alkaline and composed of basaltic to doleritic sills (Floyd et al., 1992; Floyd and Castillo, 1992). Ar/Ar radiometric ages on laser-fused samples (Pringle, 1992) give a weighted mean age of 157 Ma. The igneous units are intercalated with chert-rich sediments, which are often baked at the contact with the basalt. The sediments contain siliceous microfossils that define ages of early Bathonian to late Bajocian (~170 Ma) (Channell et al., 1995) and confirm the intrusive nature of the alkaline suite. This alkaline sequence is 60.2 m thick and overlies a Si and Fe oxyhydroxide-rich hydrothermal horizon (Sequence II) for which logging results (see resistivity log in Fig. F11) indicate a thickness of ~20 m. During Leg 129, ~63 m of volcanic rock was drilled below the hydrothermal deposit. The alteration intensity is highly variable in these rocks, and their colors vary from gray black to green gray and to light brown. Parts of these cores clearly were altered under a high fluid-flux regime (see "Basement Alteration," p. 18). These lavas are thin flows and pillows, but they lie above a series of thick flows; both are included as part of Sequence III, the Upper Massive Flows (Fig. F10). These thick flows have an exceptionally high resistivity (Fig. F11), although they appear to be similar in lithologic and geochemical character to other thick flows lower in the stratigraphy. Ar/Ar fusion dates on two samples from Sequence III define an age for these lavas from 162 to 171 Ma (Pringle, 1992).

F10. Stratigraphic column showing each cooling unit in the basement, p. 44.



F11. Paleomagnetic data from Hole 801C, p. 45.



Sequence III also defines a clear magmatic evolutionary trend toward more mafic, MgO-rich, and Zr-poor lavas from its base at ~580 mbsf to the overlying hydrothermal deposit (Fig. F12). The MgO-rich lavas contain abundant olivine phenocrysts, which are only rarely observed deeper in the section. The most evolved lavas, those with the lowest MgO and highest Zr, are commonly saturated in olivine, plagioclase, and clinopyroxene. In general, phenocrysts are scarce in the entire section. Plagioclase is the most common phase, but most of the lavas are classified as aphyric. Figure F12, in addition to highlighting alteration characteristics, shows the typical occurrence of plagioclase phenocrysts. Notwithstanding the paucity of phenocrysts, mineralogical examination and X-ray fluorescence (XRF) analyses for major and trace elements permitted definition of five geochemical units in Sequence III, which probably correspond to discrete magmatic episodes.

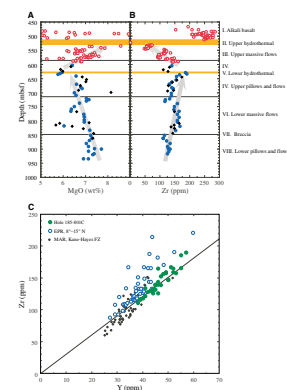
Between 600 and 720 mbsf the section is characterized by a pillow-dominated zone with well-developed interpillow horizons (Sequence IV—Upper Pillows and Flows). The amount of interpillow material of probable sedimentary origin decreases significantly downsection in this sequence. This is evident in the gamma-ray log (Fig. F11), which is smooth and decreases in intensity throughout Sequence IV. A second Si-rich hydrothermal unit similar to the larger one uphole is present within Sequence IV pillows.

From 720 mbsf to the bottom of Hole 801C at 936 mbsf, a tectonic breccia (VII) separates the Lower Massive Flows (VI, 720–890 mbsf) and a series of thin, generally <1-m-thick sheet flows and pillows, the Lower Pillows and Flows (VIII, 890–934 mbsf). The thickest flow in the former exceeds 20 m. Once more, the breccia zone also coincides with a change in geochemistry (Fig. F12), indicating that the lithologic breaks in eruption style or tectonism also correlate with the evolution in the magma composition.

The major changes in the resistivity and the natural gamma logs correspond to the major sequence divisions defined by lithology and geochemistry (Fig. F11). The logging data along with the FMS images will be integrated with the core descriptions to create as complete a section as possible from which the bulk geochemical composition of the upper oceanic crust at this site will be calculated.

This igneous sequence represents a key section recovered from fast-spreading crust (total basement penetration = 470 m) and will thus serve as an important type section with which to compare to the modern East Pacific Rise. The entire section between 530 and 890 mbsf is tholeiitic and extrusive in character. The tholeiites are all normal (N) mid-ocean-ridge basalt (MORB) (Fig. F12), with most falling on the same crystal fractionation trend from 7.5% MgO to 6% MgO (1200°–1130°C). Although it is highly altered, the capping tholeiite is very primitive, with abundant chrome spinel and >8 wt% MgO. Overall, from the base to the top of the section there is a decrease in MgO, until the lower hydrothermal unit, and then an increase in MgO until the upper hydrothermal unit (Fig. F12). During Leg 185 we recovered abundant, fresh basaltic glass in >20 cores, which represent the oldest volcanic glass sampled in oceanic crust and will be critical in assessing the primary magma compositions and possible changes in MORB melting parameters during the Jurassic. The presence of two Fe-Si hydrothermal deposits and associated intense basalt alteration within the Hole 801C section is consistent with fast-spreading crust, where hydrothermal activity is common among the spreading axis.

F12. Downhole variations in MgO and Zr from shipboard XRF data, p. 46.



Basement Alteration

The ochreous hydrothermal units are a significant characteristic of Site 801. Although similar types of deposits exist near the modern East Pacific Rise, they have never been drilled in Pacific oceanic basement elsewhere. Fluid temperatures of formation calculated for the upper hydrothermal deposit (Sequence II) are $\sim 16^{\circ}$ – 60°C (Alt et al., 1992). These fluids controlled the alteration budget of the underlying pillow basalt.

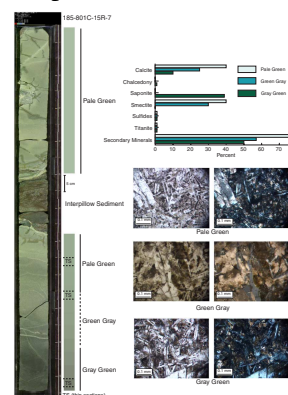
A primary objective for Leg 185 was to quantify the chemical alteration of Jurassic basement in the west Pacific in order to calculate geochemical fluxes to the Mariana subduction factory. Detailed work was done aboard ship logging vein types, breccia, hyaloclastite, interpillow units, and alteration color, as well as using the continuous multi-sensor track (MST) data and downhole logs to identify K- and U-rich zones from the natural gamma emission. Figure F13 provides examples of the major alteration types observed in the cores, as well as the interpillow sediments, which are clearly evident on the gamma logs (Fig. F11) and must contribute in a significant way to the alkali budget of the site. The dominant alteration minerals are calcite, smectite, pyrite, silica, celadonite, and Fe oxyhydroxides; different mixtures of these minerals define the alteration color of the cores (Fig. F13).

In tandem with the major change in the igneous units at ~ 720 mbsf, there is a change in the style of alteration. It is marked by a higher frequency of veins (27/m) and silica-rich interpillow material and sediment above 720 mbsf to less frequent veins (20/m) and more hyaloclastites below 720 mbsf. No interpillow sediments are found below 720 mbsf. The most extreme alteration is in the alkalic unit at the top of the basement and adjacent to the ochreous hydrothermal zones (Fig. F14). This is characterized by pervasive alteration of the igneous material to bleached pale green and buff-colored rocks, with significant concentrations of calcite, smectite, and celadonite, resulting in increases in K, CO_2 , and H_2O contents. In the pale green and buff-colored rocks all of the ferromagnesian minerals have been destroyed, and there are gains in alkalis and losses of Mg, Fe, and trace metals. Hole 801C includes four distinct oxidative alteration zones: at the top of the basement in the brown alteration zone of the alkalic unit, adjacent to the upper hydrothermal zone (462–550 mbsf), adjacent to the lower hydrothermal zone at 610–630 m, and deep in the hole at ~ 750 – 900 mbsf (Fig. F15). These oxidative zones are flanked by gray basalt minimally altered in anoxic conditions (pyrite, calcite, and saponite) and still containing glass. The alternating oxidative zones with high fluid/rock ratios and anoxic alteration assemblages of lower fluid/rock ratios is unusual given what is more typically a general decrease downhole in oxidative alteration, as found at some other drill sites into oceanic crust. The pattern of alteration found in Hole 801C was controlled by the local permeability structure, which may have been influenced by clogging of circulation pathways with secondary minerals as the result of early low-temperature hydrothermal activity associated with the formation of the Fe-Si-hydrothermal deposits. This may be typical of fast-spreading oceanic crust.

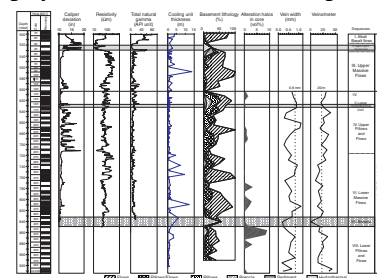
Calculating Element Budgets

Reconstructing the geochemistry of an incomplete sequence is challenging, particularly when most of the elements of interest in subduction fluxes (e.g., K, U, Ba, CO_2 , and H_2O) are distributed

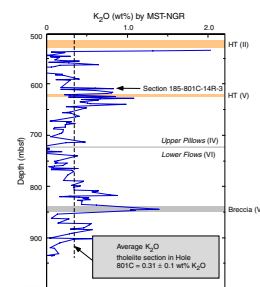
F13. Extreme alteration types observed, p. 47.



F14. Basement igneous stratigraphy and alteration features, p. 48.



F15. K_2O vs. depth, Hole 801C, p. 49.



heterogeneously. The logging data allow reconstruction of the section, particularly for quantifying brecciated and massive flow units. The gamma log provides K, U, and Th concentration data. Quantifying the number of veins and breccia intervals and integrating these data with geochemical information over the section also provides a means of calculating a mathematical average of the chemical composition of the cored section. Several scientists will work on a suite of 118 samples taken downhole to provide a comprehensive geochemical and isotope data base. Some of these samples will also be mixed to provide composite samples of the different sequences and geochemical units identified in the core (see [“Preparation of Composites,”](#) p. 25, in the “Explanatory Notes” chapter).

Two preliminary attempts were made shipboard to quantify the potassium content of the core. They both underscore the difficulties involved in making these estimations.

Firstly, shipboard measurements of K_2O and the estimation of vol% alteration (1.7% halos, 0.05% celadonite veins, 1.5% breccia and hyaloclastite, and 96.75% relatively unaltered rock) indicate that the total section cored during Leg 185 has experienced ~17% increase in K_2O and Rb contents as the result of seawater alteration. Adding interpillow sediment to this estimate increases the bulk K_2O content of the Leg 185 section to 60% greater than in fresh basalt alone (from 0.08 to 0.13 wt% K_2O), with 27% of the total alkali budget residing in interpillow sediment.

Secondly, a K_2O budget for the core can be calculated after calibrating the natural gamma-ray signal from the MST using core analyses (see [“Using Natural Gamma Ray to Calculate Potassium Budgets,”](#) p. 55, in the “Site 801” chapter and Fig. F15). The MST-NGR signal agrees well with patent alteration features in the core, as well as with K_2O determined from the natural gamma spectrometry logging tool (NGT). The bulk K_2O calculated from the MST-NGR data for the entire tholeiitic section is 0.31 ± 0.1 wt%, which is much higher than the estimate above, based on the vol% of alteration, but agrees well with the average from the downhole logging data (0.36 wt%). The MST estimate would require that the 97% of the core that did not contain patent alteration features has 0.27 wt% K_2O . An average K_2O of 0.31 wt% is lower than that calculated for DSDP Site 417 (0.56 wt%; Staudigel et al., 1995) drilled in old Atlantic crust. The technique laid out in this report could be used to calculate bulk K_2O at the few other ODP sites drilled deeply into basement (Holes 504B, 765C, 332) to start to form a better understanding of the controls on seafloor alteration fluxes.

Character of the Jurassic Quiet Zone

Hole 801C was also unique in providing the opportunity to examine the causes for the low-amplitude uncorrelated magnetic anomalies observed within the so-called Jurassic Quiet Zone. The JQZ has been variously hypothesized as a time of no geomagnetic field reversals, of anomalously low geomagnetic field intensity, or of numerous rapid reversals. In combination with the previous results from Leg 129, the basement in Hole 801C shows a series of polarity reversals downhole. Figure F11 compares results from shipboard paleomagnetic measurements on cores with the magnetic signature from the continuous downhole geophysical logs. The cores analyzed with the shipboard magnetometer show a gradual change in the magnetic field direction

from one polarity interval to the other. In both the magnetic logs and the shipboard analyses, numerous flows between those of opposite polarities display zero inclination values. These results indicate that the lavas were erupted in a period of rapid polarity fluctuations of the Earth's magnetic field. Although analysis of the core and logging data is incomplete, there appears to be a correlation between polarity changes and the different volcanic sequences. From the bottom of the hole upward, the first reversal occurs within the thin pillows and sheet flows of Sequence VIII (the major sequence change could possibly occur at the magnetic polarity change at 870 mbsf rather than at the breccia at 850 mbsf). The second polarity change is at the transition from the Lower Massive Flows (Sequence VI) to the Upper Pillows and Flows (Sequence IV). Given the spreading rate estimate of 160 km/m.y. (and, therefore, the rate at which the volcanic sequences must have formed), the lavas appear to be recording extremely rapid polarity reversals of the magnetic field. The fields may be canceling each other out, resulting in the low-amplitude uncorrelated magnetic anomalies that characterize the JQZ. The causes and rates of these rapid reversals require further research. The volcanic glass, which is preserved in small amounts down the hole, will be used to evaluate the hypothesized low intensity of the magnetic field in the Jurassic, a phenomenon that is perhaps related to the rapid reversals.

SITE 1149 PRINCIPAL RESULTS

Site 1149: Early Cretaceous Seafloor Subducting at the Izu-Bonin Trench

Leg 185, Site 1149, Holes 1149A–1149D
Days on site: 23 May–13 June 1999

Hole 1149A

Latitude: 31°20.519'N
Longitude: 143°21.078'E
Water depth (m): 5818
Total cored section (mbsf): 0–191.2
Core recovery (%): 91

Hole 1149B

Latitude: 31°20.532'N
Longitude: 143°21.060'E
Water depth (m): 5818
Total cored section (mbsf): 160.6–445.2
Core recovery (%): 12

Hole 1149C

Latitude: 31°20.550'N
Longitude: 143°21.060'E
Water depth (m): 5818
Total cored section (mbsf): 283.6–322 and 388.2–426.7
Core recovery (%): 8.3

Hole 1149D

Latitude: 31°18.792'N
Longitude: 143°24.024'E
Water depth (m): 5867
Total cored section (mbsf): 272.2–440.4
Core recovery (%): 17

Introduction

Site 1149 was the first to be continuously cored through sediment to basement in the Nadezhda Basin, a ~1000 km × 1000 km region seaward of the Izu-Bonin Trench. The sediment/basement contact was cored in three Holes (1149B, 1149C, and 1149D), and a total of 133 m of basement penetration was achieved in Hole 1149D (Table T2). Thus, the site objectives to core and log the entire sedimentary sequence and to core the upper oxidative alteration zone in basement were successfully carried out after 20 days of operation. A presite seismic survey produced an excellent image of the seismic stratigraphy that will aid in correlating sedimentary units at Site 1149 across the Nadezhda Basin and along the Izu-Bonin Trench.

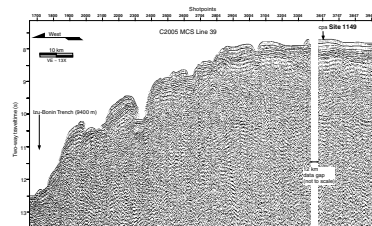
APC coring recovered ~100% of the uppermost 160 m in Hole 1149A, whereas a combination of XCB, MDCB, and RCB systems completed coring in the 410-m-thick sedimentary section in Holes 1149A and 1149B, albeit with much lower recovery rates (<15%). An excellent set of geophysical and geochemical logs from Hole 1149B will enable reconstruction of the sedimentary strata not recovered during coring. Holes 1149C and 1149D were drilled primarily to penetrate as much basement as time allowed. Only 26 m of basement was cored in Hole 1149C before chronic sticking problems prompted abandoning the hole. A thinner sedimentary section and a basement high were located on seismic Line C2005 ~5 km to the southeast of Holes 1149A, 1149B, and 1149C, where conditions were more promising for basement drilling. Despite some sticking and hole collapse problems, which slowed drilling and prevented logging of the basement section, 133 m of basement were successfully cored in Hole 1149D with 17% recovery. Site 1149 is one of only six other DSDP/ODP sites with significant (>100 m) penetration of basement into Mesozoic oceanic crust.

Geophysics

Site 1149 is located on the Pacific plate in the Nadezhda Basin southeast of Japan. It is on a slight bathymetric high ~100 km east of the Izu-Bonin Trench where the Pacific plate is flexed upward before it enters the subduction zone (Fig. F16). Although Nakanishi et al. (1992) identified magnetic Anomaly M12 in the vicinity of Site 1149, close inspection of the lineation pattern suggests instead that Site 1149 lies on the older portion of magnetic lineation M11. This stratigraphic position has a biostratigraphic age of late Valanginian and a radiometric age of ~132 Ma on the Channell et al. (1995) time scale. A model consistent with other portions of the magnetic lineation pattern of this age gives a constant spreading rate of 51 km/m.y. for this portion of the seafloor. These rates are comparable to the lower end of the range of spreading rates for the modern East Pacific Rise.

The seismic stratigraphy at Site 1149 is based on two 1976 vintage multichannel seismic lines and sonobuoy data obtained during Cruise

F16. MSC Line 39, p. 50.



C2005 of the *Robert D. Conrad*, as well as a short, presite single-channel seismic survey conducted aboard the *Resolution*. Site 1149 acoustic stratigraphy includes three or four seismic facies originally described by Ewing et al. (1968) for large portions of the western Pacific: (1) an upper transparent layer (weakly reflective), (2) an upper opaque layer (highly reflective or stratified), and (3) acoustic basement, or Horizon B. Early DSDP investigations (e.g., Legs 6, 7, 17, and 20) found that the upper transparent layer corresponds to a variety of lithofacies: pelagic clay with ash in the west Pacific, pelagic clay in the central Pacific, turbidite sequences in the north and east, and biogenic oozes along the equator. At Site 1149, this top acoustic layer corresponds to ash and diatom/radiolarian-bearing clay (Fig. F8). The upper opaque seismic layer has been correlated to the uppermost chert abundant in much of the North Pacific. Drilling at Site 1149 encountered this chert at ~180 mbsf, where it corresponds to a continuous, high-amplitude reflection at ~0.2 seconds below seafloor (sbsf). Within the opaque layer, there is a change in seismic character at ~0.28 sbsf to discontinuous, chaotic to hummocky reflections, which corresponds to a change from chert/clay to chert/chalk (+ marl) at Site 1149 (Fig. F8).

It was not until Legs 129 and 185 that material below Horizon B was sampled in the Mariana, Pigafetta, and Nadezhda Basins. Horizon B in large areas of the Nauru, Pigafetta, and East Mariana Basins correlates to mid-Cretaceous volcanic material (sills, flows, volcanogenic turbidites), and it was not clear if this material would be encountered at Horizon B or whether this would correspond to true oceanic basement. Weak and discontinuous reflections at ~0.7 sbsf in the original multichannel seismic (MCS) air-gun records at proposed site BON-10 also prompted concern that basement could lie as deep as 700 mbsf. The presite seismic survey with water guns, however, provided a clear image of a rough, undulating reflection characteristic of the top of oceanic crust at ~0.425 s (~420 mbsf at 2 km/s). Drilling in Holes 1149B and 1149C encountered oceanic basement at 410 and 401 mbsf, respectively, demonstrating that Horizon B in this portion of the Nadezhda Basin corresponds to true oceanic crust. Based on the few records available, the seismic stratigraphy of the Nadezhda Basin is laterally continuous and correlates well with the lithostratigraphy developed for Site 1149.

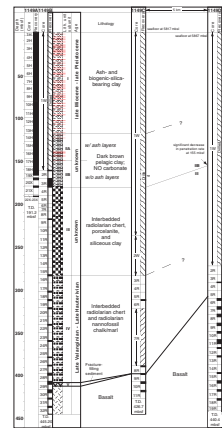
Sediments

The sedimentary section recovered at Site 1149 consists of carbonate-free clays with variable admixtures of volcanic ash and siliceous microfossils, cherts and porcelanites, and calcareous nannofossil chalks and marls. On the basis of the distribution of these lithologies, the sedimentary column above the basaltic crust has been divided from top to bottom into five lithologic units (Fig. F17):

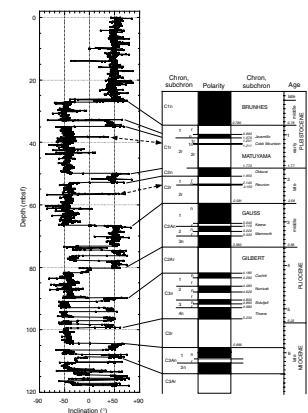
Unit I

Unit I (0–118.20 mbsf) consists of carbonate-free ash and diatom/radiolarian-bearing clay. Volcanic ash is present as both discrete ash layers and dispersed material throughout the sequence. Thickness of the discrete ash layers typically varies from a few millimeters to 5 cm; thicker layers (20–45 cm), however, are also present. As described below, dispersed ash accounts for 35%–50% of the sediment in Unit I. This unit has been dated late Miocene (i.e., 6.5 Ma) to late Pleistocene, based on an excellent magnetostratigraphic record (Fig. F18). Sedimentation

F17. Lithostratigraphic section, Site 1149, p. 51.



F18. Magnetic reversal stratigraphy, Site 1149, p. 52.



rates during deposition of Unit I as derived from the shipboard magnetostratigraphy were on the order of 18 m/m.y. (Fig. F19). The abundant assemblage of siliceous plankton, mainly diatoms, silicoflagellates, and radiolarians yield a preliminary age of Pliocene for Core 185-1149A-9H, in agreement with the paleomagnetic data.

Unit II

Unit II (118.20–179.1 mbsf in Hole 1149A; 160.6–180 mbsf in Hole 1149B) consists of undated dark brown pelagic clay with several discrete ash layers present only in the upper 30 m of the unit (Subunit IIA) and notable palygorskite in the lower half (Subunit IIB). Unit II clays are also noted by a change in porosity, pore-water chemistry, and bulk sediment chemistry. Clays from Unit II are barren of siliceous or calcareous microfossils, so their ages at this point remain undetermined. These clays, however, contain ichthyoliths that increase in abundance downhole, probably as a result of a decreased sedimentation rate. Shore-based analyses of the ichthyolith assemblages should allow for relative ages for this unit to be determined. Clays in Units I and II indicate pelagic deposition below the CCD.

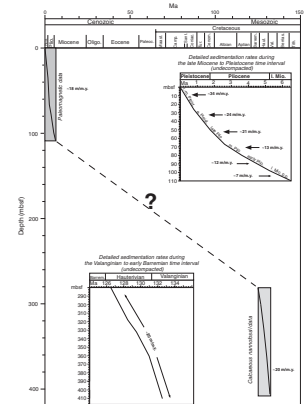
Unit III

The top of Unit III (180–191.2 mbsf in Hole 1149A; 180–282.30 mbsf in Hole 1149B) is marked by the first occurrence of indurated siliceous lithologies (i.e., chert and porcelanites). This unit is characterized by a very low recovery (<5%). The recovered sediments consist of radiolarian chert, porcelanite, and zeolitic clay, whose age is currently undetermined. These sediments are typical of a predominantly siliceous depositional environment, although the logging data indicate a high frequency of alternation of chert and clay.

Unit IV

Unit IV (282.30–416.40 mbsf) consists of radiolarian chert, porcelanite, marlstone, and chalk. Shipboard biostratigraphy of carbonates recovered in Cores 185-1149B-16R to 29R yielded well to poorly preserved calcareous nannofossil assemblages with average high diversity. Preliminary ages are the Hauterivian *Lithraphidites bollii* Zone from 311 to 340 mbsf (Core 185-1149B-16R to 21R). Downhole assemblages are dominated by *Watznaueria barnesae*, *Cruciellipsis cuvillieri*, and *Tubodiscus* sp. The first occurrence of *T. verenae* in Core 185-1149B-24R indicates the lowermost Hauterivian–uppermost Valanginian. *Rucinolithus wisei*, a species that may be restricted to the Valanginian, is present from Core 185-1149B-25R downhole. Persistence of *T. verenae* downhole to Core 185-1149B-29R confirms a Valanginian age for the base/sediment contact, consistent with the assigned M11 seafloor magnetic anomaly (132 Ma). The sedimentation rate during this time interval (i.e., 125.8 to ~132 Ma), derived from calcareous microfossil biostratigraphy, is ~20 m/m.y. (Fig. F19). Sediments from this lower unit were likely deposited when the site reached subequatorial paleolatitudes characterized by high primary productivity.

F19. Summary of sedimentation rates, Site 1149, p. 53.



Chemistry

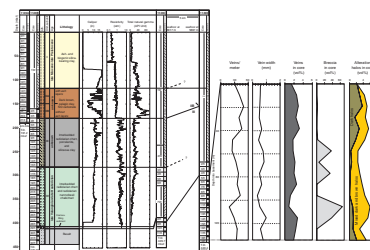
The relatively simple sedimentary sequence at Site 1149 provides an exceptional natural laboratory to examine diagenetic processes operating over a long time scale (~135 m.y.) in a sequence bounded by basaltic crust and the oceanic reservoir. The chemical components dissolved in interstitial waters recovered in sediment from the seafloor to the basement from Holes 1149A and 1149B reflect a low supply of organic matter, alteration of volcanic ash and authigenic clay formation at mid-depths, diagenesis of biogenic opal and carbonate, and ongoing basement alteration. Dissolved phosphate and ammonium have well-defined shallow maxima, although absolute concentrations are relatively low, reflecting low organic matter contents. Alkalinity remains <3 mM throughout the entire sequence, and sulfate is present at all depths (minimum value of 19 mM). The deep brown pelagic clays of Unit II define a sequence that is undergoing active authigenesis, acting as a sink for dissolved silica, strontium, and potassium, and as a source of alkalinity, ammonium, and lithium. X-ray diffraction (XRD) results and the concentration profile of dissolved silica together reflect the diagenetic transformations of opal-A to opal-CT (at ~180 mbsf) and of opal-CT to diagenetic quartz (at ~300 mbsf). Basement alteration and the relatively low diffusivity of Units IV and V lead to strong diffusive gradients in Ca and Mg, with extreme enrichments in Ca recorded (135 mM) in interstitial waters from a few meters above the basement contact (407 mbsf in Hole 1149B). Potassium and sodium uptake and high dissolved Cl (638 mM near basement) reflect hydration and alteration of the oceanic crust. These dramatic gradients and fluxes in the interstitial waters record ongoing alteration in the oceanic crust ~135 Ma after it formed.

Bulk chemical analyses of the sediments at Site 1149 corroborate several of the processes inferred from the interstitial-water results and also reveals others that are better recorded in the bulk solid phase (Fig. F20). In stratigraphic order, Site 1149 sediments preserve a well-developed metalliferous sedimentary profile in Fe/Al variations in the lower 130 m of the section (280–410 mbsf) (Fig. F21), which documents clearly the decreasing influence of hydrothermal plume precipitation with lateral distance from the ridge. The biogenic-rich sediment Units III and IV are high in Ba/Al, signaling an increase in biological export production as the site lingers near the paleoequator. Unit II pelagic clays are highly enriched in K₂O (>4 wt%), recording the K uptake inferred from the pore waters, possibly because of authigenic formation of K-rich zeolites. In addition to the discrete ash layers observed throughout Unit I and Subunit IIA, a depletion in Nb/Al with respect to average shales indicates a significant (35%–50%) dispersed ash component in the upper sediments. Shore-based studies will help to identify the source of these ashes, most probably from the Izu-Bonin or Japan volcanic arcs.

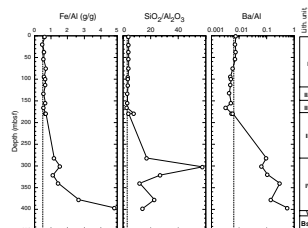
Logging

Downhole measurements in Hole 1149B were made after completion of drilling. Five logging runs were performed, consisting of one pass with the geophysical tool string, two passes with the geochemical string, and two passes with the Formation MicroScanner (FMS) sonic tool string. The logging data will be essential to reconstructing the sedimentary section, which suffered from 6% average recovery in Units III and IV. Over 90% of Site 1149 was logged or recovered. The geophysical string provided the most nearly complete logging run from ~10 m

F20. Summary of logging data, Site 1149, p. 54.



F21. Downhole variations in bulk sediment geochemistry, p. 55.



above the sediment/basement contact at ~400 mbsf (Core 185-1149B-28R) to within the clay–volcanic ash section at ~65 mbsf (Core 185-1149A-8H). The subsequent logs were limited by additional fill in the bottom of the hole and/or a 20-m-thick section of tight hole in the pelagic clays at 140–160 mbsf (Cores 185-1149A-16H to 18H) just above the uppermost cherts. Overall, the logging data agree well with the physical properties measurements and lithologic units identified from cored intervals (Fig. F20). Geophysical properties (e.g., resistivity, density, and *P*-wave velocity) accurately delineate the clay/ash layers, and the chert/clay layers. The NGT data identify regions predominantly composed of pelagic clay. The geochemical log data correlate Si-rich zones with chert layers, Ca-rich zones with the presence of nannofossil marls, and Al-rich zones with clay and ash layers. Calcium from the geochemical log is the best indicator of carbonate-rich sediment, a feature that is difficult for the other logs to distinguish.

In contrast to the East Mariana and Pigafetta Basin sediments subducting at the Mariana Trench, the Nadezhda Basin sediments subducting at the Izu-Bonin Trench lack a mid-Cretaceous volcanoclastic section and contain more siliceous and carbonate-rich biogenic material because of its longer passage beneath zones of high biological export production. Shore-based geochemical studies will demonstrate the extent to which these clear differences in sedimentary lithologies can be traced to the volcanic output from the two arc systems.

Basement

The sediment/basement boundary was recovered in three holes: at 410 mbsf in Hole 1149B, at 401 mbsf in Hole 1149C, and at 307 mbsf in Hole 1149D. Approximately 35 and 26 m of basement was drilled in Holes 1149B and 1149C, respectively, before hole conditions halted operations; a thinner sedimentary sequence in Hole 1149D may have contributed to better hole conditions there, where 133 m of basement was drilled. The contact zone between the sediments and basement in Hole 1149B is brecciated and filled with interfragment sediment. Igneous units in all three holes consist of aphyric basalt pillows, thin flows, and interpillow breccia. Cooling units are on average <50 cm thick, in contrast with Hole 801C, where the cooling unit thicknesses averaged >50 cm. The predominance of these thin, fractured, and brecciated units at Site 1149 may have contributed to the overall low recovery of basalt (<20%). Plagioclase and olivine phenocrysts are rare (usually <1%). Most basaltic glass has been highly altered; fresh glass exists on a few pieces (~10), most of which are in Core 185-1149D-9R. The chemical compositions of the least altered lavas in Hole 1149B are fairly primitive (>7.9 wt% MgO) and low in Fe₂O₃ (<10 wt%). The upper sections are N-MORBs, whereas the lowermost flows (Unit 6) are enriched (E) MORBs. This igneous section is typical of MORBs from the modern East Pacific Rise.

The volcanic rocks at Site 1149 have a spectacular pervasive dusky red alteration, which commonly displays a light gray to brown mottling. Complex, multicolored alteration halos also are present along fractures and other surfaces that were exposed to circulating fluids. The halos are up to 2 cm wide and range in color from brown to dark green. In addition to the plentiful alteration halos, another striking feature of the basalt from all three holes is an abundance of reddish fracture surfaces. In general, the alteration is more intense at Site 1149 than at Site 801. At Site 1149, alteration halos comprise 34 vol% of the recovered

basalts, as opposed to ~2 vol% at Site 801 (Fig. F20). Veining is also more intense, with 35 veins/m at Site 1149 compared to ~25 veins/m at Site 801. Finally, flow breccias and hyaloclastites are a common feature in the cored interval at Site 1149, whereas, unlike Hole 801C, massive flows and interpillow sediments are uncommon. The more intense alteration at Site 1149 may lead to greater overall budgets for K than at Site 801 (e.g., >0.3 wt% K₂O).

Although Hole 1149D was drilled in a basement high, the recovered basalts are similar in their igneous and alteration characteristics to Holes 1149B and 1149C basalts, with the exception of the E-MORB unit in the bottom 30 m of Hole 1149D. Nonetheless, the common occurrence of similar N-MORB at the top of each hole suggests that the basement topography near Hole 1149D is probably related to near-ridge processes, such as abyssal hill formation, rather than off-axis constructional magmatism.

DEEP BIOSPHERE

The fascinating possibility that microbial activity may inhabit oceanic crust as old and as deep as that at Site 801 provided the motivation for sampling the seafloor in the search for extremophilic life. Water, sediment, and rock samples were collected to determine cell abundance and community composition. Samples were examined microscopically and used to establish cultures and to extract and characterize DNA. Sample protocols were established and tracer tests conducted to determine the extent of microbial contamination potentially introduced during drilling and sample preparation.

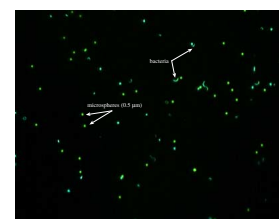
Shipboard Sampling

Water samples were collected to determine background microbial populations potentially introduced in the drilling process. Water samples were collected from the drill pipe and from the sea surface (from the z-boat) upwind of the *Resolution*. Undisturbed water in Hole 801C may be an excellent in situ microbial culture and was thus sampled using the water-sampling temperature probe (WSTP) prior to Leg 185 drilling; ~300 mL of water was recovered from a depth of 540 m in the hole.

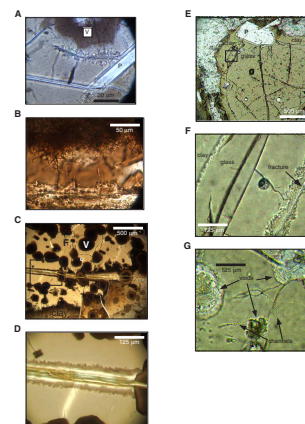
A series of samples of different rock types was collected for culturing, total cell counts, and DNA and adenosine triphosphate (ATP) analyses. Figure F22 shows an example of a bacterial population from surface seawater with fluorescent microspheres traces. Samples of basement rocks, including glass samples, were (1) taken and transported to an anaerobic chamber where they were cracked open to obtain interior pieces used to inoculate cultures and (2) used for shore-based microscopic analyses and DNA extraction. Cultures have also been started at in situ pressure (620–650 atm), and some samples have been stored under pressure for shore-based analyses.

Hole 801C and, to a lesser extent, volcanic rocks from Site 1149 preserve small amounts (several grams to a few grains) of fresh basaltic glass. These samples were studied microscopically for traces of microbial activity. Several samples preserve filament-like textures that are identical to textures attributed to microbes in deep-sea basalt from young oceanic pillow basalt (see Fig. F23 and Thorseth et al., 1992; Fisk et al., 1998; Furnes and Staudigel, 1999). Whether these textures are

F22. Example of a contaminated bacterial population, p. 56.



F23. Photomicrographs of glass, Hole 801C, p. 57.



trace fossils of past microbial activity or signs of extant microbes living in this high-pressure seafloor environment remains a fascinating subject of shore-based study.

Tracer Tests

Great strides in the study of the deep biosphere have been made using samples collected during previous drilling (e.g., Oremland et al., 1982; Whelan et al., 1986; Thorseth et al., 1992; Parkes et al., 1994; Griffin et al., 1997; Fisk et al., 1998). The drilling capabilities and extensive areas of operation of the *Resolution* give unparalleled access to samples from this environment. Critical to conducting research in the deep biosphere is the capability to core and retrieve samples without contaminating the samples with nonindigenous microbes. During Leg 185, we conducted the first extensive experiments on the *Resolution* to explicitly assess the suitability of this platform for sampling the deep biosphere.

Two types of tests were conducted to quantify the potential contamination. Particulate tracers (0.5- μm -diameter fluorescent microspheres) were introduced into the core barrel at a concentration of $\sim 10^{10}$ spheres/mL and quantified in recovered cores using epifluorescence microscopy. In addition, a chemical tracer (perfluoro[methylcyclohexane]) was added to the drilling fluid (surface seawater) to produce a 1-ppm solution. Gas chromatography was used to quantify the tracer in recovered cores. Cores were collected with the APC in unconsolidated sediments at Hole 1149A and with the DCB and RCB in sedimentary and igneous rock at Sites 801 and 1149.

Detection of the tracers on the exterior of the cores confirmed successful delivery. Contamination was low in the unconsolidated sediment cores using the APC. Spheres were never detected in the interiors of these cores ($N = 24$). The average concentration of the perfluorocarbon ($N = 12$) was equivalent to 0.03 μL of drilling fluid per gram of sediment. Contamination was also low in the igneous rock samples cored with the RCB. Spheres were not found in the interiors of igneous rock samples that were crushed ($N = 4$) but appeared in the interiors of 64% of the thin sections examined ($N = 12$). This suggests that the samples were contaminated during sectioning rather than drilling. Drilling fluid in the igneous rock samples averaged 0.01 $\mu\text{L/g}$ rock. Based on the abundance of bacteria in the surface seawater (4.2×10^8 cells/L), the potential contamination of both sample types is on the order of 1–10 cells/g of cored material.

The tracer techniques adapted for use on the *Resolution* are a sensitive means of evaluating microbial contamination in deep-sea cores and should be deployed in the future when microbiological samples are collected. The perfluorocarbon tracer is also useful for evaluating the incursion of drilling fluid into pore-water samples. The methods used in these tests are described in detail in “[Methods for Quantifying Potential Microbial Contamination during Deep Ocean Coring](#)” (Smith et al., 2000) so that they may be routinely employed when coring for samples to be used in microbiological research in future ODP legs.

SUMMARY

The operational and scientific objectives of Leg 185 were achieved. Two sites were drilled in deep water and into the oldest crust of the Pa-

cific Ocean (Figs. F24, F9). Hole 801C in the Pigafetta Basin was reentered and deepened in order to drill the upper oxidative alteration zone in basement. Four holes at Site 1149 in the Nadezhda Basin were drilled through sediment and into basement in order to characterize seafloor subducting at the Izu-Bonin Trench. In addition to satisfying these basic drilling objectives, the Leg 185 scientific party achieved a number of scientific goals.

Legacy Site into Pacific Jurassic Crust

Hole 801C was deepened by 340 m, providing a total basement section of 470 m, making it the sixth deepest ODP or DSDP site into normal oceanic crust. We exceeded our conservative drilling objective, to deepen the hole by 250 m. Recovery was very good (47%), and a high quality set of logs was run to 388 m in basement. Hole 801C is the only site to drill into Jurassic Pacific oceanic crust. The hole is in good condition and remains a legacy site into the Earth's oldest oceanic crust. Hole 801C is an important geochemical, geophysical, and biological reference site into old (~170 Ma), fast-spreading crust. The basalts from Hole 801C have been sampled using a coordinated strategy to develop a common set of samples for all geochemical investigators, as well as composite samples, which will be another legacy of the site. This is a novel approach, which will lead to an unprecedented geochemical data set for this unique section of oceanic crust.

Complete Sedimentary Sequence in the Nadezhda Basin, Western Pacific

Drilling at Site 1149 satisfied a primary objective of providing the first complete section through the pelagic sediments (~400 m) of the Nadezhda Basin, a ~1000 km × 1000 km region in the western Pacific. More than 90% of the sedimentary section was either recovered or logged. Thus, Site 1149 is an important reference site for Mesozoic equatorial sedimentation from the upper Valanginian and for sediment that is being subducted along the 1000-km Izu-Bonin Trench.

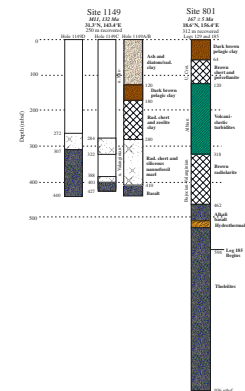
Early Cretaceous Seafloor Subducting at the Izu-Bonin Trench

Basement drilling at Site 1149 achieved significant (133 m) penetration into Anomaly M11 (132-Ma oceanic crust), ranking this as one of the few ODP sites to drill >100 m into Mesozoic oceanic crust. Consequently, Site 1149 will serve as an important reference site for fast-spreading, Mesozoic Pacific crust (102 mm/yr full rate) and its associated alteration and igneous composition as it subducts at the Izu-Bonin Trench.

Mass Balance Equation for Crustal Recycling at the Mariana Arc

After drilling Hole 801C, the remaining piece of the crustal input inventory is complete for the Mariana subduction factory. Shore-based geochemical analyses of the basement section in Hole 801C will provide the first robust estimates for any subducting oceanic crust. Sediment and basement input fluxes will then be compared to volcanic

F24. Lithostratigraphic summary of Leg 185 holes, p. 59.



outputs at the Mariana arc and backarc. The basaltic inventory for K, U, Ba, CO₂, and H₂O will provide not only seawater-basalt fluxes but also crust-mantle fluxes for these key tracers and volatiles.

Comparisons of the Input and the Output at the Mariana and Izu Arcs

Having provided the first continuous sedimentary section to basement of sediments subducting along the Izu-Bonin margin, Leg 185 data enable comparison of the inputs to the Mariana and Izu arcs. In contrast to the sediments subducting at the Mariana Trench, the Nadezhda Basin sediments subducting at the Izu-Bonin Trench lack a mid-Cretaceous volcanoclastic section and contain more siliceous and carbonate-rich biogenic material because of the longer passage beneath zones of high biological export production. Shore-based geochemical studies will demonstrate the extent to which these different sedimentary histories can be traced to the volcanic output from the two arc systems. For example, does the sedimentary and basaltic input on the incoming plate provide suitable Pb isotope mixing end-members for the Izu arc volcanics, or are other mantle and upper plate sources required? Does the extensive biogenic section in the lower half of Site 1149, which has very low concentrations of alkali elements, contribute to the low alkali content of the Izu arc? The coordinated shipboard sampling and analytical effort organized by Leg 185 scientists will provide an unprecedented geochemical data set (major elements, trace elements, and Pb, Nd, Sr, Os, Hf, Li, B, Be, Cl, Se, C, N, O, H, and S isotopes) of crustal inputs to the two subduction factories.

Jurassic Quiet Zone

Hole 801C Jurassic basement records up to six geomagnetic reversals. There are several reversals, and some sections preserve gradual changes in the magnetic field direction from one polarity interval to the other. Therefore, igneous basement at Hole 801C was extruded at a time of rapid polarity alternations of the geomagnetic field. These data may provide an explanation for the JQZ in a series of superposed flows with opposite polarity, essentially canceling out one another. The presence of fresh basaltic glass at various depths in Hole 801C will also provide suitable material for paleointensity studies, to test the hypothesis that the JQZ was a time of low geomagnetic field intensity.

Deep Biosphere

Leg 185 was the first ODP leg to invest a significant effort in conducting microbial contaminant tests, equipping a microbiology laboratory, and establishing techniques for core handling of biological samples. Contaminant tests using perfluorocarbon and fluorescent microsphere tracers demonstrated that sediments cored with the APC showed less susceptibility to contamination than those cored with RCB. Several APC core interiors were free of contaminants, and RCB coring resulted in the presence of chemical, but not particulate, tracers in the interior of the cores. These tests, which demonstrate that potential biological contamination can be assessed and surmounted, pave the way for establishing ODP as a new platform for microbiological studies. Leg 185 samples were used to start culturing experiments in various media at

both atmospheric and in situ pressures and for shore-based DNA extraction and community characterization. Several glass samples from Hole 801C show textural evidence for microbial alteration and prompt the intriguing question of whether there is current microbiological activity in ~170-Ma volcanic basement.

Calibrating Magnetic Anomaly M11

Based on a re-evaluation of existing seafloor magnetic anomaly lineations, Site 1149 lies in crust of Anomaly M11, which is consistent with the presence of *T. veranae* found in the basal core in Hole 1149B. Obtaining a radiometric date on the basement at Site 1149 could provide a reasonably precise date of Anomaly M11 and help to refine the time scale during this age near the breakup of Gondwana.

Mesozoic and Cenozoic Pelagic Sequences

The equatorial paleolatitude history of Site 1149 during the mid-Cretaceous, combined with a predictable subsidence history, is ideal for testing variations in the Cretaceous CCD. Site 1149 sediments record a well-developed metalliferous sedimentary profile, which clearly documents the decreasing influence of plume precipitation with lateral distance from the ridge. Very high sediment accumulation rates (~30 m/m.y.) and the mineral composition of the youngest sediments suggest that Site 1149 was in the reach of the Asian dust plumes after the early Pleistocene.

Petrology of Mesozoic Crust

Fresh basaltic glass was recovered from both Site 1149 and Site 801, providing pristine samples of the igneous liquid that forms Mesozoic Pacific crust. These valuable samples record mid-ocean ridge processes, mantle composition, and mantle temperature at a time preceding the Cretaceous superplume event in the Pacific.

Architecture of Fast-Spreading Crust

Sites 801 and 1149 provide the first sections into Mesozoic fast-spreading crust, Layer 2A. Geochemical alteration of the volcanic section in Hole 801C is found in several discrete zones associated with ocherous Si-Fe-hydrothermal deposits and tectonic breccia. These zones control the alteration pattern of crust and contrast with “accepted” models for a gradual decrease downhole in the oxidative alteration of oceanic basement. The pattern of alteration at Site 801, controlled by local pathways for hydrothermal fluids, may be a feature of fast-spreading crust.

Continued Diffusive Exchange between Basement and Sediments

Although it is generally accepted that there is diffusive exchange between interstitial waters in the volcanic section of oceanic crust and the overlying sediments, the organic-poor nature of the sediments at Site 1149 allows modeling of S and metal budgets between basement and sediments, as well as assessing the potential for bacteria in the basement to affect the redox state of the overlying sediments.

REFERENCES

- Abrams, L.J., Larson, R.L., Shipley, T.H., and Lancelot, Y., 1992. The seismic stratigraphy and sedimentary history of the East Mariana and Pigafetta basins of the western Pacific. *In* Larson, R.L., Lancelot, Y., et al., *Proc. ODP, Sci. Results*, 129: College Station, TX (Ocean Drilling Program), 551–569.
- Alt, J.C., France-Lanord, C., Floyd, P.A., Castillo, P., and Galy, A., 1992. Low-temperature hydrothermal alteration of Jurassic ocean crust, Site 801. *In* Larson, R.L., Lancelot, Y., et al., *Proc. ODP, Sci. Results*, 129: College Station, TX (Ocean Drilling Program), 415–427.
- Alt, J.C., Honnorez, J., Laverne, C., and Emmermann, R., 1986. Hydrothermal alteration of a 1 km section through the upper oceanic crust, Deep Sea Drilling Project Hole 504B: mineralogy, chemistry, and evolution of seawater-basalt interactions. *J. Geophys. Res.*, 91:10309–10335.
- Alt, J.C., and Teagle, D.A.H., 1999. The uptake of carbon during alteration of ocean crust. *Geochim. Cosmochim. Acta*, 63:1527–1535.
- Arculus, R.J., Gill, J.B., Cambray, H., Chen, W., and Stern, R.J., 1995. Geochemical evolution of arc systems in the western Pacific: the ash and turbidite record recovered by drilling. *In* Taylor, B., and Natland, J. (Eds.), *Active Margins and Marginal Basins of the Western Pacific*. Am. Geophys. Union, 88:45–65.
- Armstrong, R.L., 1968. A model for Sr and Pb isotopic evolution in a dynamic earth. *Rev. Geophys.*, 6:175–191.
- Arthur, M.A., Dean, W.E., Schlanger, S.O., 1985. Variations in the global carbon cycle during the Cretaceous related to climate, volcanism, and changes in atmospheric CO₂. *In* Sundquist, E.T., and Broecker, W.S. (Eds.), *The Carbon Cycle and Atmospheric CO₂: Natural Variations Archean to Present*. Geophys. Monogr., Am. Geophys. Union, 32:504–529.
- Carbotte, S.M., Mutter, J.C., and Xu, L., 1997. Contribution of volcanism and tectonism to axial and flank morphology of the southern East Pacific Rise, 17°10'–17°40'S, from a study of layer 2A geometry. *J. Geophys. Res.*, 102:10165–10184.
- Castillo, P.R., Floyd, P.A., France-Lanord, C., and Alt, J.C., 1992. Data report: Summary of geochemical data for Leg 129 igneous rocks. *In* Larson, R.L., Lancelot, Y., et al., *Proc. ODP, Sci. Results*, 129: College Station, TX (Ocean Drilling Program), 653–670.
- Channell, J.E.T., Erba, E., Nakanishi, M., and Tamaki, K., 1995. Late Jurassic–Early Cretaceous time scales and oceanic magnetic anomaly block models. *In* Berggren, W.A., et al. (Eds.), *Geochronology, Time Scales and Global Stratigraphic Correlation*. Spec. Publ.—Soc. Econ. Paleontol. Mineral., 54:51–63.
- Detrick, R., Collins, J., Stephen, R., and Swift, S., 1994. *In situ* evidence for the nature of the seismic layer 2/3 boundary in oceanic crust. *Nature*, 370:288–290.
- Elliott, T., Plank, T., Zindler, A., White, W., and Bourdon, B., 1997. Element transport from subducted slab to volcanic front at the Mariana Arc. *J. Geophys. Res.*, 102:14991–15019.
- Erba, E., 1992. Middle Cretaceous calcareous nannofossils from the western Pacific (Leg 129): evidence for paleoequatorial crossings. *In* Larson, R.L., Lancelot, Y., et al., *Proc. ODP, Sci. Results*, 129: College Station, TX (Ocean Drilling Program), 189–201.
- Ewing, J., Ewing, M., Aitken, T., and Ludwig, W.J., 1968. North Pacific sediment layers measured by seismic profiling. *In* Knopoff, L., Drake, C.L., and Hart, P.J. (Eds.), *The Crust and Upper Mantle of the Pacific Area*. Geophys. Monogr., Am. Geophys. Union., 12:147–173.
- Fisk, M.R., Giovannoni, S.J., and Thorseth, I.H., 1998. Alteration of oceanic volcanic glass: textural evidence of microbial activity. *Science*, 281:978–980.

- Floyd, P.A., and Castillo, P.R., 1992. Geochemistry and petrogenesis of Jurassic ocean crust basalts, Site 801. *In* Larson, R.L., Lancelot, Y., et al., *Proc. ODP, Sci. Results*, 129: College Station, TX (Ocean Drilling Program), 361–388.
- Floyd, P.A., Winchester, J.A., and Castillo, P.R., 1992. Geochemistry and petrography of Cretaceous sills and lava flows, Sites 800 and 802. *In* Larson, R.L., Lancelot, Y., et al., *Proc. ODP, Sci. Results*, 129: College Station, TX (Ocean Drilling Program), 345–359.
- Francheteau, J., Armijo, R., Cheminée, J.L., Hekinian, R., Lonsdale, P., and Blum, N., 1992. Dyke complex of the East Pacific Rise exposed in the walls of Hess Deep and the structure of the upper oceanic crust. *Earth Planet. Sci. Lett.*, 111:109–121.
- Fryer, P., 1992. A synthesis of Leg 125 drilling of serpentine seamounts on the Mariana and Izu-Bonin forearcs. *In* Fryer, P., Pearce, J.A., Stokking, L.B., et al., *Proc. ODP, Sci. Results*, 125: College Station, TX (Ocean Drilling Program), 593–614.
- Furnes, H., and Staudigel, H., 1999. Biological mediation in ocean crust alteration: how deep is the deep biosphere? *Earth Planet. Sci. Lett.*, 166:97–103.
- Gill, J.B., Hiscott, R.N., and Vidal, P., 1994. Turbidite geochemistry and evolution of the Izu-Bonin arc and continents. *Lithos*, 33:135–168.
- Gillis, K.M., 1995. Controls on hydrothermal alteration in a section of fast spreading oceanic crust. *Earth Planet. Sci. Lett.*, 134:473–489.
- Gillis, K.M., Ludden, J.N., Plank, T., and Hoy, L.D., 1992. Low-temperature alteration and subsequent reheating of shallow oceanic crust at Hole 765D, Argo Abyssal Plain. *In* Gradstein, F.M., Ludden, J.N., et al., *Proc. ODP, Sci. Results*, 123: College Station, TX (Ocean Drilling Program), 191–199.
- Gradstein, F.M., Agterberg, F.P., Ogg, J.G., Hardenbol, J., van Veen, P., Thierry, J., and Huang, Z., 1994. A Mesozoic time scale. *J. Geophys. Res.*, 99:24051–24074.
- Griffin, W.T., Phelps, T.J., Colwell, F.S., and Fredrickson, J.K., 1997. Methods for obtaining deep subsurface microbiological samples by drilling. *In* Amy, P.S., and Haldeman, D.L. (Eds.), *The Microbiology of the Terrestrial and Deep Subsurface*. Boca Raton (CRC Press, Lewis Publishers), 23–43.
- Haggerty, J.A., Premoli Silva, I., Rack, F., and McNutt, M.K. (Eds.), 1995. *Proc. ODP, Sci. Results*, 144: College Station, TX (Ocean Drilling Program).
- Harland, W.B., Armstrong, R.L., Cox, A.V., Craig, L.E., Smith, A.G., and Smith, D.G., 1990. *A Geologic Time Scale 1989*: Cambridge (Cambridge Univ. Press).
- Hawkesworth, C.J., Turner, S.P., McDermott, F., Peate, D.W., and van-Calsteren, P., 1997. U-Th isotopes in arc magmas: implications for element transfer from the subducted crust. *Science*, 276:551–555.
- Haymon, R.M., Fornari, D.J., Edwards, M.H., Carbotte, S.M., Wright, D., and Macdonald, K.C., 1991. Hydrothermal vent distribution along the East Pacific Rise crest (9°09′–54°N) and its relationship to magmatic and tectonic processes on fast-spreading mid-ocean ridges. *Earth Planet. Sci. Lett.*, 104:513–534.
- Hofmann, A., 1997. Mantle geochemistry: the message from oceanic volcanism. *Nature*, 385:219–229.
- Ikeda, Y., and Yuasa, M., 1989. Volcanism in nascent back-arc basins behind the Shichito Ridge and adjacent areas in the Izu-Ogasowara arc, Northwest Pacific: evidence for mixing between E-type MORB and island arc magmas at the initiation of back-arc rifting. *Contrib. Mineral. Petrol.*, 101:377–393.
- Karig, D.E., and Kay, R.W., 1981. Fate of sediments on the descending plate at convergent margins. *Philos. Trans. R. Soc. London*, 301:233–251.
- Karl, S.M., Wandless, G.A., and Karpoff, A.M., 1992. Sedimentological and geochemical characteristics of Leg 129 siliceous deposits. *In* Larson, R.L., Lancelot, Y., et al., *Proc. ODP, Sci. Results*, 129: College Station, TX (Ocean Drilling Program), 31–79.
- Kimura, G., Silver, E.A., Blum, P., et al., 1997. *Proc. ODP, Init. Repts.*, 170: College Station, TX (Ocean Drilling Program).
- Lancelot, Y., Larson, R.L., et al., 1990. *Proc. ODP, Init. Repts.*, 129: College Station, TX (Ocean Drilling Program).

- Langmuir, C., 1987. Testing the relationship between MORB chemistry and axial depth: new data from the Mid-Atlantic Ridge between the Kane and Hayes Fracture Zones. *Eos*, 68:1540.
- Langmuir, C.H., Bender, J.F., and Batiza, R., 1986. Petrological and tectonic segmentation of the East Pacific Rise, 5°30'N–14°30'N. *Nature*, 322:422–429.
- Larson, R.L., Fisher, A.T., Jarrard, R.D., Becker, K., and Ocean Drilling Program Leg 144 Shipboard Scientific Party, 1993. Highly permeable and layered Jurassic oceanic crust in the western Pacific. *Earth Planet. Sci. Lett.*, 119:71–83.
- Larson, R.L., and Sager, W.W., 1992. Skewness of magnetic anomalies M0 to M29 in the northwestern Pacific. In Larson, R.L., Lancelot, Y., et al., *Proc. ODP, Sci. Results*, 129: College Station, TX (Ocean Drilling Program), 471–481.
- McLennan, S.M., 1988. Recycling of the continental crust. *Pure Appl. Geophys.*, 128:683–724.
- Morris, E.L., Tanner, I., Meyerhoff, H.A., and Meyerhoff, A.A., 1990. Tectonic evolution of the Caribbean region: alternative hypothesis. In Dengo, G., and Case, J.E. (Eds.), *The Caribbean Region*. Geol. Soc. Am., Geol. of North Am. Ser., H:433–457.
- Nakanishi, M., Tamaki, K., and Kobayashi, K., 1989. Mesozoic magnetic anomaly lineations and seafloor spreading history of the Northwestern Pacific. *J. Geophys. Res.*, 94:15437–15462.
- , 1992. Magnetic anomaly lineations from Late Jurassic to Early Cretaceous in the west-central Pacific Ocean. *Geophys. J. Int.*, 109:701–719.
- Oremland, R.S., Culbertson, C., and Simoneit, B.R.T., 1982. Methanogenic activity in sediment from Leg 64, Gulf of California. In Curray, J.R., Moore, D.G., et al., *Init. Repts. DSDP*, 64 (Pt. 2): Washington (U.S. Govt. Printing Office), 759–762.
- Parkes, R.J., Cragg, B.A., Bale, S.J., Getliff, J.M., Goodman, K., Rochelle, P.A., Fry, J.C., Weightman, A.J., and Harvey, S.M., 1994. A deep bacterial biosphere in Pacific Ocean sediments. *Nature*, 371:410–413.
- Perfit, M.R., and Chadwick, W.W., 1998. Magmatism at mid-oceanic ridges: constraints from volcanological and geochemical investigations. *Geophys. Monogr., Am. Geophys. Union.*, 106:50–115.
- Pick, T., and Tauxe, L., 1993. Geomagnetic paleointensities during the Cretaceous normal superchron measured using submarine basaltic glass. *Nature*, 366:238–242.
- Plank, T., and Langmuir, C.H., 1993. Tracing trace elements from sediment input to volcanic output at subduction zones. *Nature*, 362:739–743.
- , 1998. The chemical composition of subducting sediment and its consequences for the crust and mantle. *Chem. Geol.*, 145:325–494.
- Plank, T., and Ludden, J.N., 1992. Geochemistry of sediments in the Argo Abyssal Plain at Site 765: a continental margin reference section for sediment recycling in subduction zones. In Gradstein, F.M., Ludden, J.N., et al., *Proc. ODP, Sci. Results*, 123: College Station, TX (Ocean Drilling Program), 167–189.
- Plank, T., Stern, R., and Morris, J., 1998. The subduction factory science plan, MARGINS Program. *Nat. Sci. Found.* <<http://www.soest.hawaii.edu/margins/SubFac.html>>
- PLATES Project, 1998. Atlas of paleogeographic reconstructions (PLATES Progress Report No. 215), *Univ. Texas Inst. Geophys. Tech. Rep.*, 181.
- Pringle, M.S., 1992. Radiometric ages of basaltic basement recovered at Sites 800, 801, and 802, Leg 129, western Pacific Ocean. In Larson, R.L., Lancelot, Y., et al., *Proc. ODP, Sci. Results*, 129: College Station, TX (Ocean Drilling Program), 389–404.
- Reymer, A., and Schubert, G., 1984. Phanerozoic addition rates to the continental crust and crustal growth. *Tectonics*, 3:63–77.
- Roth, P.H., 1981. Mid-Cretaceous calcareous nannoplankton from the central Pacific: implication for paleoceanography. In Thiede, J., Vallier, T.L., et al., *Init. Repts. DSDP*, 62: Washington (U.S. Govt. Printing Office), 471–489.
- Sager, W.W., and Pringle, M.S., 1988. Mid-Cretaceous to Early Tertiary apparent polar wander path of the Pacific Plate. *J. Geophys. Res.*, 93:11753–11771.

- Smith, D.C., Spivack, A.J., Fisk, M.R., Haveman, S.A., Staudigel, H., and the Leg 185 Shipboard Scientific Party, 2000. Methods for quantifying potential microbial contamination during deep ocean coring. *ODP Tech. Note*, 28 [Online]. Available from World Wide Web: <<http://www-odp.tamu.edu/publications/tnotes/tn28/INDEX.HTM>>. [Cited 2000-05-23]
- Smith, W.H.F., and Sandwell, D.T., 1997. Global seafloor topography from satellite altimetry and ship depth soundings. *Science*, 277:1956–1962.
- Smith, W.H.F., and Wessel, P., 1990. Gridding with continuous curvature splines in tension. *Geophysics*, 55:293–305.
- Staudigel, H., Albarede, F., Blichert-Toft, J., Edmond, J., McDonough, W., Jacobsen, S., Keeling, R., Langmuir, C., Nielsen, R., Plank, T., Rudnick, R., Shaw, H., Shirey, S., Veizer, J. and White, W., 1998. Geochemical Earth Reference Model (GERM): description of the initiative. *Chem. Geol.*, 145:153–160.
- Staudigel, H., Davies, G.R., Hart, S.R., Marchant, K.M., and Smith, B.M., 1995. Large scale Sr, Nd, and O isotopic anatomy of altered oceanic crust: DSDP Sites 417/418. *Earth Planet. Sci. Lett.*, 130:169–185.
- Staudigel, H., Kastner, M., and Sturz, A., 1986. ^{18}O and $^{87}\text{Sr}/^{86}\text{Sr}$ of calcites from the basaltic basement of Deep Sea Drilling Project Site 597: timing and temperature of alteration. In Leinen, M., Rea, D.K., et al., *Init. Repts. DSDP*, 92: Washington (U.S. Govt. Printing Office), 499–503.
- Stein, C.A., and Stein, S., 1994. Constraints on hydrothermal heat flux through the oceanic lithosphere from global heat flow. *J. Geophys. Res.*, 99:3081–3095.
- Stern, R.J., Lin, P.-N., Morris, J.D., Jackson, M.C., Fryer, P., Bloomer, S.H., and Ito, E., 1990. Enriched back-arc basin basalts from the northern Mariana Trough: implications for the magmatic evolution of back-arc basins. *Earth Planet. Sci. Lett.*, 100:210–225.
- Tatsumi, Y., Murasaki, M., and Nodha, S., et al., 1992. Across-arc variations of lava chemistry in the Izu-Bonin Arc. *J. Volcanol. Geotherm. Res.*, 49:179–190.
- Taylor, B., 1992. Rifting and the volcanic-tectonic evolution of the Izu-Bonin-Mariana arc. In Taylor, B., Fujioka, K., et al., *Proc. ODP, Sci. Results*, 126: College Station, TX (Ocean Drilling Program), 627–651.
- Taylor, R.N., and Nesbitt, R.W., 1998. Isotopic characteristics of subduction fluids in an intra-oceanic setting, Izu-Bonin Arc. *Earth Planet. Sci. Lett.*, 164:79–98.
- Thierstein, H.R., 1979. Paleoceanographic implications of organic carbon and carbonate distribution in Mesozoic deep sea sediments. In Talwani, M., Hay, W., and Ryan, W.B.F. (Eds.), *Deep Drilling Results in the Atlantic Ocean*. Am. Geophys. Union, Maurice Ewing Ser., 3:249–274.
- Thorseth, I.H., Furnes, H., and Heldal, M., 1992. The importance of microbiological activity in the alteration of natural basaltic glass. *Geochim. Cosmochim. Acta*, 56:845–850.
- Thorseth, I.H., Torsvik, T., Furnes, H., and Muehlenbachs, K., 1995. Microbes play an important role in the alteration of oceanic crust. *Chem. Geol.*, 126:137–146.
- Van der Hilst, R.D., Widiyantoro, S., and Engdahl, E.R., 1997. Evidence for deep mantle circulation from global tomography. *Nature*, 386:578–584.
- Wessel and Smith, 1995. New version of the Generic Mapping Tools released. *Eos*, 76:329.
- Whelan, J.K., Oremland, R., Tarafa, M., Smith, R., Howarth, R., and Lee, C., 1986. Evidence for sulfate-reducing and methane producing microorganisms in sediments from Sites 618, 619, and 622. In Bouma, A.H., Coleman, J.M., Meyer, A.W., et al., *Init. Repts. DSDP*, 96: Washington (U.S. Govt. Printing Office), 767–775.
- Woodhead, J.D., and Fraser, D.G., 1985. Pb, Sr, and ^{10}Be isotopic studies of volcanic rocks from the Northern Mariana Islands: implications for magma genesis and crustal recycling in the western Pacific. *Geochim. Cosmochim. Acta*, 49:1925–1930.

Figure F1. Input to and output from "The Subduction Factory."

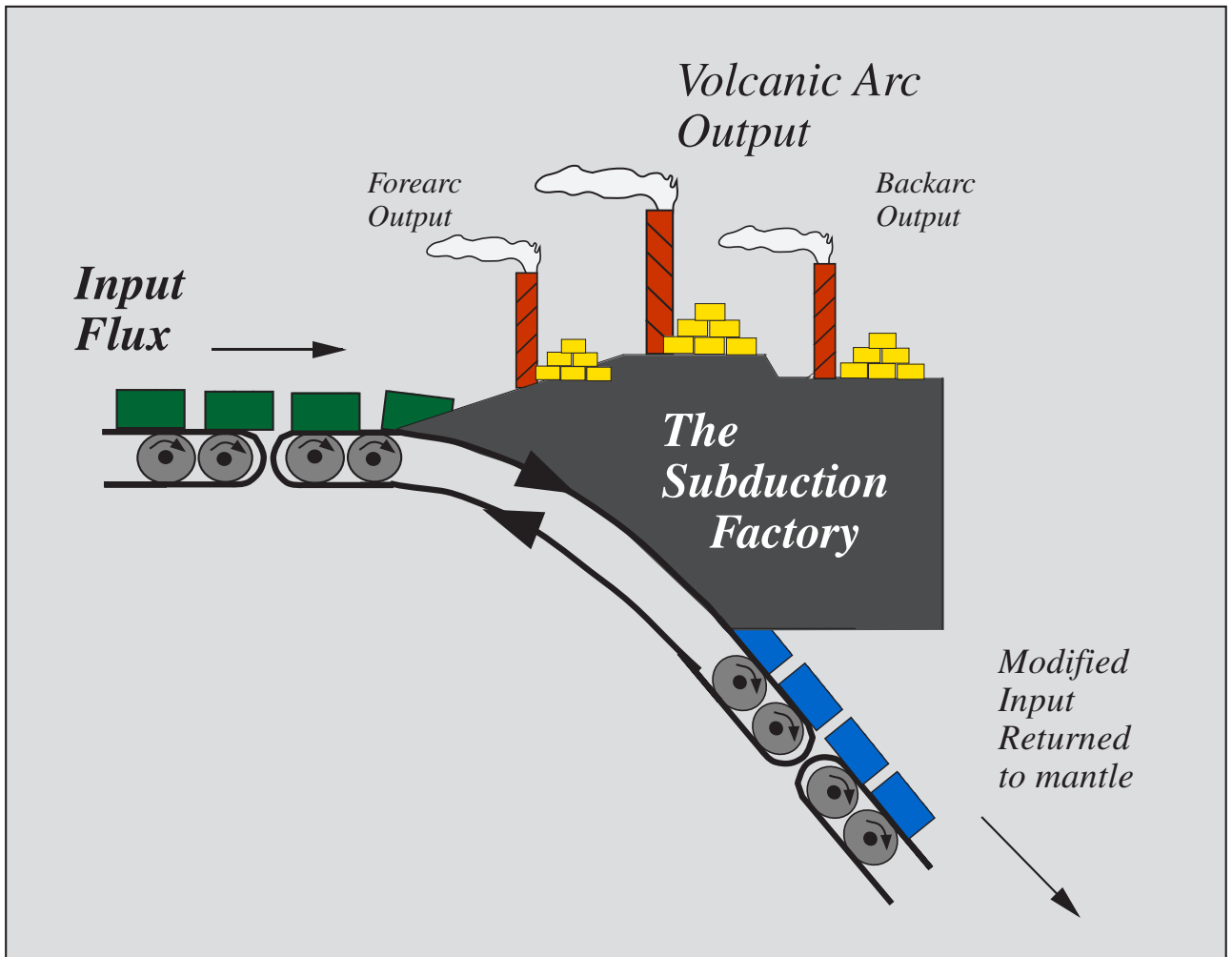


Figure F2. Predicted topography of the northwest Pacific (Smith and Sandwell, 1997) and magnetic lineations of the western Pacific compiled from Nakanishi et al. (1989) and the PLATES Project (1998). Ages of selected lineations (solid black lines) are given using the time scale of Channell et al. (1995). Open circles show locations of selected DSDP/ODP sites. Site 1149 is located 2200 km northwest of Site 801 along a fracture zone bounded flow line spanning ~36 m.y. White dashed lines = locations of fracture zones (GMT software; Wessel and Smith, 1995).

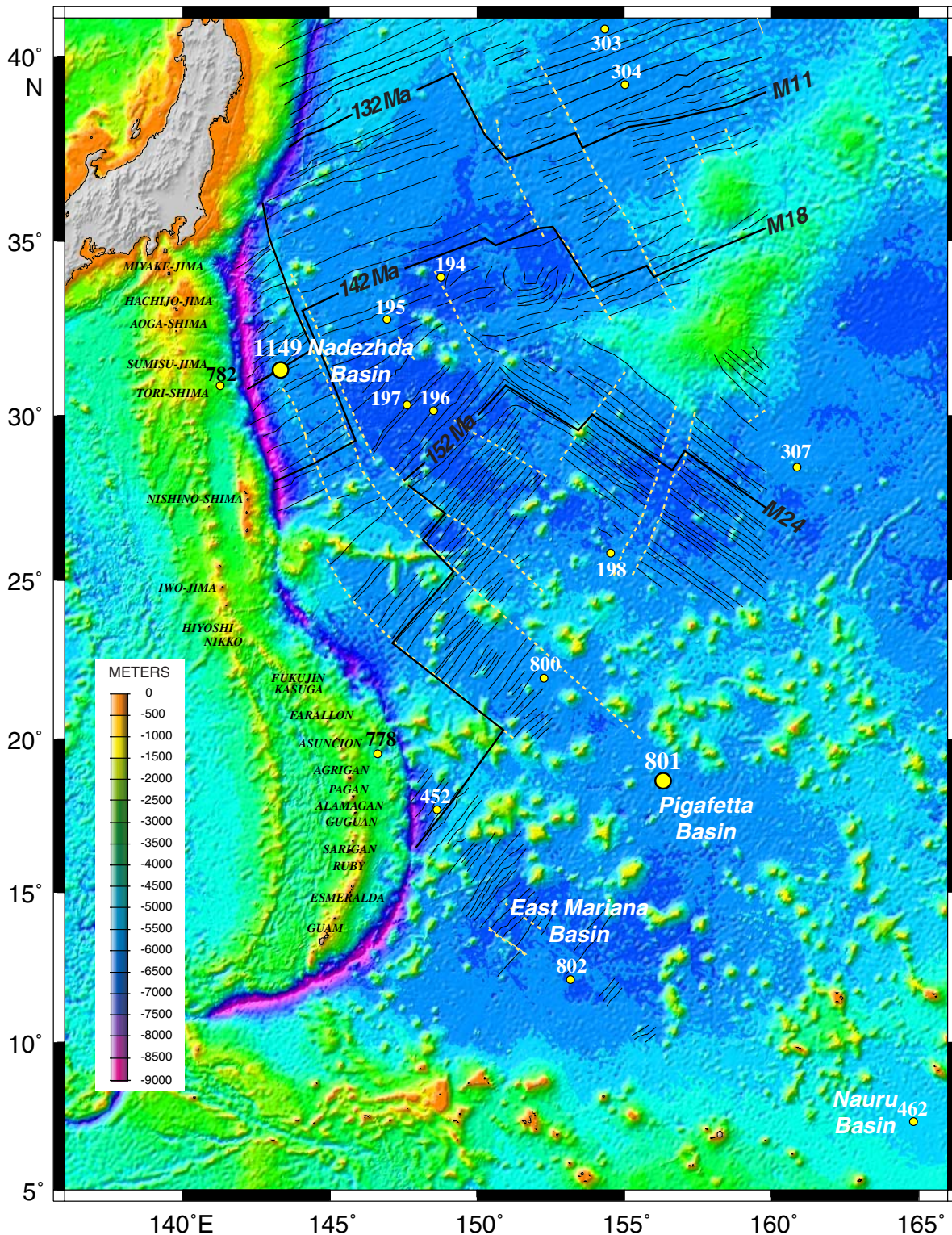


Figure F3. Perspective map of Izu and Mariana arcs and Leg 185 Sites 801 and 1149. Predicted bathymetry based on satellite altimetry (Smith and Sandwell, 1997) displayed with GMT software (Smith and Wessel, 1990).

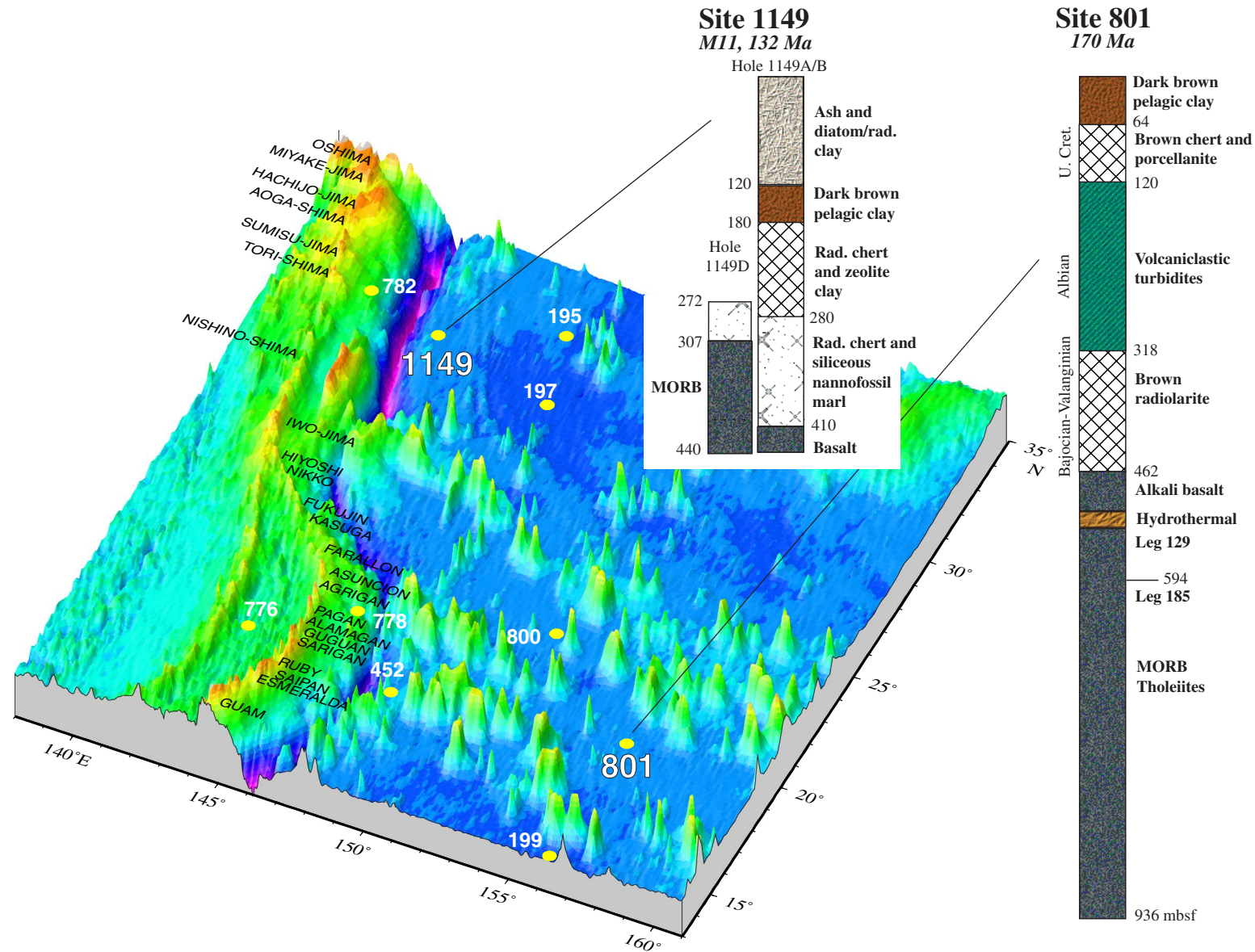


Figure F4. Competing models for input-output studies. **A.** The grass control model indicates that the kind of milk (dark vs. light) is controlled by the kind of grass (dark vs. light) that the cow eats. **B.** In the cow control model the breed of the cow is the important control in determining the kind of milk produced. Different cows (Guernsey vs. Jersey) eating the same kind of grass may produce different kinds of milk (dark vs. light). These models are directly analogous to subduction recycling studies, where the grass is the subducted input (sediments and oceanic crust), the milk is the volcanic arc output and the cow is the subduction zone.

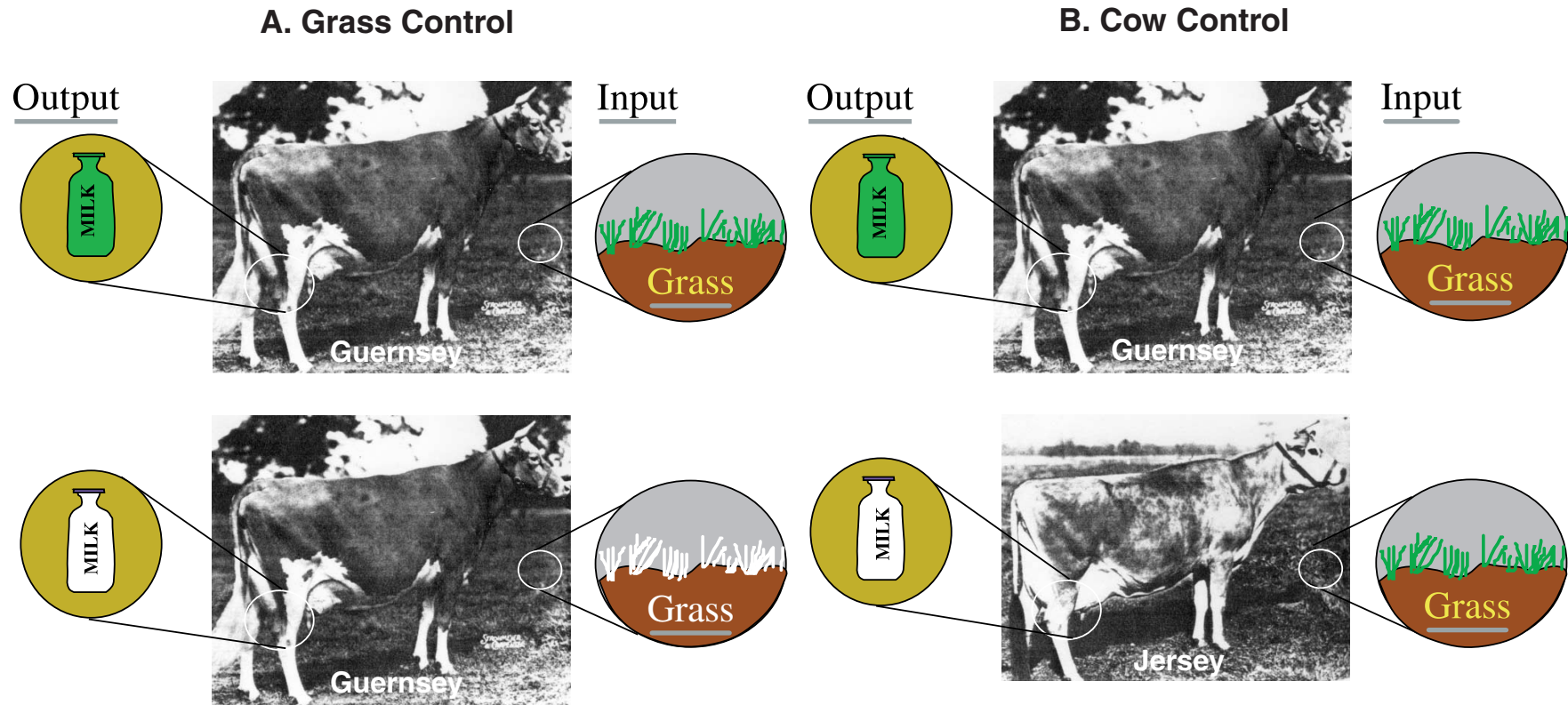


Figure F5. A. Correlation between Ba flux in subducted sediment and Ba enrichment of arc basalts for various arcs (Ant = Northern Antilles, Mar = Mariana, T = Tonga, Mex = Mexico, J = Java, Al = Aleutians, and G = Guatemala) around the world (after Plank and Langmuir, 1993). Open circles = three different sediment flux estimates for the Mariana, based on the three ODP sites drilled during Leg 129 (800–802) (Plank and Langmuir, 1998). Note Izu volcanics are lower in Ba/Na than Mariana volcanics by a factor of two. Drilling at Site 1149 will help to test if the low Ba/Na of the Izu volcanics is related to a lower Ba sediment flux. Shown for reference are the average Mariana Ba sediment flux and the flux for a 400-m section of chert (with 125 ppm Ba, similar to the upper radiolarites in Hole 801C; Karl, et al., 1992). **B.** Contrasting Pb isotopic composition of Mariana (open circle) and Izu-Bonin (solid circle) arc volcanics. Mariana volcanics form a mixing trend (arrow), almost perfectly coincident with mixtures of ODP Site 801 sediment (open boxes) and basalt (solid boxes) averages. Drilling at Site 1149 will test whether the Izu-Bonin arc trend (arrow) is consistent with different subducted material than that from the Mariana. Modern Pacific MORB data are shown for reference. Data sources: Elliott et al., 1997; Gill et al., 1994; Plank and Langmuir, 1998; Castillo et al., 1992.

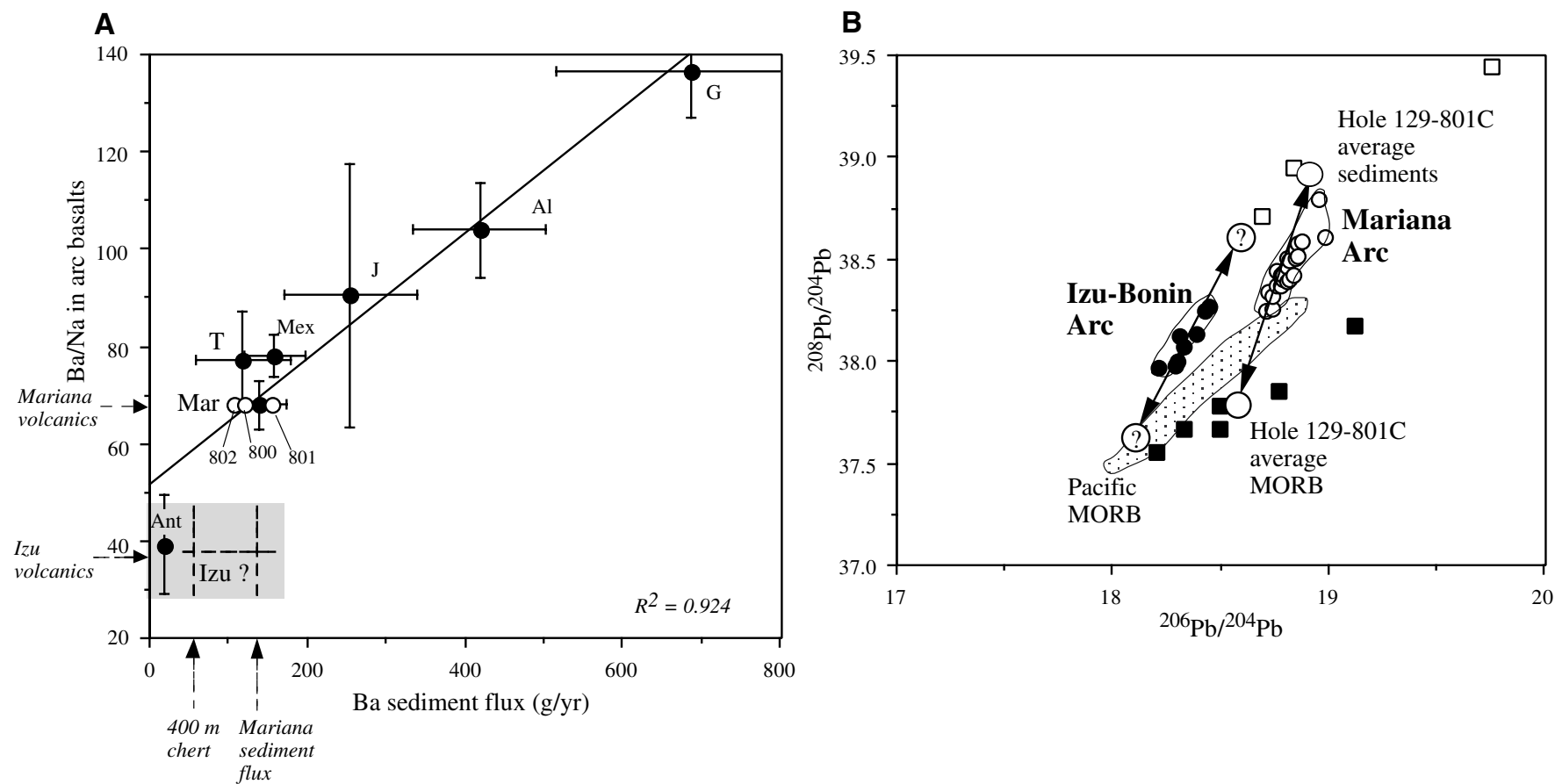


Figure F6. Lithologic columns for Leg 20 sites (Sites 194–197), Hole 801C, and Site 1149. Reflections may represent basaltic basement in Leg 20 sites.

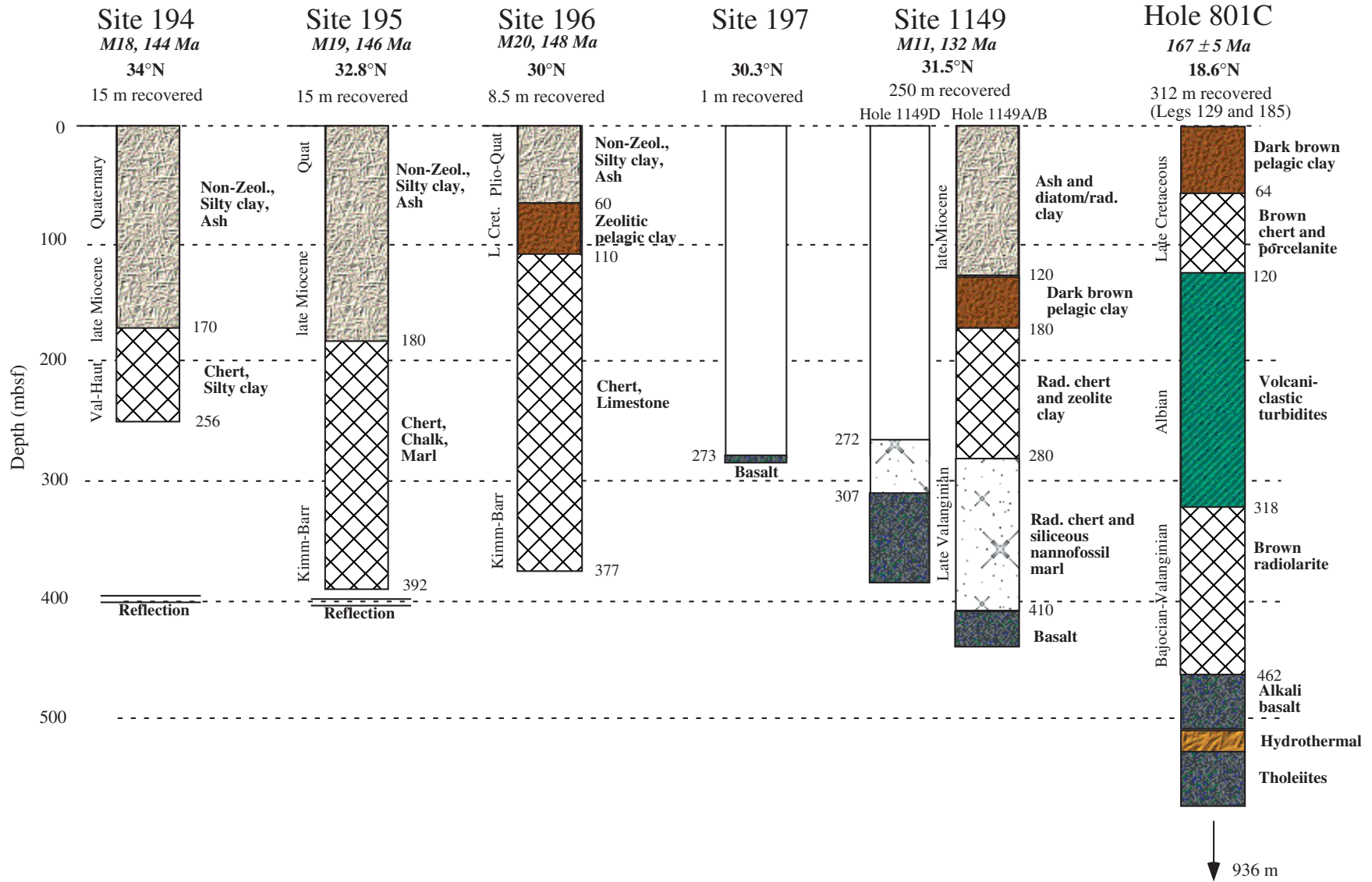


Figure F7. Theoretical Mesozoic paleolatitude histories of ODP Sites 801 and 1149 based on the combined polar wander paths for the Pacific plate of Sager and Pringle (1988) for 60–100 Ma and Larson and Sager (1992) for 100–155 Ma. Great circle distances are measured at 5-m.y. intervals on the combined polar wander path to the present-day site locations and then converted to paleolatitudes to construct these histories. The paleolatitudes of 155–165 Ma for ODP Site 801 are based on measured remanent inclinations in Jurassic core samples from that site.

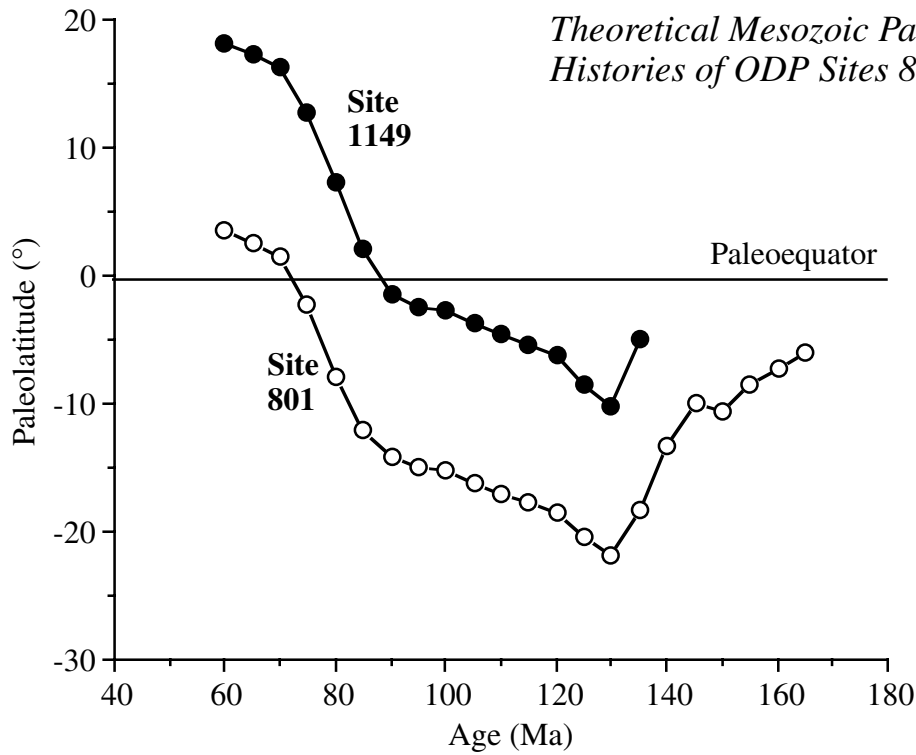


Figure F8. Summary of seismic stratigraphy in Holes 1149A, 1149B, and 1149C showing generalized correlations with lithologic units, ages, and seismic facies. UT = upper transparent, UO = upper opaque, and HB = Horizon B. The basement age of 132 Ma corresponds to Chron M11 from Channell et al., 1995. Holes 1149A, 1149B, and 1149C were imaged with SCS water guns (two 80 in³) obtained on approach to Site 1149 during Leg 185. Track-line orientation and locations are shown in Figure F7, p. 59, in the “Site 1149” chapter. Seismic data were processed and displayed with the following parameters: mute, band-pass filter 30–100 Hz, three-trace mix, skip every other trace, 500-ms automatic gain control, and vertical exaggeration of ~25× at the seafloor.

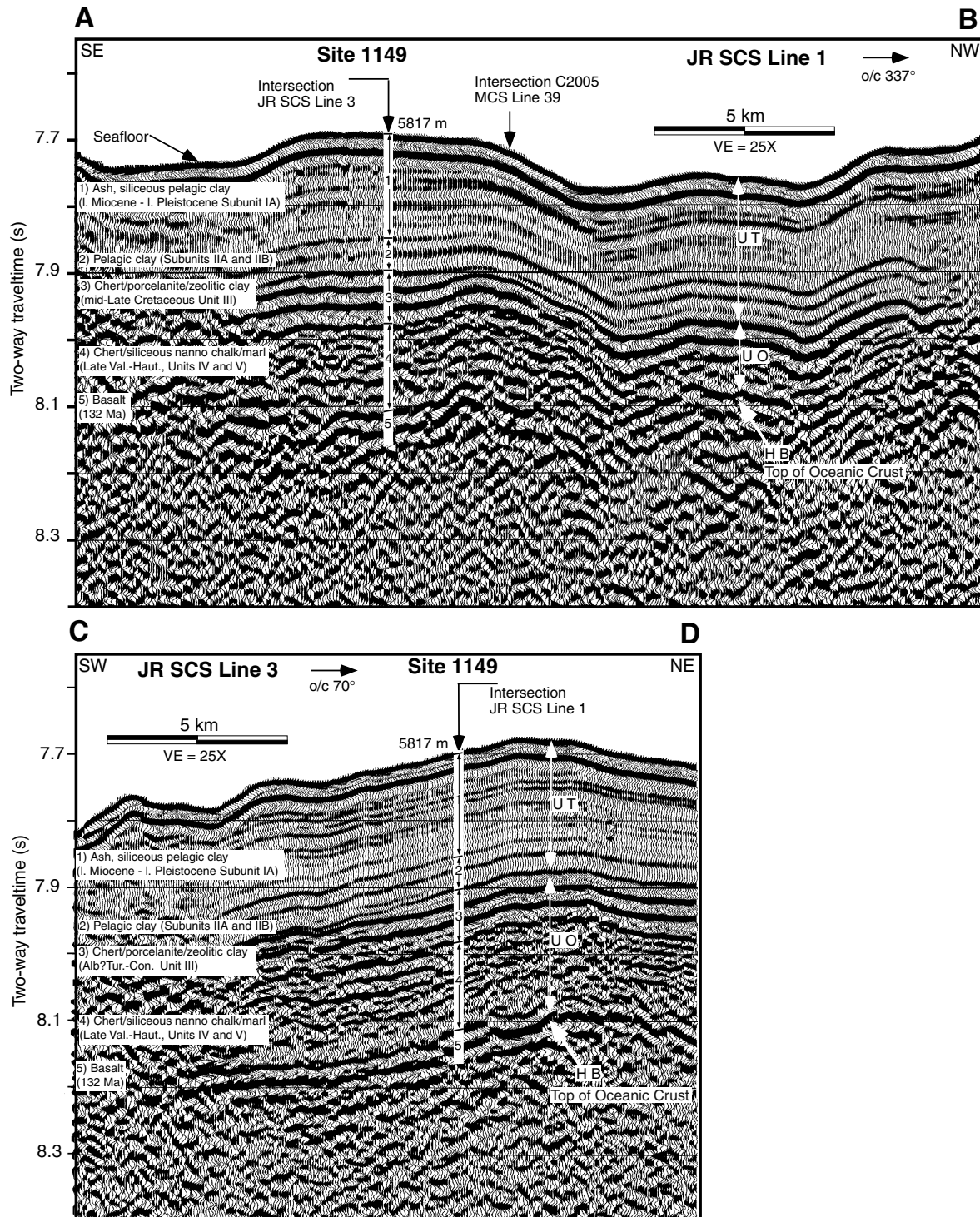


Figure F9. Original drilling objectives for Leg 185 sites and drilling achieved.

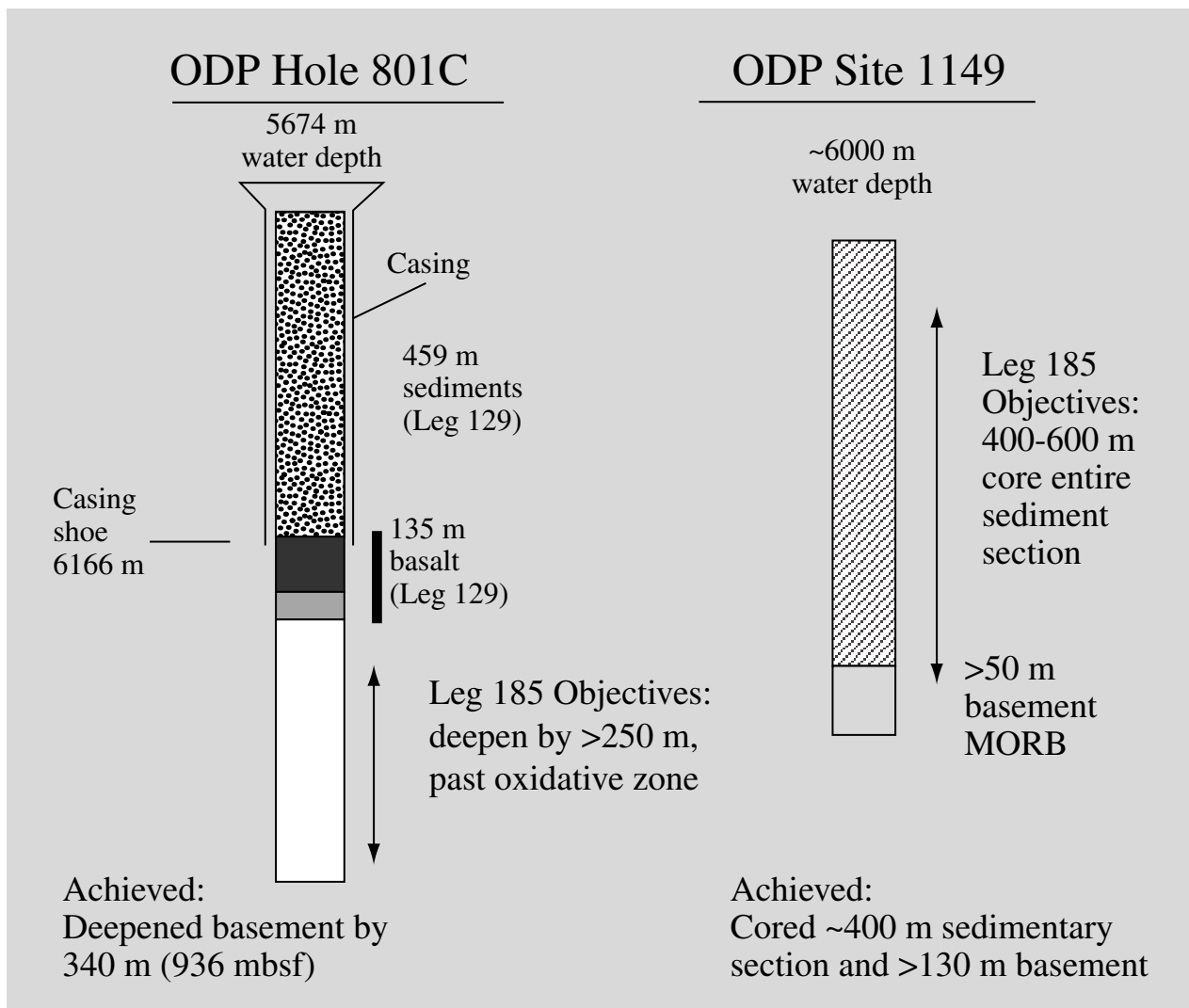


Figure F10. Stratigraphic column showing each cooling unit in the basement at Hole 801C drilled during Legs 129 and Leg 185. The sequences (i.e., I–VIII) correspond to major lithologic changes and are also related to the presence of breccia zones, hydrothermal deposits, and changes in magma chemistry.

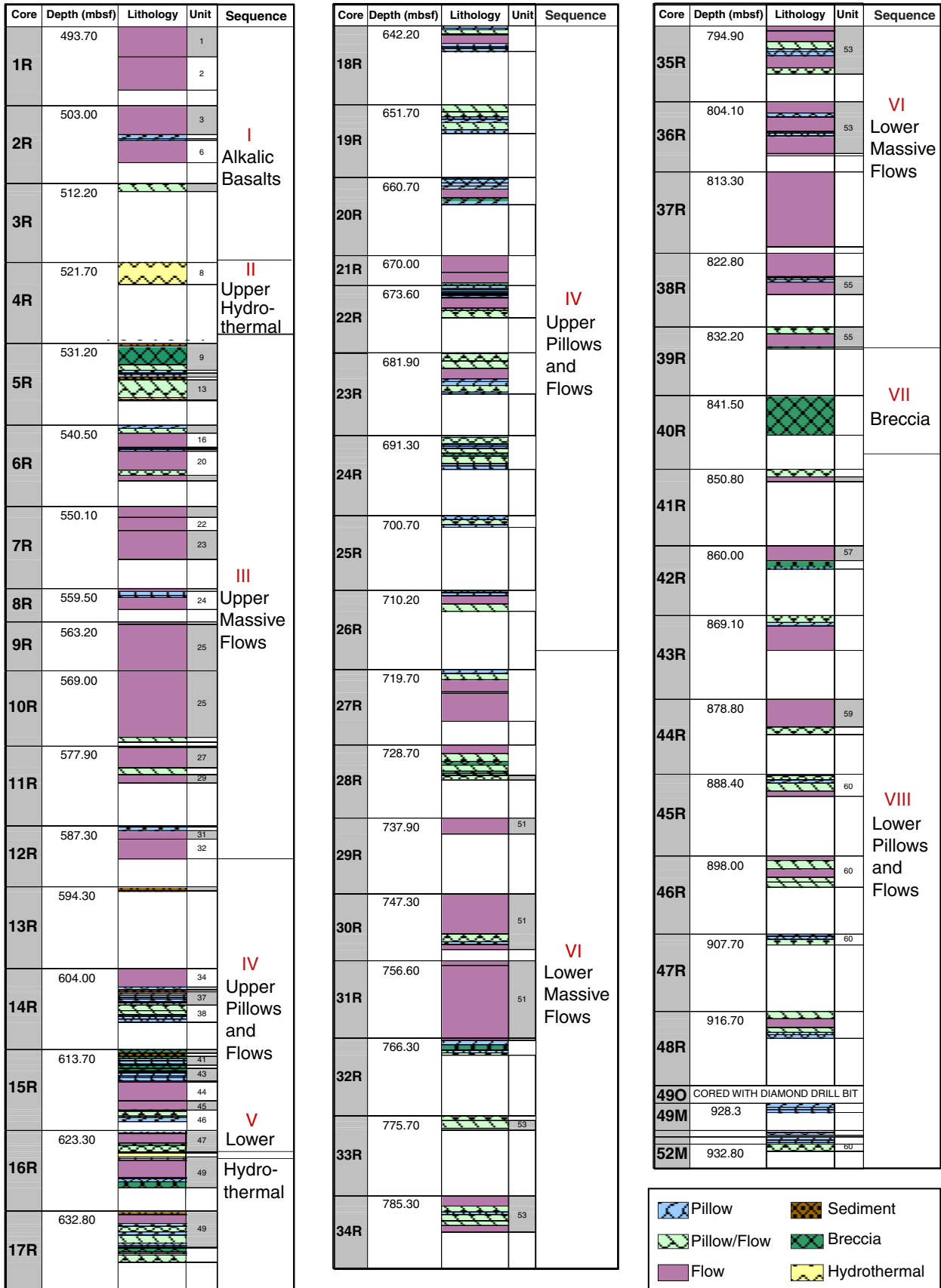


Figure F11. Data from Hole 801C showing recovery resistivity, natural gamma logs, magnetic logs of vertical and horizontal intensity, and the magnetic inclination measured in half-round cores. In addition, the major lithologic sequences for the section are given.

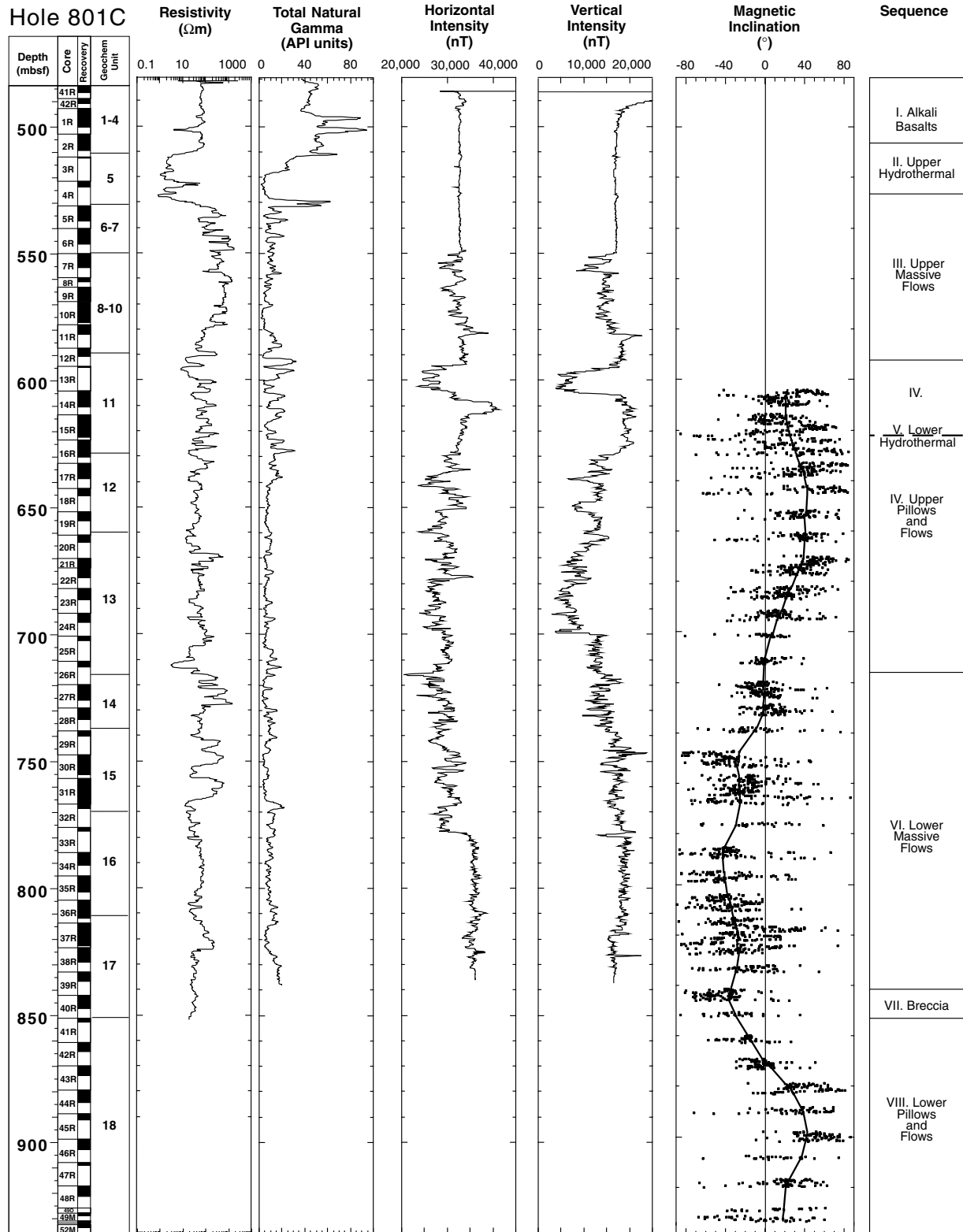


Figure F12. Downhole variations in (A) MgO and (B) Zr from shipboard XRF data, demonstrating the magmatic trends upsection. Smaller scale variation is observed within the various igneous sequences. The alkaline suite in Sequence I is identified by enriched Zr relative to the tholeiites. Leg 185 basalts are in solid circles and open diamonds (>2 wt% LOI, >1 wt% K₂O). Leg 129 basalts are in open circles. The Zr/Y diagram (C) demonstrates that Site 801 tholeiites are comparable to modern East Pacific Rise and mid-Atlantic Ridge MORB (Langmuir et al., 1986; Langmuir, 1987).

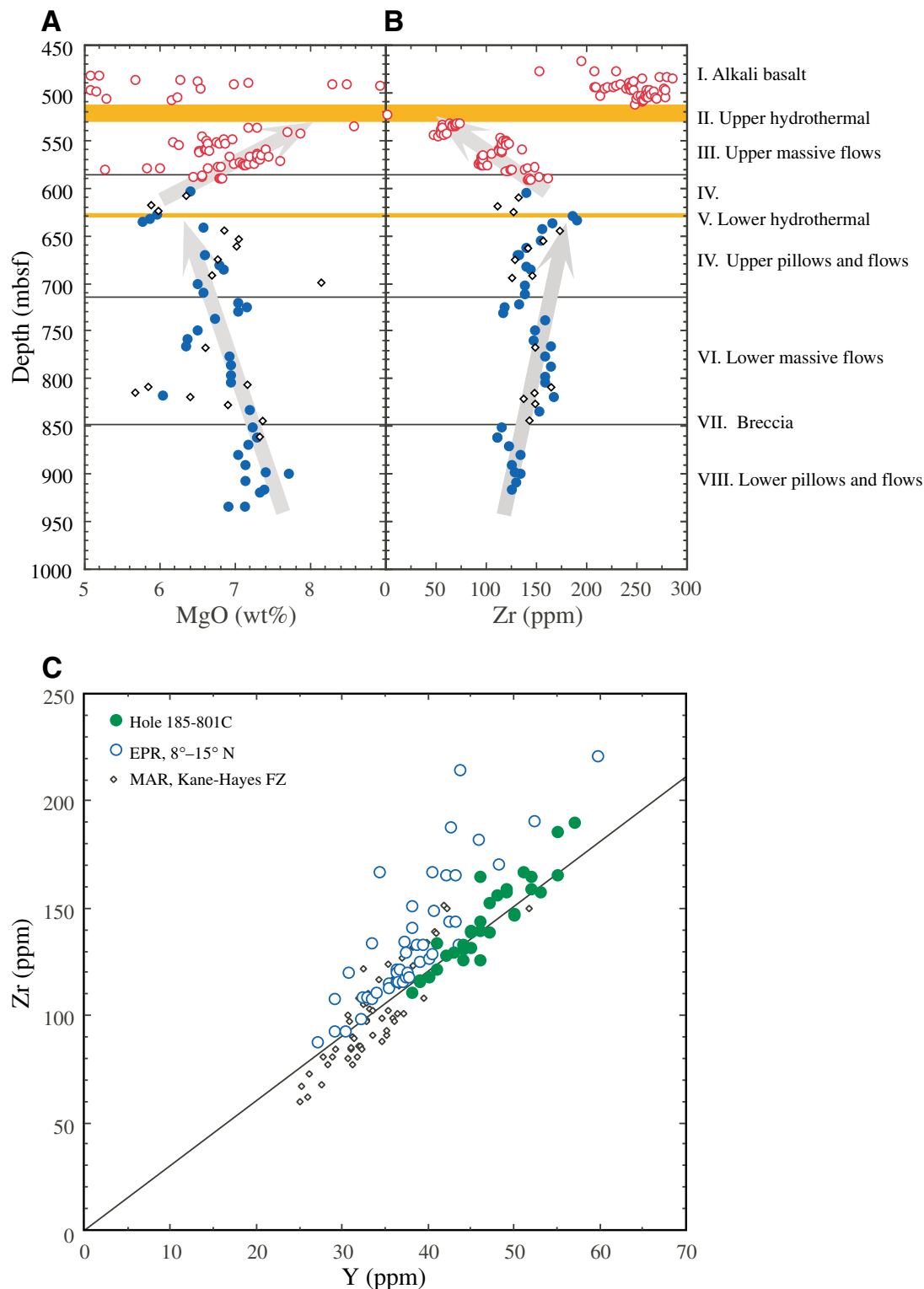


Figure F13. Section 185-801C-15R-7 showing extreme alteration types observed. The pale green alteration flanks an interpillow sediment. The gray-green alteration at the bottom of the core is typical of much of the background alteration in the cores. Proportions of the main secondary minerals are given, as are photomicrographs in which saponite, smectite, and calcite are visible. The two photomicrographs of the pale green alteration show a plagioclase phenocryst, which is otherwise rare in these dominantly aphyric lavas.

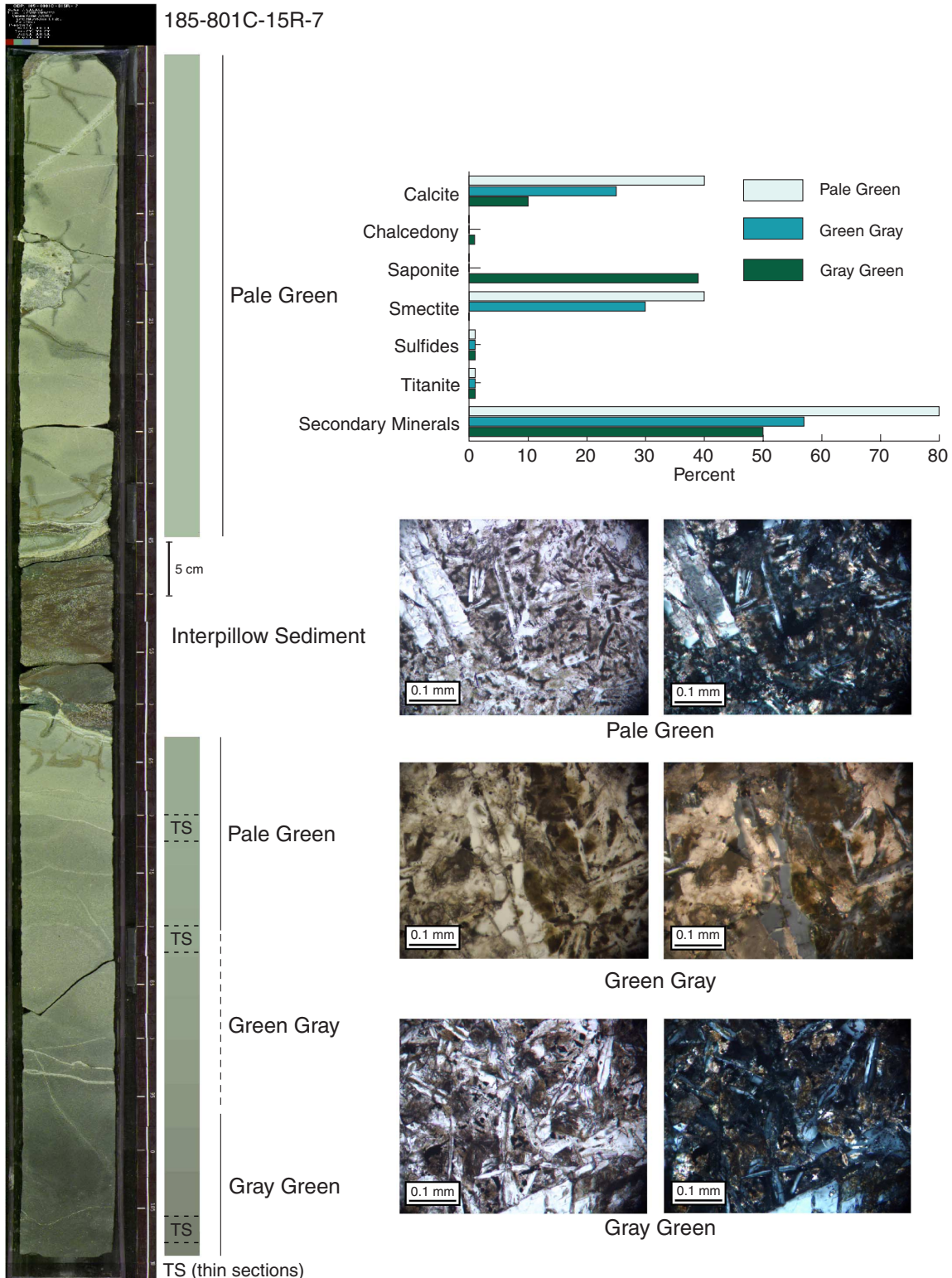


Figure F14. Summary of basement igneous stratigraphy and alteration features downcore.

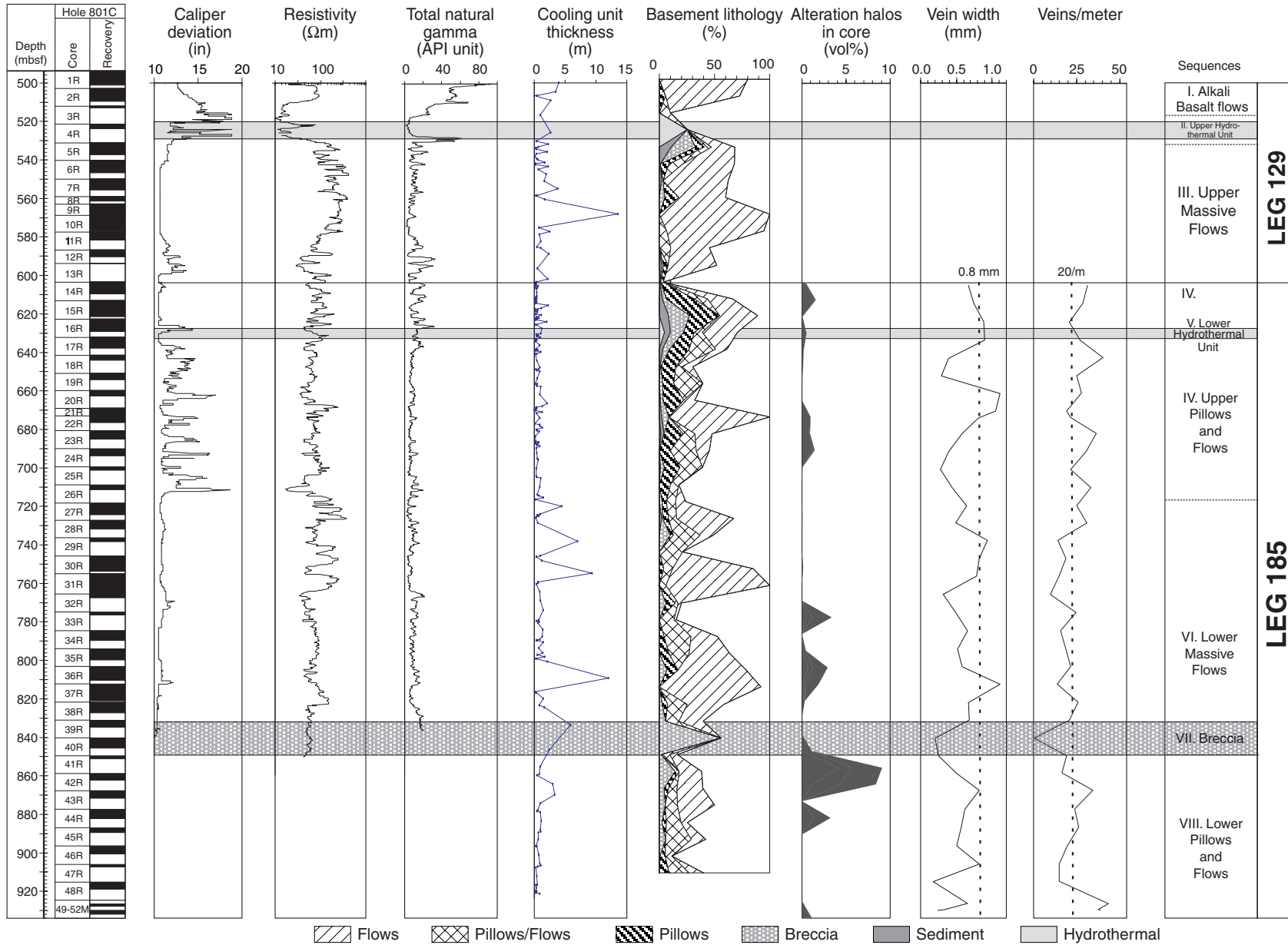


Figure F15. K_2O vs. depth in Hole 801C (tholeiitic section only), calculated from the natural gamma ray (NGR) data on the whole-round cores analyzed on the multisensor track (MST).

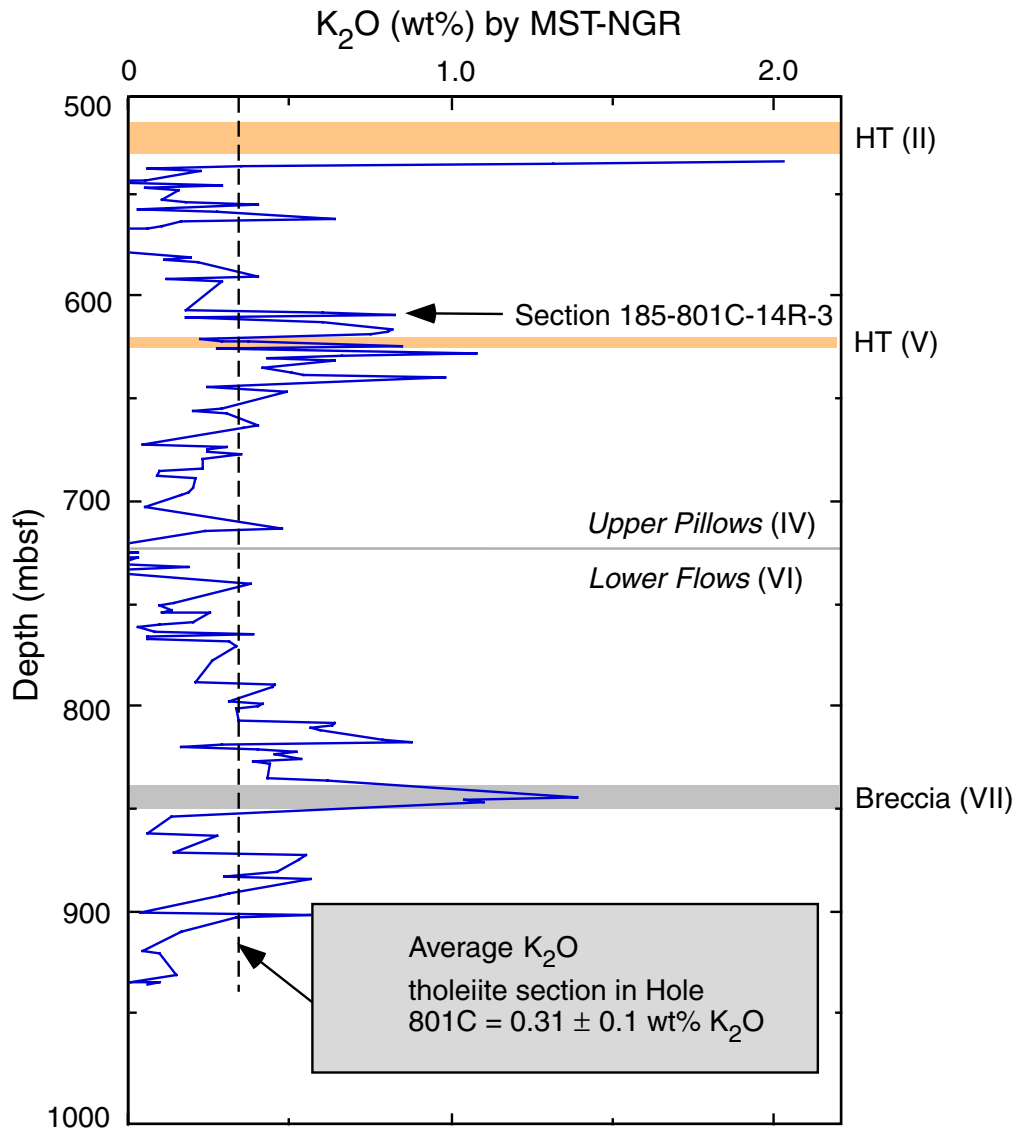


Figure F16. MSC Line 39 recorded in 1976 during *Conrad* Cruise 2005 illustrating the proximity of Site 1149 to the Izu-Bonin Trench axis; cpa = closest point of approach.

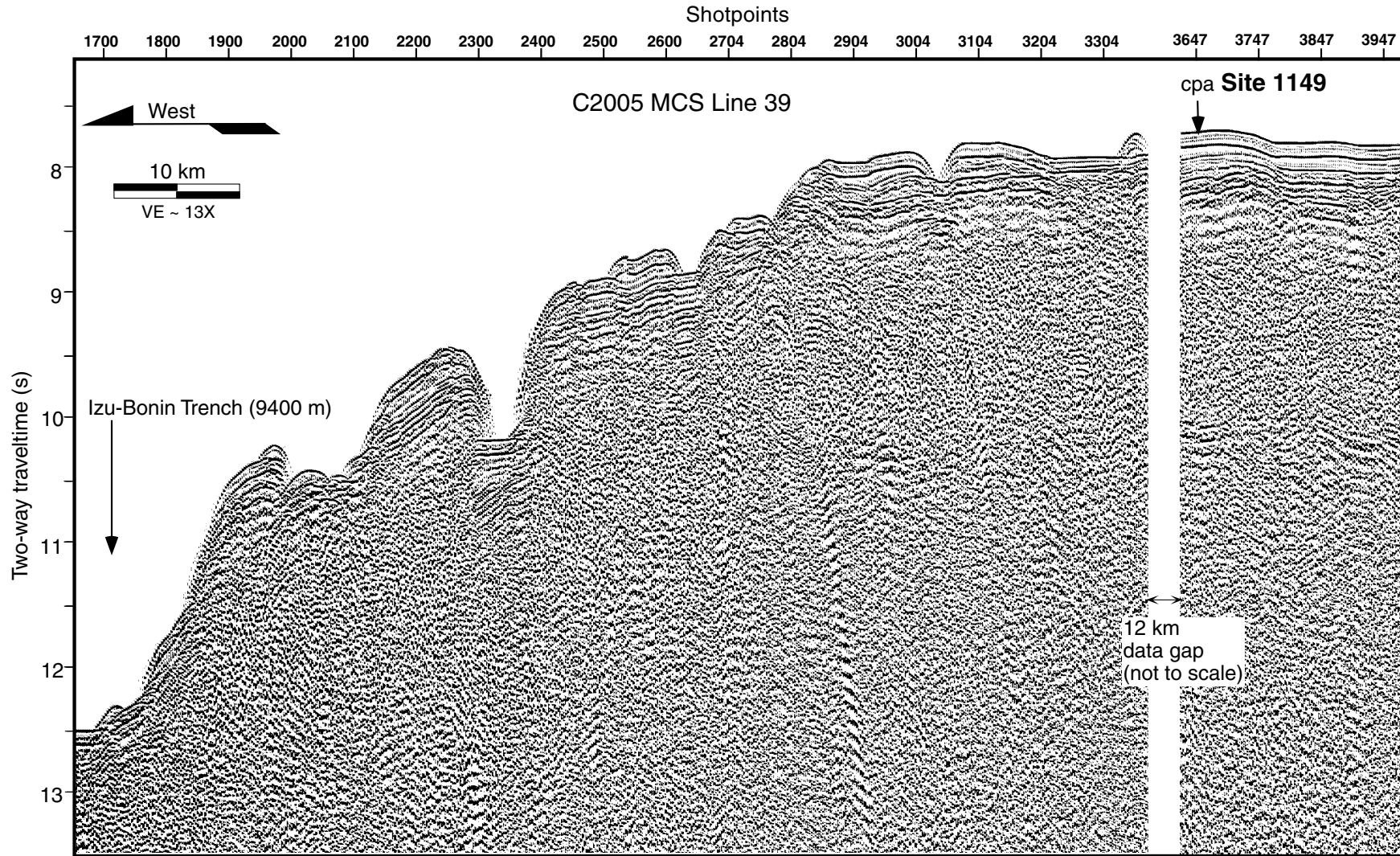


Figure F17. Summary of the lithostratigraphic section at Site 1149.

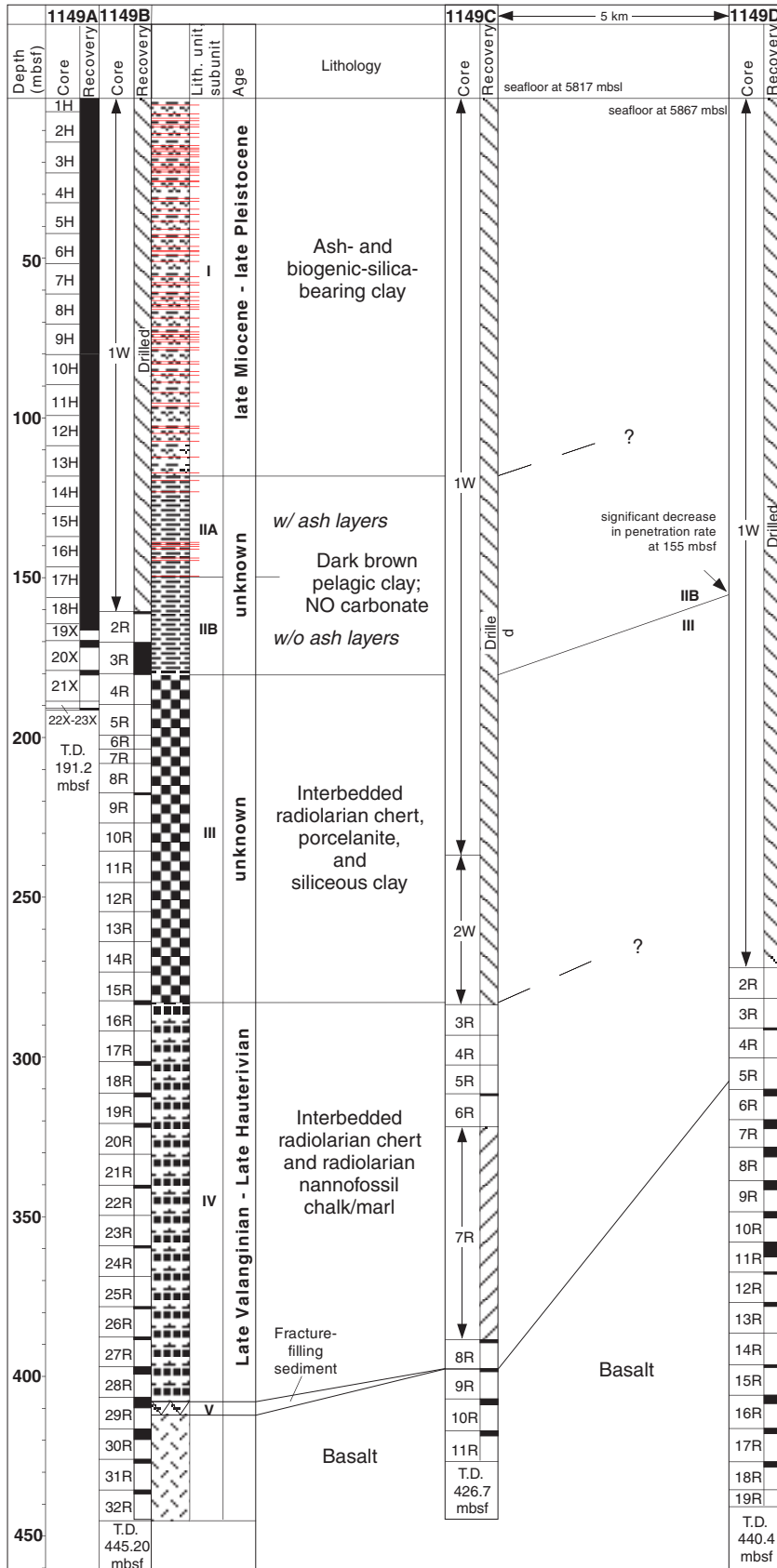


Figure F18. Magnetic reversal stratigraphy in the upper 120 m of Site 1149.

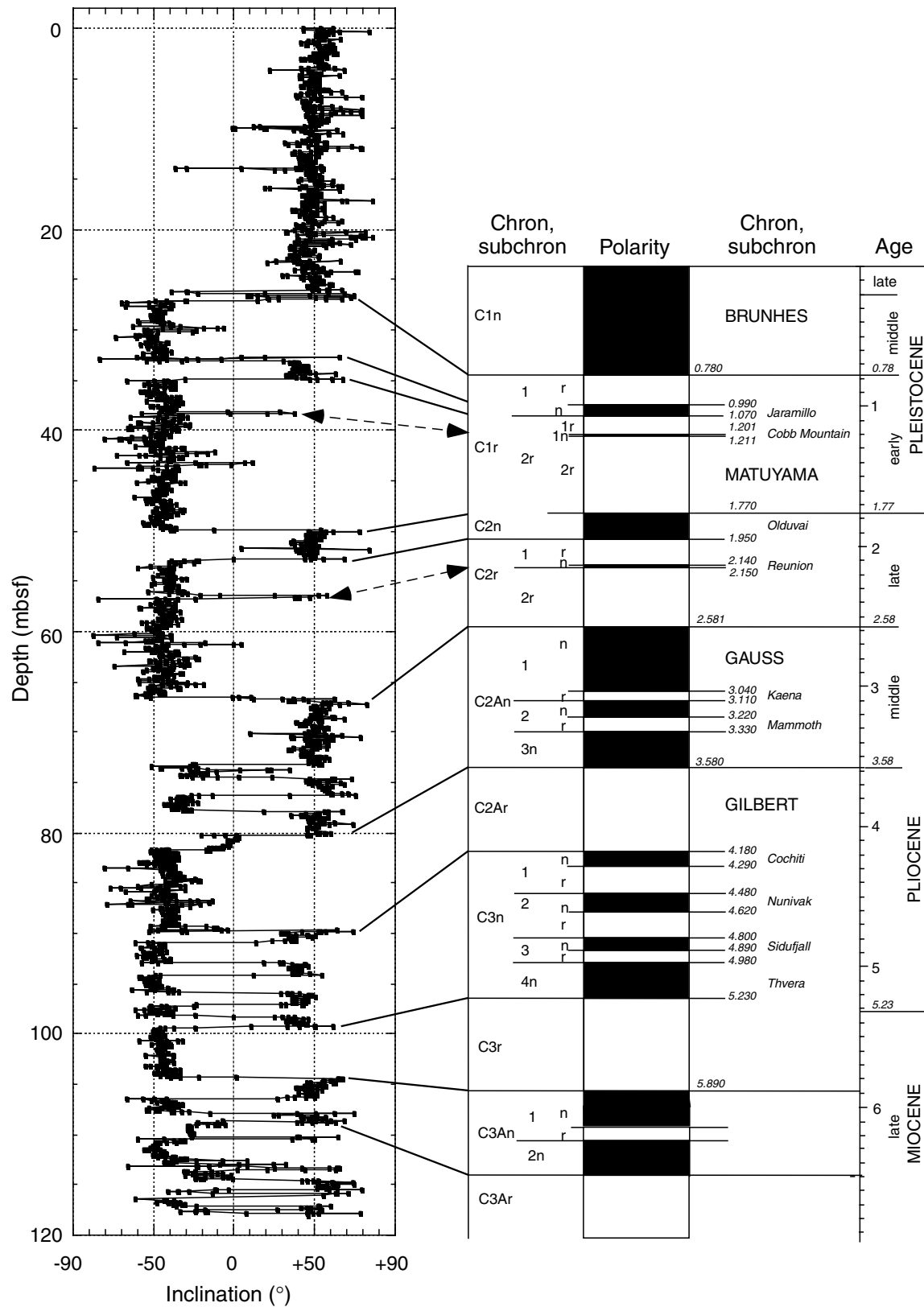


Figure F19. Summary of sedimentation rates, based on magnetostratigraphy and calcareous nannofossil biostratigraphy of Site 1149.

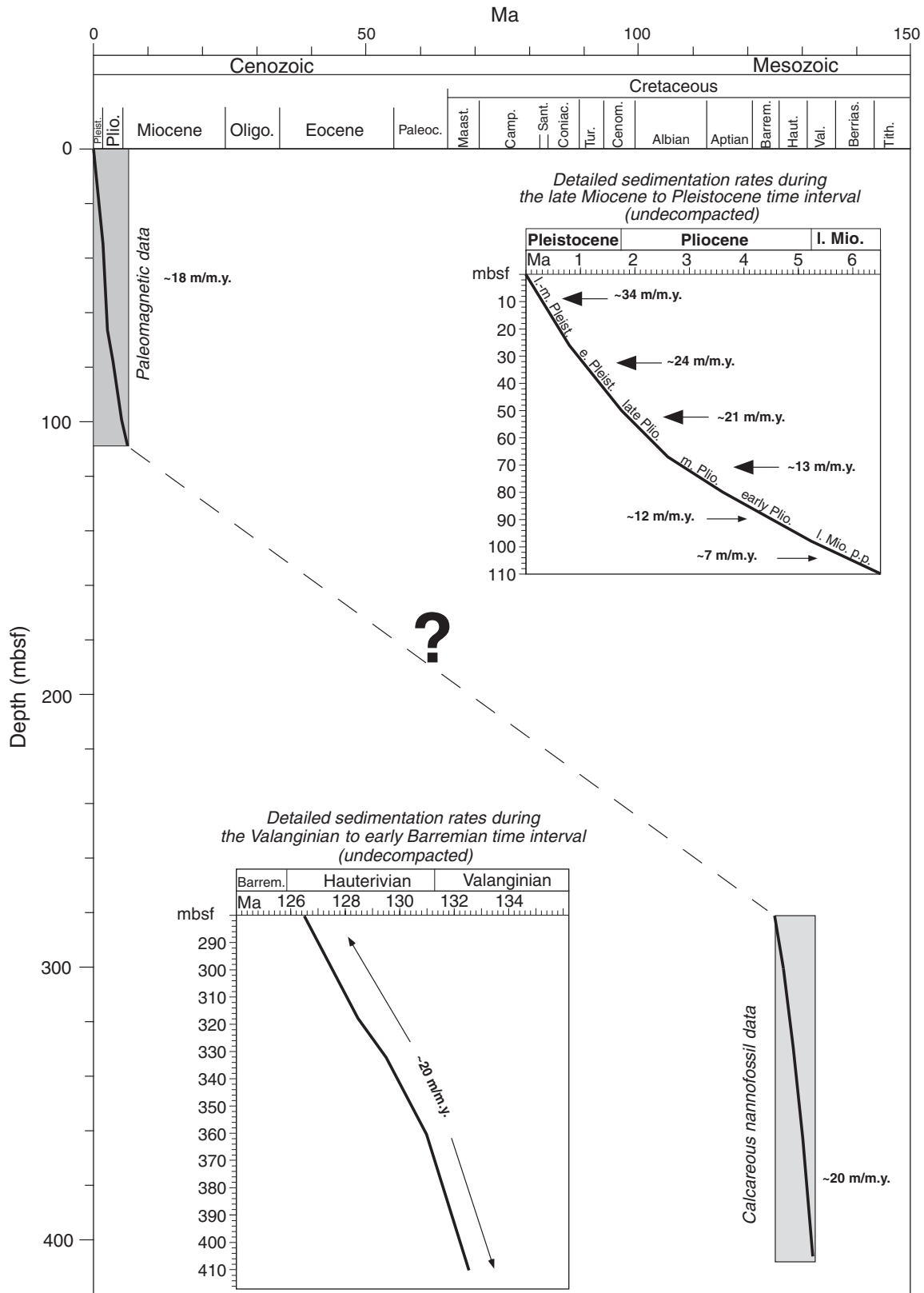


Figure F20. Summary of logging data in sedimentary section and basement alteration features at Site 1149.

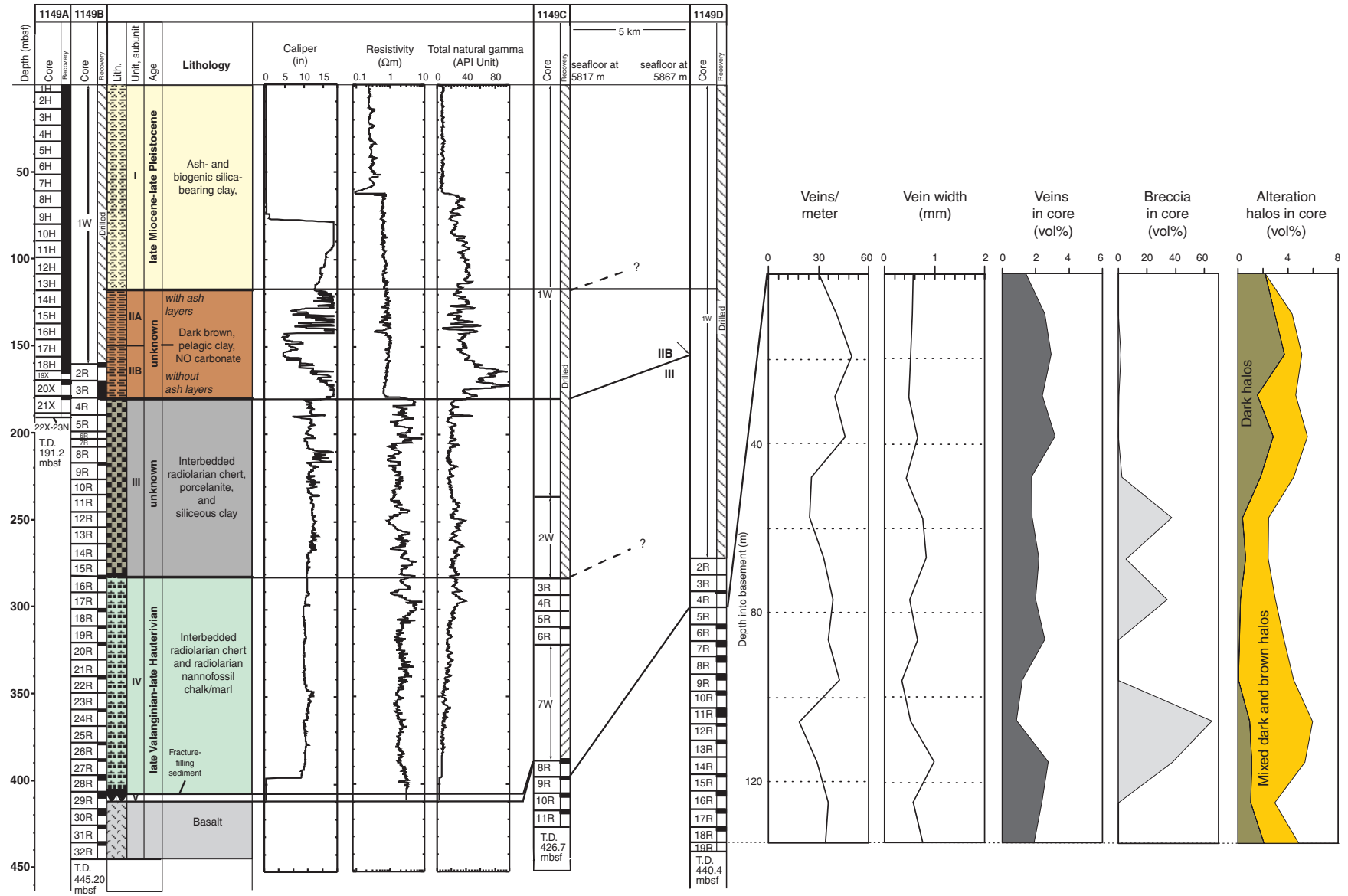


Figure F21. Downhole variations in bulk sediment geochemistry. Variations in Fe/Al show influence of hydrothermal particulates at the base of the site. Si/Al variations reflect chert-rich lithologies in Units III and IV. Ba/Al ratios increase downhole with increases in both biogenic and hydrothermal fluxes. Dashed line = values in average shale.

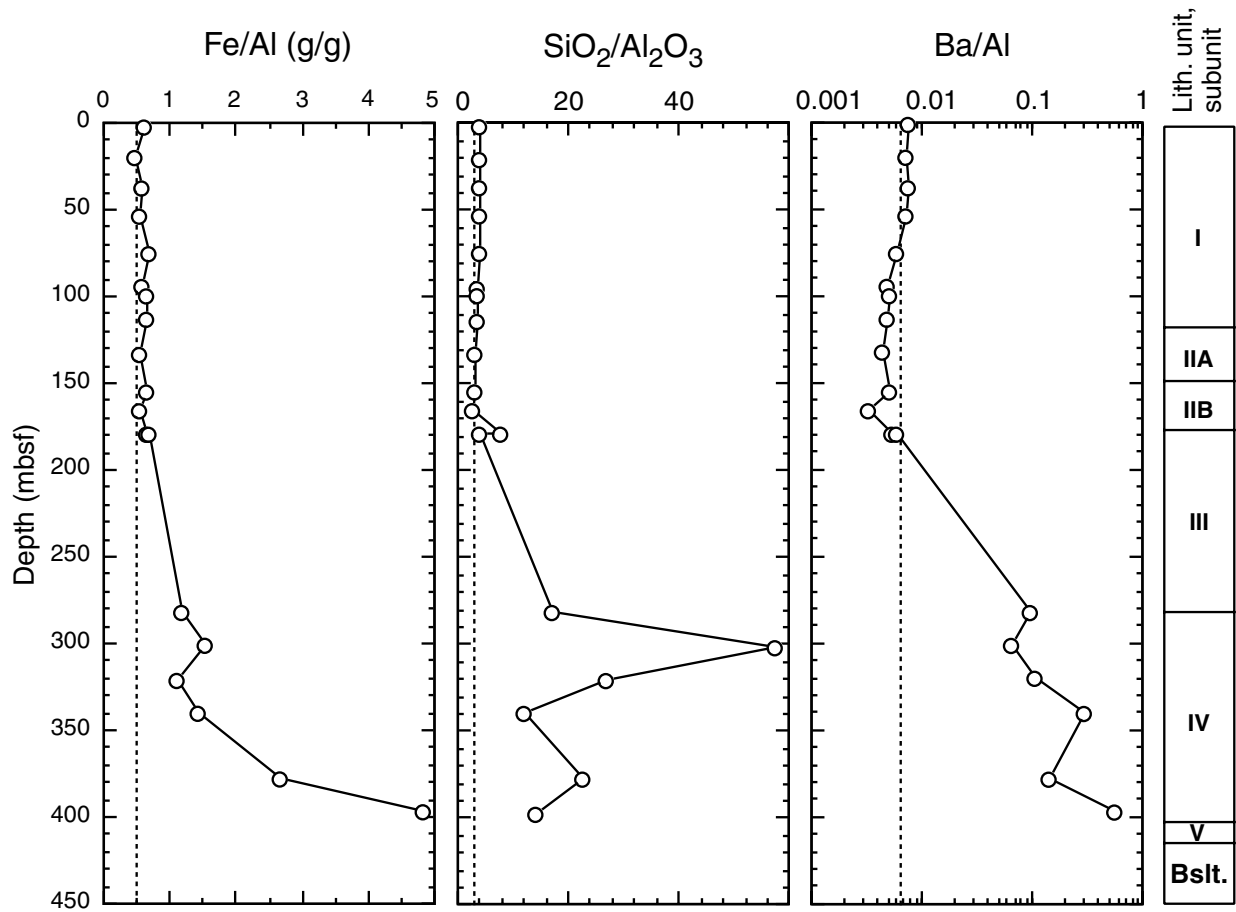


Figure F22. Example of a bacterial population contaminated with fluorescent microspheres.

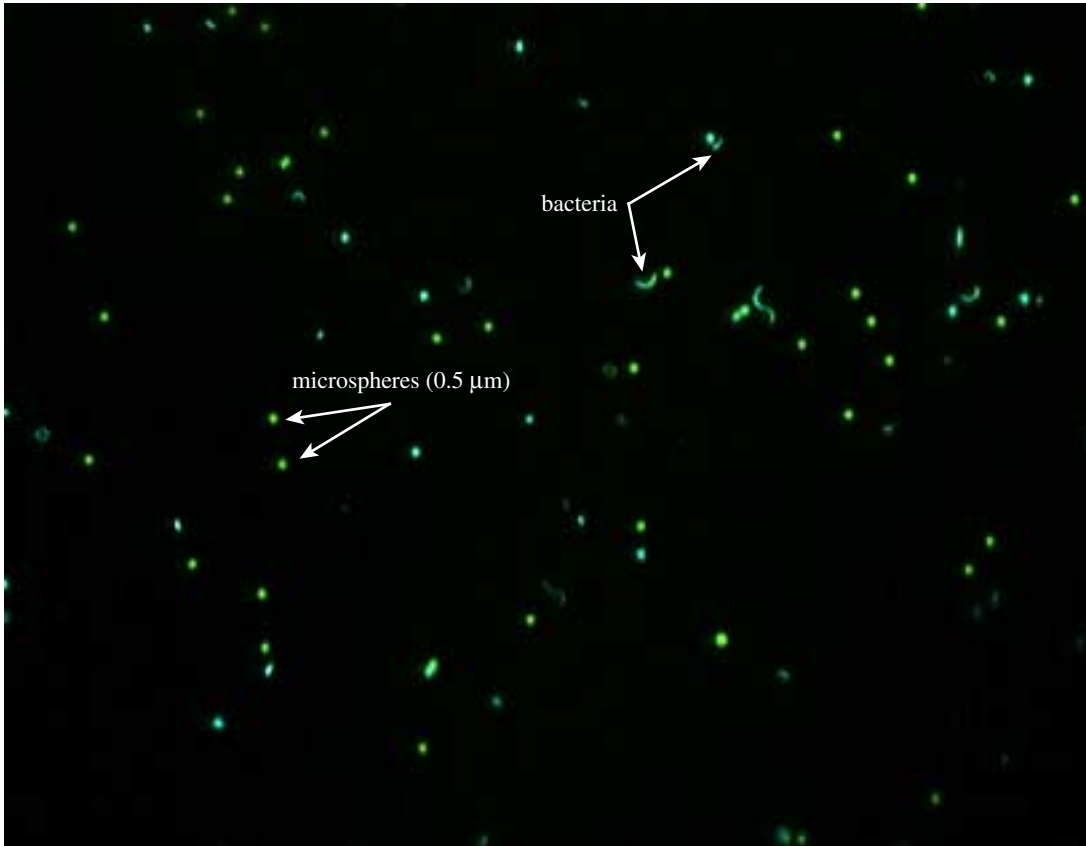


Figure F23. Photomicrographs of glass from Hole 801C viewed in plane-polarized light demonstrating microbial alteration textures. **A.** Sample 185-801C-12R-1, 85–89 cm, pillow margin. Brown variolitic (V) and clear glass with a single white plagioclase feldspar lath (P) in the lower right. A fine (5 μm wide) fracture extends into the glass in the center of the photograph from a fracture that lies along the edge of the feldspar. This 5- μm fracture is surrounded by delicate, hollow, ornamented channels that extend 5–10 μm from the fracture. These are similar to decorations found in a variety of subseafloor volcanic glasses that have been attributed to microbial activity. **B.** Sample 185-801C-17R-3, 85–91 cm, flow margin. This glass has parallel fractures and one of these lies at the bottom of the photograph and a second one is just beyond the top of the photograph. Surrounding the top fracture is a dense network of channels that extend 50–100 μm from the fracture and make the glass opaque. Some individual channels can be seen extending toward the center of the photograph. Where these intersect the surface of the thin section the channel cross section is $\sim 5 \mu\text{m}$. The fracture across the bottom of the photograph has not developed the dense network of channels. **C.** Sample 185-801C-48R-2, 121–123 cm. This photograph shows variolitic glass (V) and fresh glass (F), which is cut by a 100- μm -wide fracture. Near the bottom of the photograph, fresh glass is being replaced with clay and the boundary between them is irregular, much like the dark boundary in B. The glass next to the fracture is being converted to clay along an irregular alteration front. The box shows the location of D. **D.** Detail of Sample 185-801C-48R-2, 121–123 cm. Brown variolitic glass is around the edges of the photograph. The fracture is $\sim 20 \mu\text{m}$ wide and is filled with clay. The dark bands in the glass along the fracture contains irregular interconnected voids $\sim 1 \mu\text{m}$ across. This irregular texture is not preserved as the glass-to-clay alteration front advances. **E.** Sample 185-801C-801C-42R-2, 126–128 cm. Hyaloclastite thin section viewed in plane-polarized light. The white in the upper left corner is calcite. The glass is tan and contains a 500- μm white plagioclase feldspar (P). The outer 100–200 μm of the glass has been altered to clay that is the nearly same color as the glass. The glass is altered to clay along fractures. The area in the square is shown in F. **F.** Detail of Sample 185-801C-42R-2, 126–128 cm. The edge of the glass (upper left of photo) is scalloped and the edges of the fracture are irregular. In both areas the glass is being replaced by clay. **G.** Detail of Sample 185-801C-42R-2, 126–128 cm. The interior of a separate piece of glass from that shown in E and F. Three voids are labeled and 2- to 4- μm -diameter tunnels lead from the voids into the glass. The tunnels are 100–200 μm long and have irregular edges from which 1- μm tunnels branch. This is the only location in Hole 801C where this type of tunnel was observed. They are also similar to a style of tunneling seen in ocean floor basalts from other ODP holes. (Figure shown on next page.)

Figure F23. (Caption on previous page.)

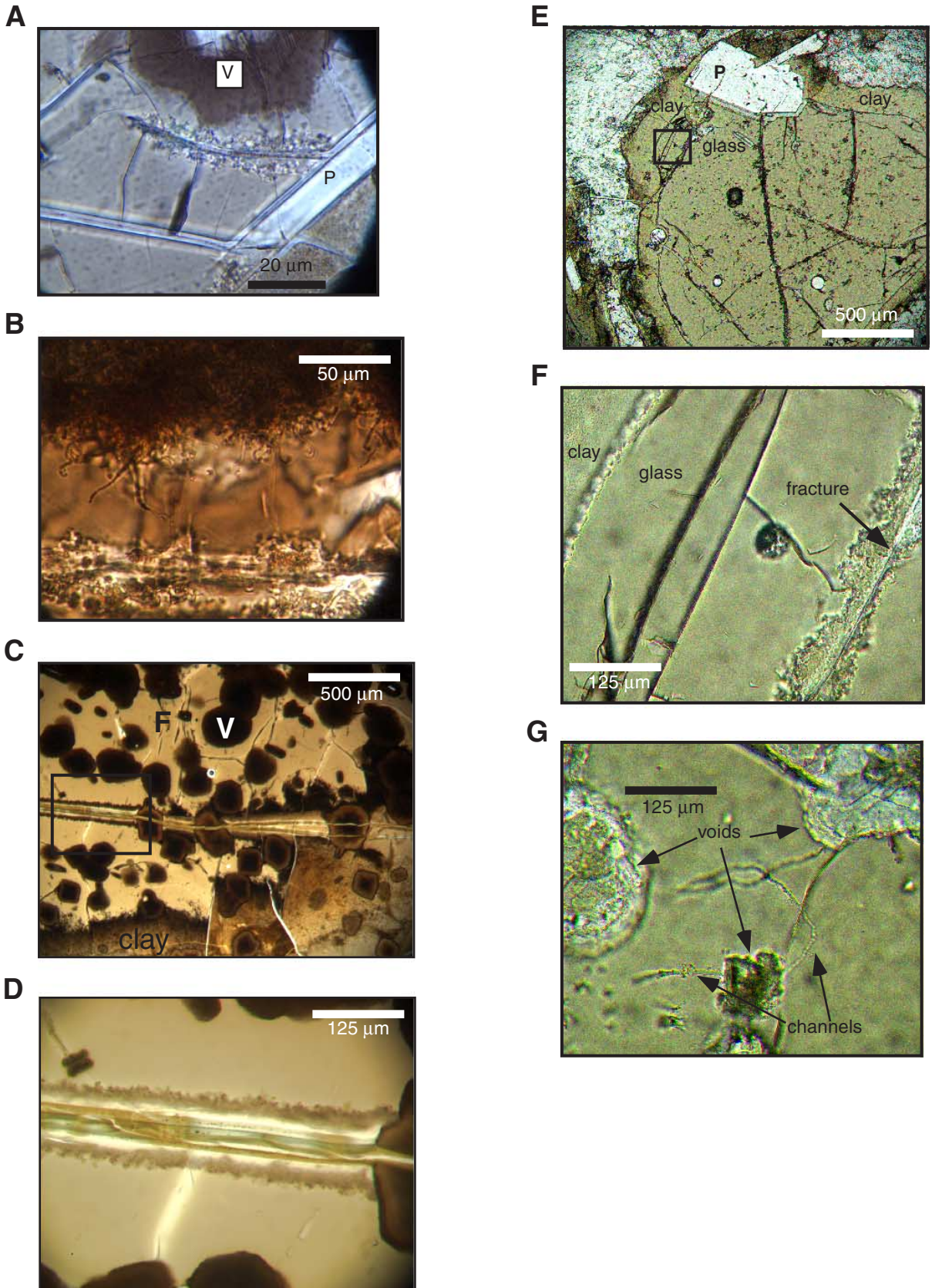


Figure F24. Lithostratigraphic summary of holes drilled during Leg 185 (including Hole 801C of Leg 129).

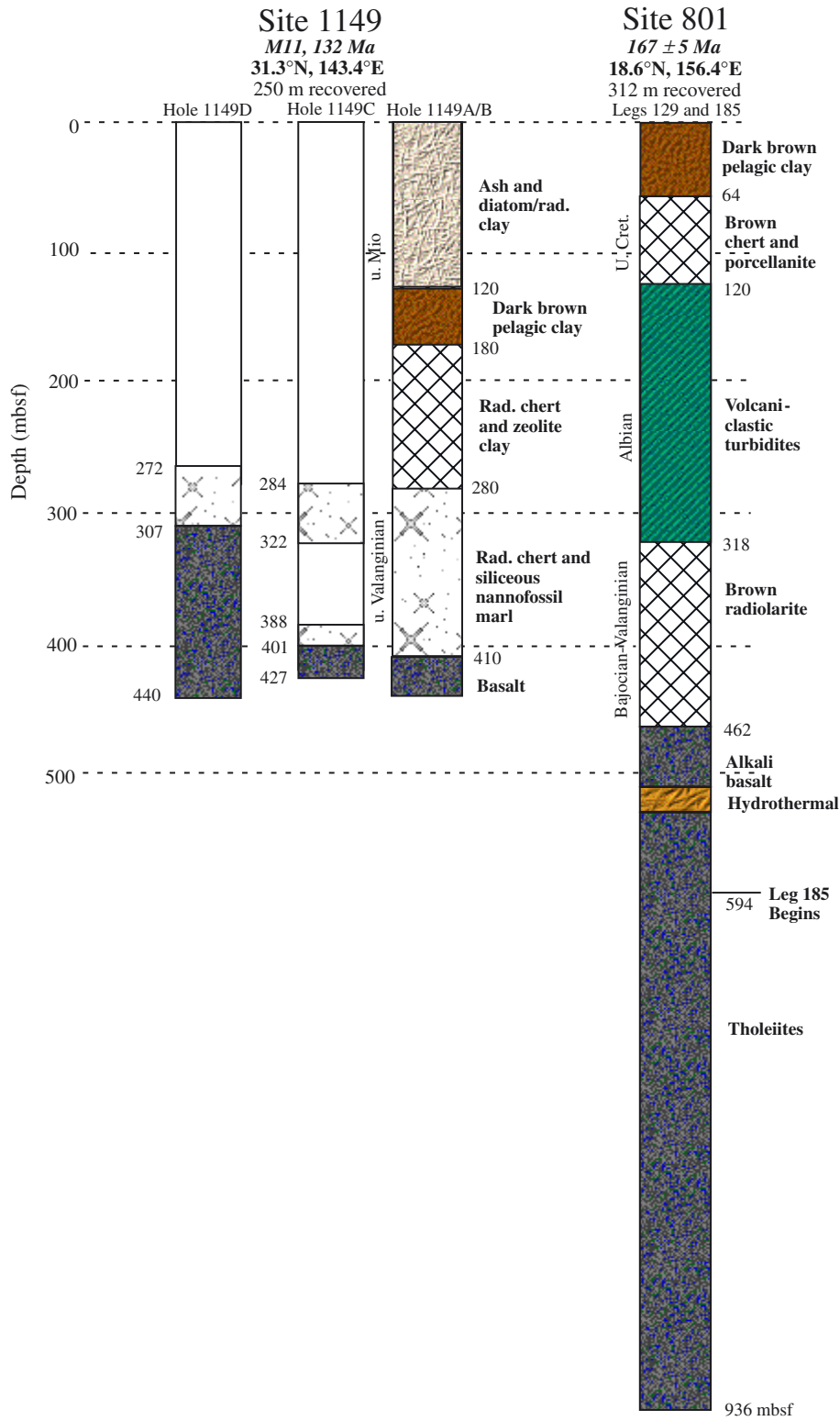


Table T1. The oldest crust drilled by ODP in the different ocean basins.

Leg 185, Site 801: West Pacific, Pigafetta Basin

Water depth (m): 5674
Total depth (m): 6609.7
Penetration (m): 935.7
Basement (mbsf): 461.6
Basement penetration (m): 474.1
Magnetic lineation: >M36
Oldest sediment: Bajocian–Bathonian (166 Ma)
Basement age: Alkalic cap (155 Ma)
Tholeiites: >155 <171 Ma
The oldest basement drilled in the oceans.

Leg 76, Site 534: West Atlantic, Blake-Bahama Basin

Water depth (m): 4973
Total depth (m): 6639.5
Penetration (m): 1666.5
Magnetic lineation: M28
Oldest sediment: mid-Calloviaian (~155 Ma)
Basement: core catcher, no radiometric age
The oldest Atlantic basement drilled.
The deepest penetration.

Leg 123, Site 765: Argo Abyssal Plain, Indian Ocean

Water depth (m): 5713.8
Total depth (m): 6908.7
Penetration (m): 1194.9
Casing string (m): 937
Basement (mbsf): 947.9
Basement penetration (m): 247
Magnetic lineation: M25a
Oldest sediment: early Berriasian (140 Ma)
Basement age: >156 Ma; Ar/Ar fusion
Celadonite age: 155 Ma; K/Ar
The oldest Indian Ocean basement drilled.
The greatest total depth.

Table T2. Leg 185 operational summary.

Hole	Latitude (N)	Longitude (E)	Water depth (m)	Number of cores	Interval cored (m)	Core recovered (m)	Recovery (%)	Drilled (m)	Penetration (m)	
801C	18°38.538´	156°21.588´	5674	40	339.3	160.4	47.3	0	935.7	
801D	18°38.538´	156°21.646´	5673.6	0	0	9.4	0.0	0	19.3	
801 summary	18°38.538´	156°21.618´	5673.8	40	339.3	169.8	50.0	0	955.0	
1149A	31°20.52´	143°21.07´	5817.6	23	191.2	174.4	91.2	0	191.2	
1149B	31°20.520´	143°21.06´	5817.5	31	284.6	36.7	12.9	151.1	445.2	
1149C	31°20.55´	143°21.06´	5817.6	8	76.9	8.7	8.3	0	426.7	
1149D	31°18.79´	143°24.03´	5817.5	18	168.2	29.9	17.8	0	445.2	
1149 summary	31°20.095´	143°21.805´	5817.6	80	720.9	249.8	32.6	151.1	1508.3	
Leg 185 totals:		Mean:	5745.7	120	1060.2	410.2	Mean:	41	151.1	2463.3

Note: hr = hour, d = day.

Table T2 (continued).

Hole	Time on hole	APC cores (number)	XCB cores (number)	RCB cores (number)	DCB cores (number)	MDCB cores (number)	Seafloor (mbrf)	Rig floor elevation (m)	Total penetration (mbrf)	
801C	485.00 hr	0	0	36	4	0	5685.0	11.0	935.7	
801D	22.50 hr	0	0	0	0	0	5685.0	11.4	19.3	
801 summary	21.1 d	0	0	36	4	0	5685.0	11.2	477.5	
1149A	64.42 hr	18	4	0	0	1	5829.3	11.7	6020.5	
1149B	180.58 hr	0	0	31	0	0	5829.3	11.8	6274.5	
1149C	103.33 hr	0	0	8	0	0	5829.3	11.7	6256.0	
1149D	155.00 hr	0	0	18	0	0	5829.3	11.8	6274.5	
1149 summary	21.0 d	18	4	57	0	1	5829.3	11.8	6206.4	
Leg 185 totals:	42.1 d	18	4	93	4	1	5757.2	Mean:	11.5	6683.9

Table T3. Proposed analyses of the communal and composite samples, Hole 801C.

Measurements	Investigator
Major elements by ICP-AES	Kelley/Plank
Trace elements (ICP-MS)	Kelley/Plank
Mineral comparisons by EMP, SEM, Petrography	Alt
Mineral identification by XRD, EMP, Petrography	Honnorez
S, Se, metals by MC-ICP-MS	Rouxel/Ludden/Armstrong
Trace elements by LAM-ICPMS	Plank
Hf isotopes	Ludden/Chauvel
Os isotopes	Ludden/Reisberg
Sr, Nd, Pb isotopes	Schmidt/Staudigel
Cl isotopes and halogens	Spivack
Li, B isotopes	Valentine
C, O, H, S isotopes	Alt
N isotopes	Bebout/Emilio
Ion Probe by C, O, S, traces	Ludden/Rouxel
Total number of communal samples:	118
Total number of composites:	12

Note: ICP-AES = inductively coupled plasma-atomic emission spectroscopy, ICP-MS = inductively coupled plasma-mass spectrometry, MC-ICP-MS = multi-collector ICP-MS, LAM = laser ablation microprobe.

Table T4. Proposed analyses of the communal glass samples.

Measurement	Investigator	Number of analyses	Aliquot
Fourier transform infrared spectroscopy water	Armstrong, Robin	5 to 10	5 mm chips
Microprobe for major elements	Fisk, Martin	30 to 40 + 20 thin sections	5 mm chips and thin sections
Microprobe and optical microscopy for biological alteration	Fisk, Martin	20 thin sections	thin sections
Ion probe for C, S, and trace element distribution and Pb isotopes	Ludden, John	10 to 20	1 to 5 mm bio + chips
LA-ICP-MS for trace elements	Plank, Terry	20 to 30	>1 mm chips
Ion probe for S, Se, metals	Rouxel, Olivier	same 10-20 chips of Ludden	1 to 5 mm bio + chips
Mass spectrometry Sr, Nd, Pb isotopes	Schmidt, Angelika	1	0.5 g
Cl isotopes and halogens	Spivack, Arthur	2 to 3	250 mg
Microscopy of biological alteration	Staudigel, Hubert	same as/share with Fisk	thin sections
Magnetic intensity	Steiner, Maureen	10 to 12	50 mg
Li, B isotopes	Valentine, Robbie	2	1 g
N isotopes	Bebout	2-3	<1 g

Note: LA-ICP-MS = laser ablation-inductively coupled plasma-mass spectrometry.